Musculoskeletal Modelling for Hip Joint Replacement

Master's Thesis

Neha Saini
2150066

Academic Supervisor:
Professor Mark Taylor

October 2019

Submitted to the College of Science and Engineering in partial fulfilment of the requirements of the degree of Bachelor of Engineering (Mechanical) (Honours), Master of Engineering (Biomedical) at Flinders University, Adelaide Australia

Abstract

Osteoarthritis (OA), specifically in the hip joint, is a progressive chronic joint disorder that leads to pathological changes including pain, limited mobility and muscle atrophy. Increasing prevalence of OA is a result of an ageing population and obesity. Total hip arthroplasty (THA), one of the most successful surgeries, is used to replace the degenerated articular surfaces providing pain relief and improved mobility. Conversely, several complications are associated with THA resulting in failure and revision surgery, leading to low quality of life and higher indirect and direct costs. Estimation of hip joint contact forces (HCF) can assist in preventing implant failure and consequent revision surgery. Musculoskeletal modelling has become a conventional method to predict HCF, however muscle symmetry is typically assumed in present studies. This assumption may not be a close representation of clinical observations. This thesis was designed to estimate resultant HCF and muscle forces by introducing abductor muscle asymmetry to imitate muscle atrophy.

OpenSim 4.0 was used with previously designed statistical shape scaled model (Bahl et al, 2019). Maximum isometric forces defined by Delp (1990) to introduce asymmetry in gluteus medius and minimus; 20%, 40% and 60%. Muscle asymmetry was introduced in the affected OA hip in six end-stage OA patients awaiting surgery by altering maximum isometric forces that are directly correlated to muscle cross sectional area.

Only one patient out of six showed a two peak profile while others showed only one peak profile in 100% gait cycle in the affected hip. For majority of the patients, insignificant changes were present in resultant HCF for all muscle asymmetry models. However, for 60% abductor muscle asymmetry model, evident changes in resultant HCF were present with a significant increase in two patients while a decrease in one patient. This was due to

compensatory action by the individual muscles taking over for the weak abductors. Further assessing the anterior - posterior HCF, a direction change was present for one patient as the muscle asymmetry was increased.

An increasing trend in used available muscle force capacity was present in all abductors; gluteus medius, minimus, maximus and tensor fascia latae. Additionally, patients using their full abductor available muscle force capacity due to muscle asymmetry were further compensated by flexors and extensors. Low gait speeds were also associated with lower HCF but only true for some patients.

The results strongly indicated; the impact of abductor muscle asymmetry on the resultant HCF and individual muscle forces was very case dependent. Further suggesting various other factors can impact patient's ability to withstand muscle weakness. In most cases, abductor muscles were reaching their maximum available force capacity may result in muscle fatigue, risk of dislocation and further volume reduction post THA.

This study has provided a method to predict resultant HCF and muscle forces with manipulating the muscle asymmetry in end-stage OA patients. Additionally, the impact of muscle asymmetry on the peak resultant HCF was also analysed to be case dependent. Therefore, future studies should be conducted with patient specific data for muscle volume and fatty infiltration using CT data.

Declaration

I certify that this work does not incorporate of any previously submitted material without acknowledgement, for a degree or diploma in any university; and that to the best of my knowledge and belief it does not contain any material previously published or written by another person except where due to reference is made in the text.

Neha Saini
October 2019

Acknowledgements

I would like to sincerely thank my supervisor Professor Mark Taylor for providing constant support, advice and assistance throughout the thesis. I would like to extend my gratitude to Francesca Bucci supporting me with musculoskeletal modelling in OpenSim and providing advice regarding the thesis. I would like to acknowledge and thank Jasvir Bahl for providing all the data and scaled models for OpenSim. I would also like to genuinely thank David Hobbs for providing support and advice on various occasions. To my friends for all the support and encouragement. To my family, gratitude to my parents and sisters for constant support, encouragement and love.

Table of Contents

List of Tables

List of Figures

Chapter 1

1 Introduction

Hip structure of a ball and socket provides range of movements (Byrne et al., 2010) where the head of the femur is attached to acetabulum of the pelvic bone (Drake et al., 2015). The structure supported by muscles allows forces to be transmitted ground up as well as sustaining forces from the trunk, head and upper extremities. (Byrne et al., 2010). The hip movements can be categorised into flexion, extension, adduction, abduction, lateral and medial rotation. The pelvic stability during gait, abduction and rotation of the hip is supported by the abductor muscles. (Flack et al., 2012). The abductor muscle group includes gluteus minimus, gluteus medius, gluteus maximus and tensor fascia latae.

Osteoarthritis (OA) is a chronic joint disorder that can be classified into primary and secondary disorder depending on the progression. (Cucchiarini *et al.*, 2016). OA can impact various joints in the body but weight-bearing joints are most significantly impacted such as the hip joint. Progression of OA leads to pathological changes including pain, synovial inflammation, deformity and loss of function in the structural joint. Further progressive changes include articular cartilage degradation, subchondral bone thickening, osteophyte

formation and degeneration of ligaments.(Loeser et al., 2012). The disease also affects the patient's lifestyle due to limited mobility, financial and social issues.

There is an estimation of 9.6% and 18.0% men and women, respectively aged over 60 years with symptomatic osteoarthritis. 80% of OA patients have limitations with movement and 25% cannot perform daily activities. (World Health Organization, 2013) OA patients demonstrate asymmetric gait pattern with reduction in stride length, hip motion and hip joint muscle moment (Hurwitz et al., 1997) Altered gait cycle results from pain and limited mobility further leading to disuse atrophy and hip abductor muscle weakness. (Arokoski et al.,2002)

According to Australian Bureau of Statistics (ABS), in 2014 to 2015 approximately 2.1 million people had OA; 1 in 11 Australians (9%). The number increases with age as 21% and 35% are affected from age of 45 and 80 years, respectively. (ABS, 2015) 1 in 4 people with OA reported fair or poor health conditions, twice as much compared to people without the condition. (AIHW, 2018) World Health Organization (2013) states OA to be one of the ten most disabling diseases in the developed countries. There has been an increasing prevalence of OA is due to the ageing population and obesity. (Bijlsma et al., 2011) There are treatments for OA such as non-steroidal anti-inflammatory drugs and arthroscopic lavage and debridement as well as replacement surgery but have not been sustainable to fully reverse the OA phenotype. (Cucchiarini *et al.*, 2016)

Total hip arthroplasties (THA) is one of the most successful surgeries providing pain relief and improved walking abilities. THA can have a positive impact on the patient's quality of life but can also lead to a negative impact due to failure. Analyses from long term studies show abnormal gait cycles post THA. (Colgan *et al.*, 2016) The consequences can result from surgical methods and atrophy, fatty degeneration and function loss in the hip muscles.

Hip replacement data estimated with Nationwide Inpatient Sample and United States Census Bureau data between 1990 to 2003 shows an increase of 174% THA from 208,600 in 2005 to 572,000 by 2030. (Kurtz et al., 2007) There are also several complications associated with THA that lead to failure and revision surgery resulting in low quality of life and higher costs. (Patil et al., 2008; Vanhegan et al., 2012) The design of the implants can be improved to reduce revision surgery to support the growing demand. Estimation of loading on the implant

through magnitude and direction of hip contact forces (HCF) can assist in preventing failure and design applications. In vivo data for HCF has been collected but only for post-operative stages. A common method in the recent years to study HCF has been musculoskeletal modelling as it is cost effective, subject specific and non-invasive.

OpenSim is an opensource musculoskeletal modelling software equipped with basic models such as lower limb model (Delp et al., 2007) used to study hip joint contact forces. Previous research with lower limb modelling has several limitations such as muscle symmetry. As various studies show there is abductor muscle volume reduction as well as fatty infiltration further impacting the quality of the abductor muscle. Therefore, leading to the decrease of maximum isometric forces due to reduction in contractile force capacity and cross-sectional area of the abductor muscle. As the muscle volume is directly proportional to the maximum isometric force that muscles can produce. (Arokoski *et al.*, 2002)

1.1 Objectives

This objective of this master's thesis was to develop a musculoskeletal modelling (OpenSim) method to predict the impact of the asymmetry in osteoarthritic patients on resultant HCF. Correspondingly, study the impact of abductor asymmetry on the HCF and muscle forces in patients with Osteoarthritis in normal gait cycle. The abductor muscle asymmetry was created through changing the maximum isometric forces in OpenSim assigned to each muscle. The focus key muscles for this study was gluteus medius and gluteus minimus. Kinematics and force plate data required was collected with Vicon system in six patients conducting multiple walking trails by a previous study (Bahl et al., 2019).

Phase one was conducted for comparison between linear scaling and statistical shape scaling designed by an earlier study (Bahl et al., 2019) for predicting result HCF and muscle forces. Phase two analysed the different maximum isometric forces reported by earlier studies for lower limb extremity muscles. Phase three introduced asymmetry within abductor muscles to analyse the impact on resultant HCF and muscle forces in each patient.

1.2 Aims

1. Define a method to introduce muscle abductor asymmetry into the musculoskeletal model.
2. Assess the impact of statistical shape scaling and linear scaling on resultant HCF
3. Assess the influence of maximum isometric forces on the resultant HCF
4. Impact of muscle abductor; gluteus medius and minimus asymmetry on the resultant, directional HCF and individual muscle forces

Chapter 2

2 Literature Review

2.1 Hip Anatomy

Hip comprises of a ball and socket joint surrounded by muscles providing the ability to access range of movements. (Byrne *et al*., 2010). Head of the femur and acetabulum of the pelvic bone has a synovial articulation between it. (Drake, 2005). The structure of the hip allows the forces to be transmitted ground up as well as sustaining forces from the trunk, head and upper extremities. (Byrne *et al*., 2010). The hip joint is a multiaxial ball and socket with three degree of freedom allowing rotations. Movements can include flexion, extension, adduction, abduction, lateral and medial rotation and circumduction.

Figure has been removed due to Copyright restrictions.

Figure 1: Hip anatomy consisting of a femoral head on the femur and pelvis as a hip joint structure - Reproduced from Towson Orthopaedic Associates. (2019)

The spherical head of the femur and lunate surface of the acetabulum of the pelvic bone make up the articular surfaces of the hip joint. The joint stability results from the almost entire enclosure of hemi-spherical head of the femur by the acetabulum. Whereas, the non-articular acetabular contains loose connective tissue and hyaline cartilage covers the lunate surface. Thick and strong fibrous membrane encloses the hip joint. Connective tissue forms the ligament of the head of the femur that is attached to the acetabular fossa.

2.1.1 Hip Muscles and Movement

Muscles are divided into three different tissue groups; visceral, cardiac and skeletal. Skeletal muscle classified as voluntary formed by small progenitor cells connected together to form long multinucleated fibres. (Drake *et al*., 2005). Skeletal muscles are primarily connected to bone through tendons; dense connective tissue of collagen fibres. Tendons are woven into covering muscles and bones in order to withstand high stress when pulled by muscles. Origin and insertion are defined as the stationary bone and moving bone connected to the muscle via tendon, respectively. The middle part between tendons is responsible for the contraction.

Contraction of muscles is stimulated by motor neuron signals at the neuromuscular junction (NMJ). Neurotransmitter chemicals are released by motor neurons at the NMJ connected to motor end plate part of the sarcolemma. Neurotransmitters cause the opening of ion channels in the motor end plate resulting in positive ions entering the muscle fiber. Further channels are opened as the ions spread inside the sarcolemma and T-tubules by increasing the number of open channels. Ca2+ are released into myofibrils subsequently of positive ions reach sarcoplasmic reticulum. Ca2+ bind to troponin inducing change in shape and transporting close to tropomyosin molecules. As the tropomyosin is moved away to expose the myosin binding sites to actin molecules for binding to occur. The mechanism involves thick filaments bending and pulling on actin molecules of thin filaments to the center of the sarcomere causing contraction. (Berchtold *et al.*, 2000)

The strength of the muscles is controlled by number of employed motor units and degree of stimulation from nervous system. There are different types of contractions; twitch contraction, isometric contraction and muscle tone. Skeletal are divided into two types

dependent on amount of energy produced and utilized; Type I and Type II. (Berchtold et al., 2000)

Muscles inserted on the femur, mostly originate at the pelvic girdle aiding in movement (Figure 2). Iliopsoas group are made up psoas major and iliacus. Gluteus maximus are the largest group followed by gluteus medius and gluteus minimum. Flexion and abduction of the thigh is conducted by gluteus medius and iliopsoas acting as synergist. Lateral rotation of the femur at the hip is directed by piriformis, obturator internus, obturator externus, superior gemellus, inferior gemellus and quadratus femoris. Adductor longus, brevis and magnus hold ability to medially and laterally rotate the thigh depending on the foot placement. Adductor longus and adductor magnus flex and extend the thigh, respectively. Pectineus formed at the junction of hip and leg consisting of femoral nerve, artery, vein and inguinal lymph nodes, adducts and flexes the femur. (Flack *et al.*, 2012)

Figure has been removed due to Copyright restrictions.

Figure 2: Hip muscles involved in flexion, extension, abduction, adduction, internal and external rotation from anterior and posterior view. Reproduced from Lumen (2019)

2.1.2 Hip Abductors

The hip abductors contribute to pelvic stability during gait, abduction and rotation at the hip joint. (Flack *et al*., 2012) The hip abductors also contribute to movement of the thigh away from the body's centre axis. The abductor muscle group includes gluteus minimus, medius and maximum and tensor fascia latae (Figure 2).(Soderberg and Dostal, 1978; Lyons *et al.*,

1983; Gottschalk *et al.*, 1989; Kumagai *et al.*, 1997; Anderson and Pandy, 2003) The gluteus medius and minimus are identified as major stabilisers of the hip joint. Medius consists of three parts responsible for stabilisations in the initial phase of the gait cycle as well as initiating pelvic rotation. Minimus is a primary hip stabiliser as well but during the mid and late stance phases of the gait cycle. (Gottschalk *et al.*, 1989)

Gluteus minimus also contribute to medial rotation of the hip. (Attum and Varacallo, 2018) It is a fan shaped muscle originating from the external surface of the expanded upper part of ilium between the inferior and anterior gluteal line. The tendon formed by muscle fibres converged inferiorly and laterally inserts into a linear facet on the anterolateral of the greater trochanter. (Drake, 2005) The anterior gluteus medius fibres rotates the hip medially while posterior fibres rotate hip laterally. (Attum and Varacallo, 2018) It is also fan shaped and overlies the minimus. The medius muscle group has an origin from the external surface of the ilium between the anterior and posterior gluteal line. It inserts into elongate facet on the greater trochanter's lateral surface. Both the gluteal minimus and medius abduct the hip joint as well as reduction of pelvic drop through securing the position of pelvis on the stance limb during the swing phase. (Drake, 2005)

The gluteus maximus is also involved in extension of the hip as well as lateral rotation. (Attum and Varacallo, 2018) It is the largest gluteal muscle and a quadrangular shaped. Maximus extends from the roughened area of ilium behind the posterior gluteal line to the external surface of sacrotuberous ligament. The muscle contributes to extension of the flexed thigh and stabilisation knee and hip joint due to insertion into iliotibial tract. (Drake, 2005)

The tensor fascia latae maintains the stabilization of the knee and hip joint. (Attum and Varacallo, 2018) It originated from the outer boundary of ilium crest from anterior superior iliac spine. The muscle stabilises of knee in extension and supports the head of femur in the acetabulum to support the hip joint. It also works with the gluteal maximus on the iliotibial tract to the greater trochanter. (Drake, 2005)

2.1.3 Level Gait

Various studies have described level gait hip biomechanics(G Bergmann *et al*., 1993; Davy et al., 1988; Givens-Heiss *et al*., 1992; Rydell, 1966). A full gait cycle consists of two main phases stance and swing divided into 8 different periods (Vu *et al.*, 2018).

Figure has been removed due to Copyright restrictions.

Figure 3: One Gait cycle comprising of eight phases from initial heal contact (0%) to next initial contact of the same foot (100%) within the two main phases of stance and swing. First and second double support during the loading response and pre-swing phase. First and second single limb support during the other phases between 8% to 50% and 60% to 100%. Reproduced from Neumann et al, (2010)

Kinematics

During a normal stride in the gait cycle, hip rotations is approximately 40^{o} in the sagittal plane. Maximum flexion occurs in the later swing phase (85%) at 30 - 35^{o}. Whereas, maximum extension is reached near toe-off (50%) at approximately 10^{o} (Perry, 1992). Maximum hip adduction occurs in the frontal plane during the early stance (40%) (Krebs et al., 1998). Hip abduction occurs in the early swing phase between 5 - 7^{o} (Perry, 1992). Maximum internal rotation occurs closer to midstance (10%) and external rotation during swing phase (60 – 100%) (Krebs *et al*., 1998).

Kinetics

Ground reaction forces comprise of six degrees of freedom divided into vertical compression, fore-aft, mediolateral horizontal shears and three twisting moments (Krebs *et al.*, 1998). Gait cycle from initial heel strike to terminal stance progression results in changes in forces vector from anterior to posterior. In the Initial contact (0%) period, peak flexion torque occurs followed by a decrease to extension torque during midstance (10 -30%) until late stance. Adduction torque in the coronal plane is sustained during the stance phase (Perry, 1992).

Muscle Activity

Hamstrings and gluteus maximus help hip extension to conduct the initial contact (Perry, 1992). During the midstance, abductors stabilise the pelvis contributing to the increased muscle activity in the coronal plane (Krebs *et al.*, 1998). Lateral pelvic stabilization is conducted by both gluteus medius and minimus during the terminal stance. During the late stance and pre-swing hip flexion, iliacus and tensor fascia latae are active. Hamstrings and gluteus maximus are active during the terminal swing in order to decelerate hip flexion and knee extension. (Perry, 1992)

Table 1:Muscle activation during the 100% gait cycle of lower limb extremity hip muscles – Adapted from Bonnefoy-Mazure and Armand, (2015) and Thelen and Anderson, (2006)

Hip Muscle	**Bonnefoy-Mazure and Armand, (2015)**	**Thelen and Anderson, (2006)**
Gluteus Medius	0 – 40% & 85 – 100%	0 – 60%
Gluteus Maximus	0 – 20%	0 – 20%
Tensor Fasciae Latae	-	20 – 60%
Semimembransus	-	0 – 10%
Biceps Femoris	0 – 20%	0 – 5%
Sartorius	60 – 70%	40 – 60%
Rectus Femoris	50 – 70%	45 – 60%
Iliacus	60 – 75%	-
Adductor Longus	30 – 50%	30 – 50 %

2.2 Osteoarthritis

Osteoarthritis (OA) is a chronic joint disorder that can be classified into primary and secondary OA. (Cucchiarini *et al.*, 2016) The classification is dependent upon etiology, progressive articular cartilage breakdown as well as subchondral bone, synovium, meniscus, tendons/ligaments and muscle changes. The pathological changes of the disease can result in pain, deformity and loss of function in the entire joint structure. (Lane, 2007; Dibonaventura *et al.*, 2011; Constantinou *et al.*, 2014; Eitzen *et al.*, 2015; Loeser et al., 2012) Further changes can include articular cartilage degradation, subchondral bone thickening, osteophyte formation, degeneration of ligaments and synovial inflammation. OA can affect any joint but weightbearing joints are most significantly affected. (Cucchiarini *et al.*, 2016) The disease affects the daily lifestyle of patients and contributes to further financial and social issues.

Hip OA has no cure and further progresses to advanced stages and prosthetics such as hip replacement have a focus on reducing pain and improving mobility. (Puett and Griffin, 1994; McNair *et al.*, 2009; Arnold and Faulkner, 2010) During daily activities, excessive joint loading with muscle weakness are risk factors in the development of hip OA. (Felson, 2013)

OA can be classified as primary and secondary types. Primary hip OA affects multiple joints and usually occurs in the elderly populations without a known cause. Secondary OA is developed due to disorder affecting the joint articular surface and defined as monoarticular condition. Although, primary OA is reported to be majority of the all hip OA. (Felson, 2013)

2.2.1 Osteoarthritis Population Statistics

1 in 4 people with OA reported fair or poor health conditions, twice as much compared to people without the condition. (AIHW, 2018) The increasing trend in OA is due to the ageing population and obesity. (Bijlsma *et al*., 2011) Traditional treatments such as non-steroidal anti-inflammatory drugs and arthroscopic lavage and debridement as well as replacement surgery have not been sustainable to fully reverse the OA phenotype. (Cucchiarini *et al.*, 2016) According to Australian Bureau of Statistics (ABS), in 2014 to 2015 approximately 2.1 million people had OA; 1 in 11 Australians (9%). The number increases with age as 21% and 35% are affected from age of 45 and 80 years, respectively. (ABS, 2015)

World Health Organization (2013) states OA to be one of the ten most disabling diseases in the developed countries. There is an estimation of 9.6% and 18.0% men and women, respectively aged over 60 years with symptomatic osteoarthritis. 80% of OA patients have limitations with movement and 25% cannot perform daily activities.

2.2.2 Pain and Mobility

OA patients experience joint pain, stiffness, joint range of motion and muscle strength reduction. (Lane, 2007; Dibonaventura *et al.*, 2011; Constantinou *et al.*, 2014; Eitzen *et al.*, 2015) It has also been reported OA patients have demonstrated asymmetric gait patterns including stride length decrease, hip motion decrease and affected leg hip joint muscle moment reduction. (Hurwitz *et al.*, 1997) Due to the pain and limited mobility of the OA hip leads to the altered gait cycles further resulting in disuse atrophy and hip abductor muscle weakness. (Arokoski *et al.*, 2002) Further, OA patients have reduced performance of daily activities further resulting in diminish in quality of life. (Castaño-Betancourt *et al.*, 2013) Common activities that intensify the hip pain in OA patients are prolonged inactivity and physical activity, abduction, external & internal rotation and bending. Pain flares with dynamic activity and after prolonged period of sitting or resting. Hip joint stiffness also makes it difficult to walk or bend. The range of motion at the joint also affects the walking abilities and OA patients often limp to avoid loading the affected side due to pain. (Lespasio *et al.*, 2018)

2.2.3 Hip Muscle Atrophy

Osteoarthritis (OA) can result in muscular weakness (Arokoski *et al*., 2002; Madsen, et al., 1997; Rasch et al, 2007; Suetta et al., 2004), joint pain and reduced ambulatory capacity in the affected hip. (Loureiro et al., 2018; Zacharias *et al*., 2016) Further research on OA patients show muscle weakness combined with muscle atrophy (Grimaldi *et al*., 2009; Rasch *et al.*, 2009; C. Suetta *et al.*, 2007; Suetta *et al*., 2004), muscle inhibition (Suetta *et al*., 2007), and muscle density reduction. (Rasch *et al*., 2009; Rasch *et al*., 2007; C. Suetta *et al*., 2007) The research suggests that muscle weakness is one of the primary risk factors of OA and progression of the disease may also impact atrophy or weakness of periarticular muscles.

Gluteal msucle atrpohy in hip OA may lead to imacprieemnt of protective reflexes, joint instability and increased peak HCF. (Zacharias *et al.*, 2017)

Following these finding intensive research has been conducted on activation, strength, size and function of the hip muscle groups affected by hip OA. (Zacharias *et al.*, 2016) Major stabilisation at the hip joint is the abductor muscle groups; gluteus medius and minimus. Studies show hip abductor weakness in hip OA that can be impacted in reduction of muscle size or activity. Cross-sectional area (CSA); contractile and non-contractile, is directly proportional to the force produced by the muscle. In muscle atrophy as muscle fibres degenerate, the empty space is occupied by the fatty tissue. Therefore, fatty infiltration can impact the muscle function therefore calculations of CSA should exclude all non-contractile tissues. (Zacharias *et al.*, 2016) Muscle volume and strength studies are normally conducted with OA and healthy patients with MRI and isokinetic dynamometer.

2.2.4 Muscle Volume and Strength

Lower hip abductor strength was reported in OA subjects compared to healthy control subjects. (Zacharias *et al.*, 2016) Gluteus minimus muscles also showed lower volume with other muscle groups as well. Muscle asymmetries were not detected, potentially as a result of having both unilateral (12 subjects) and bilateral (7 subjects) hip OA. (Zacharias *et al.*, 2016)

Louriero et al. (2018) reported there was a hip volumes reduction of 5-30% across all muscle assessed except tensor fasica latae and gluteus medius. Arokoski et al. (2002) found CSA reduction of 6-13% on the affected compared to the contralateral hip. Furthermore, Various studies have reported 12-19% reduction in cross-sectional area (CSA) of muscles in the affected hip. (9,10,11, Grimaldi, 2009). Hip strength for the hip abductors has been reported 31% (Arokoski *et al*, 2002) and 11-29% (Rasch *et al*, 2006) lower compared to healthy hip. Lourier et al, (2018) also reported 22-26% lower muscle strength but compared to the control group.

The gluteus medius strength reduction may be due to unilateral OA and it can further contribute to development of contralateral hip OA. As a result of weaker muscle leading to the inability of sustaining load transfer during gait. (Amaro *et al*., 2008) Hence, the absence

of muscle strength asymmetry can be present during progression of the disease. (Zacharias *et al.*, 2016; Loureiro *et al.*, 2018; Silva *et al.*, 2018) Reduction in muscle volume was more evident with increased OA severity and progression. (Zacharias *et al.*, 2016; Loureiro *et al.*, 2018; Silva *et al.*, 2018) Muscle atrophy has also been detected through electromyography and magnetic imaging showing abnormalities. (Andary *et al.*, 1998)

The results of muscle asymmetry were different to the previous study (Loureiro *et al.*, 2018) as reduced muscle volume of the gluteal group was observed on the affected side (Zacharias *et al.*, 2016). This contradiction between results may be due to difference in the grades in the Zacharias *et al.*, (2016) and Loureiro *et al.*, (2018) studies. Zacharias et al. (2016) results show atrophy was demonstrated in gluteal muscle with KL grade of 3. However, Loureiro et al. (2018) study had 42% subjects with KL grade = 2 therefore suggesting muscle asymmetry becomes more prominent with increasing severity of OA.(Zacharias *et al.*, 2016) Muscle strength had absence of difference could result from unloading of both sides of hip reducing the overall physical activity due to pain. (Loureiro *et al.*, 2018)

2.2.5 Fatty Infiltration

Fatty infiltration has also been associated with age increase, higher body-mass index and low physical activity (Daguet *et al*., 2011). As the OA patients have limited mobility and pain leading to lower physical activity, this further induces reduction in muscle quality.

Skeletal muscle represents approximately 40% of the body weight and tissue is constantly changing due to internal and environmental stresses. (Reid and Fielding, 2012) There can be positive impacts due to exercise and nutrition resulting in muscle hypertrophy. However, chronic disease can also lead to muscle atrophy and deconditioning with some functional limitations. Studies have shown evidence loss of muscle strength is higher than loss of muscle mass in advancing age or muscle inactivity. (Prior *et al.*, 2007; Goodpaster *et al.*, 2008) Further suggesting there are other factors such as Intermuscular adipose tissue (IMAT) or accumulation of fatty infiltrations that play a critical role in muscle weakness. Adipocyte clusters are fat cells under the epimysium (between bundle of muscle fibres) and perimysium (between muscle fibres). IMAT are naturally present in all healthy skeletal muscle but due to increased and accumulation within the muscles dysfunction, deconditioning as well as

disturbed regenerating process. (Marcus *et al.*, 2010; Uezumi et al., 2014; Sciorati *et al.*, 2015) Increased accumulation of fatty infiltration (FA) is closely associated with muscle deconditioning due to inactivity. (Manini *et al.*, 2007; Leskinen *et al.*, 2009; Tuttle *et al.*, 2011) Furthermore, inactivity leads may lead to structural changes like increased intramuscular fatty tissues hence, muscle strength decrease (Manini et al., 2007) as well as reduced mobility. (Visser *et al.*, 2002) These signs and impacts are also commonly seen in OA populations.

Gluteal muscles in elderly with osteoarthritis can lead to degeneration and FA. (Muller et al., 2011). Furthermore, in the elderly patients, satellite cells decline with reductions in the regenerative capacity as a result of increasing age. (Kadi *et al.*, 2004; Müller *et al.*, 2011) The satellite cells also have a reduction in proliferative capacity. (Schultz and Lipton, 1982) Kovalak *et al.* (2018) also reported FA was increased in the operated hips. Zacharias et al. (2016) found muscle atrophy ranging from medium to high effects in affected side gluteus medius, minimus and maximus compared to the contralateral side. Zacharias *et al.* (2016) study results were also in a good correlation with previous study (Chi *et al.*, 2015) for healthy controls but significantly increased levels of FA for OA population.

Furthermore, there is increased muscle atrophy, strength deficits and FA in the affected side compared to contralateral side and healthy subjects. This is commonly seen in OA population and has been identified by numerous studies. While muscle volume is shown to be more evident in the advanced OA population compared to initial stages. (Marshall, 2016). There is also growing evidence of strong correlation between severity of OA and extent of atrophy as well as FA. (Zacharis *et al*., 2017)

2.2.6 Contralateral Hip OA

Patients with unilateral hip implant also have a risk of developing OA in the contralateral unaffected hip. Damm et al. (2018) also reported a decrease in the lean muscle on the contralateral hip which may be impacted by the hip implant. Studies have reported patients with end stage OA or THA have a greater risk of developing OA in the contralateral non-affected hip. (Husted *et al.*, 1996; Shakoor *et al.*, 2002; Pivec *et al.*, 2012) Pivec *et al*. (2012) reported a probability of 36% for development of the OA in the contralateral non-affected

limb. Risk increase of THA may cause abnormal loading in the hip joint (Schmidt *et al.*, 2017). It has also been reported, unilateral hip OA patients display higher loads in the contralateral non-affected hip compared to the affected hip. (Hurwitz *et al.*, 1997; Shakoor *et al.*, 2003; Miki *et al.*, 2004; Foucher, Hurwitz and Wimmer, 2007; Chiu, Lu and Chou, 2010; Foucher and Wimmer, 2012; Schmitt, Vap and Queen, 2015) Shakoor et al. (2013) reported the asymmetry in loads remained after the THA as well.

2.3 Total Hip Arthroplasty

THA is an orthopaedic procedure consisting of surgical removal of femur head and proximal neck and removal of acetabular cartilage and subchondral bone. A mental femoral prosthesis with stem and head with small diameter is inserted into femoral medullary canal (Figure 4).

Figure has been removed due to Copyright restrictions.

Figure 4: components in the THA, implant with all the components and the implant in the hip. Reproduced from Orthoinfo (2019)

THA can have a positive impact on the subjects' quality of life but can also lead to a negative impact due to failure. Although it is one of the most successful surgeries providing pain relief and improved walking abilities, but gait cycles remain abnormal. Diverse studies analysing long term gait cycles post THA show inability of walking cycles to return to normal. (Colgan *et al.,* 2016) The consequences can result from surgical methods and atrophy, fatty degeneration and function loss in the hip muscles. Previous research shows muscle atrophy and fatty degeneration lead to negative influence on the postoperative outcomes. Numerous studies have been conducted over time on in vivo joint contact forces after THA.
Both total hip revision is reported to increase by 137% between 2005 and 2030. The total hip arthroplasties are also approximated to increase to 174% to 572,000 by 2030 from 208,600 in

2005. This data was estimated with Nationwide Inpatient Sample between 1990 to 2003 and used in conjunction with United States Census Bureau data. (Kurtz *et al*., 2007)
There are also several complications associated with THA that lead to failure and revision surgery resulting in low quality of life and higher costs. (Patil et al., 2008; Vanhegan et al., 2012) Delaunay et al. (2013) conducted a study to evaluate the causes for failure of primary THA in France. The results indicated a revision due to mechanical loosening (42%), periprosthetic fracture (12%), infection (11%), dislocation (10%), surgical technique error (6%), wear/osteolysis (11%) and implant failure (3%). Further studies have reported misalignment of prosthetic resulting in a major risk factor for aseptic loosening, implant wear and main reason for revision THA. (MacInnes *et al*., 2012)

The wear of the implant can be improved by reducing the stresses. The design of the implant has to be studied and improved to support the growing demand of surgeries in the younger adults. Acetabular inlay excessive edge loading needs to prevent, and it is one of the major criteria for defining patient specific load-based cup alignment. The design can be improved through the study of loads applied on the implants due to different activities.

2.3.1 Post-operative THA Volume and Strength

Fukumoto et al. (2013) conducted study with women with unilateral total hip arthroplasty (THA) and age matched healthy women to evaluate the maximal isometric strengths. Measurements were taken for hip flexors, extensors and abductors and knee extensors & flexors. THA group showed muscle strength lower than healthy group for abductors. Six months after results showed an improvement in muscle strength for both sides compared to preoperative stage but remained lower than results of healthy individuals also supported by some of the previous studies. Preoperative muscle strength was 55% to 66% of involved side and 72% to 81% on uninvolved side of that in the healthy group. These results show that a reduction in strength was present before surgery also with subjects with unilateral hip OA. Therefore, previous studies with reference point of preoperative or uninvolved leg muscle strength could have led to overestimated of after surgery muscle strength. (Fukumoto *et al.*, 2013)

Fukumoto et al, can also be supported by another study conducted for assessment of maximal voluntary isometric strength with 20 elderly patients; unilateral OA preoperative, 6 months and 2 years post THA. (Rasch *et al*., 2010) The measurements were taken with strain gauges while in sitting and standing positions. There was a deficit of 18% and 12% for preoperative and 6 months post THA, respectively. Hip muscles showed a 6% deficit after 2 years post THA compared to the contralateral healthy leg also supported by previous study. *(Rasch et al.*, 2010). Muscle atrophy was present after two years of THA in abductor muscle groups in a similar study. The study conducted showed a reduction in cross-sectional area of hip abductors of 8.4% also represented with radiological densities of gluteus maximus (10.1 Hounsfield units and gluteus medius/minimum (5.6 Hounsfield units). (Rasch *et al*., 2009)

Increasing age and loss of satellite cells results in metabolic response and recovery impairment of the hip muscles post-surgery. Further leads to degeneration and reduced hip abductor muscle mass in the THA hip compared to contralateral non THA hip. Elderly patients (over 70 years) showed poor functional outcomes and higher FA postoperatively in comparison to younger patients. This could be due to reduced regenerative capacity of the hip muscles as well as increased weakness. (Müller *et al.*, 2011)

Post three months THA, damaged gluteal muscle lead to high in vivo joint loads. The results showed decrease of 25% in volume and increase in fatty infiltration ratio of gluteus minimus also recorded in the previous literature. (Adolphson *et al*., 1993; Rasch *et al*., 2009; Suetta *et al*., 2004). There were only minor changes present in the gluteus medius and maximus. The major findings were the increased tensor fasciae latae volume by 14% and lean volume by 34% with decreased fat ratio of 57%. (Damm *et al*., 2018)

Results from knee OA patients also show reduction in functional capacity leading to joint pain, stiffness and muscular strength deficit. Some studies have also been conducted on the dynamic loading, muscle strength and proprioceptive acuity at the knees in unilateral hip OA. The results show asymmetries in the muscle strength and proprioception between the unilateral and contralateral hip OA. (Rasch *et al.*, 2009)

Figure has been removed due to Copyright restrictions.

Figure 5: Measured strengths in flexion, abduction, adduction and leg press – Reproduced from Rasch et al., (2009)

A short-term study conducted by Rasch *et al.* (2009) using similar methods to previous study (Rasch *et al*., 2010) follow the same trend of results. Figure 5 shows a decrease at day 2, however, an increase in abductor muscles activity was noted at day 8. Although the abduction muscle strength did not return to the pre-operative values, but this could be due to the short time phase or general pattern also shown in previous studies (Rasch *et al*., 2010; Fukumoto *et al.*, 2013).

Some studies also assess the muscle strength and recovery by comparing the values obtained for the affected unilateral hip to contralateral hip or preoperative values. (Rasch *et al*., 2010; Fukumoto *et al.*, 2013;Suetta *et al*., 2004) Preoperative values could be reduced due to progression of OA and muscle recovery to that value may not occur therefore using them as reference might be insufficient. Contralateral unaffected hip values as a reference may be inaccurate due to altered by disuse atrophy. (Arokoski *et al.*, 2002) These findings can be supported by previous studies that show hip and knee muscle strength for both involved and uninvolved side was considerably lower compared to healthy subjects after 4 to 5 months or 2 years postoperative. (Sicard-Rosenbaum *et al.*, 2002; Bertocci *et al.*, 2004)

2.3.2 Different Surgical Methods

Winther et al. (2016) conducted study with 60 subjects with different surgical methods; direct lateral (DLA), posterior (PA) or anterior approaches (AA). The abductor strength was investigated over 3 months period post-operative. DLA method affects the gluteus medius & maximus and PA affects gluteus maximus, piriformis muscle and gemelli muscles. AA method doesn't affect muscles but tensor fascia latae and gluteus medius are stretched. The operated leg was 15% weaker in abduction than bilateral (unoperated) leg (figure 2) compared to preoperative strength (100%). Observations show DLA surgery decrease in muscular strength compared to PA and AA methods. In the last period of investigation at 3 months, the PA group showed increased muscle strength compared to both DLA and AA groups (Winther *et al.*, 2016). As the abduction exercise mainly employs gluteus medius and minimus can be the result for DLA method showing decreased muscle strength. Furthermore, piriformis muscle, tensor fascia latae as well as gluteus maximus upper fibers contribute with lesser degree (Winther *et al.*, 2016) therefore AA and PA don't account for major change in strength. The tensor fascia latae results in the preoperative muscle strength studies also show minor differences in muscle strength and volume. (Zacharias *et al.*, 2016; Loureiro *et al.*, 2018)

Figure has been removed due to Copyright restrictions.

Figure 6: Different surgical methods measurement of abduction strength post-operative; 2 days, 8 days, 6 weeks and 3 months - Reproduced from Winther *et al.* (2016)

2.3.3 Gait Patterns

Studies have also shown slower walking speeds to be directly correlated with gait adaptations. (Murray et al., 1971; Wadsworth et al., 1972) Further studies have also been conducted with postoperative THA patients compared to healthy individuals. Systemic studies show low walking speeds, strike length, lower sagittal and coronal plane range of motion (ROM) in the hip joint and lower peak hip abduction moment. These systemic reviews don't account for the pre-operative results of the patient. This is a limitation as the comparison of THA patient to healthy individuals as it could be inadequate to represent the differences without considering the pre-operative end-stage OA functionality. (Bahl et al, 2018) (Li *et al.*, 2014) Altered gait kinematics of OA patients before operation will persist after surgery.

A recent study conducted compared the preoperative and post-operative results of OA patient showing improvements over time in walking speed, stride length and step length post THA. In comparison to healthy individuals, lower walking speeds were still present at 12 months despite the early improvements. Further research into muscle function in THA patients need to be conducted to gain a greater understanding of the results. (Bahl *et al.*, 2018) The difference in healthy standard data and THA results can be due to altered articulating surfaces and reconstruction leading to changes in soft tissue. Hence, patients' characteristics can alter the hip contact forces at the bearing surface. (De Pieri *et al.*, 2019). Wesseling et al, (2018) also conducted research to overcome the limitations with joint loading before and up to one-year post-operative with healthy individual controls. Bilateral hip loading showed a decrease for pre and 12 months post-operative compared to healthy controls.

2.4 Hip Joint Contact Forces

The loading on the implants can be estimated by approximation of magnitude and orientation of hip joint forces (HJF). The HJF can further be used to define the edge loading risk in the preoperative planning process stages. The highest loads occur in the upright position during activities such as level walking, one-leg stance, stair climbing and jogging. (Bergmann et al., 2016). Joint contact forces can help to understand the function of normal and diseased joint, designing implants and rehabilitation treatments, evaluation of treatments, optimization of

performance and understanding progression of diseases. The gait cycle is normally used to calculate the joint contact forces as its regarded as one of the most frequent daily activities with high contact forces. There has also been a great interest in the muscles that contribute to distribution of loads in the hip joint. As knowing the contribution of individual muscle forces can help to reduce implant failure rates. Major group that contributes to distributing and stabilising the hip is abductors being the most influential muscle group.

2.4.1 In Vivo Studies

Joint contact forces have been measured with various activities and body joints with in vivo and modelling methods. Previous intensive studies have also been conducted by Bergmann et al. (1988) with in vivo data collection for various activities. Activity dependent hip contact force magnitudes and directions have been measured with nine instruments implants in seven patients for up to 9 years post-operative. Multichannel strain gauges were used to measure spatial hip contact forces in orthopaedic implants. (Bergmann *et al*., 1988) Furthermore, Graichen & Bergmann. (1991) also continued to work on four channel telemetry system used in in vivo hip joint force measurements which was used in later studies as well. These prostheses were first implanted in three patients that was used to measure different activities. Graichen et al., (1999) implanted protheses with sensors to measure joint contact forces and temperature along the entire length of the implant. Further studies on hip contact forces were also conducted with stumbling (Bergmann *et al*., 1993), stair walking (Bergmann et al., 1995a), load carrying (Bergmann *et al*., 1997) and effect of shoe and floor materials (Bergmann *et al.*, 1995).

A previous study conducted by Rydell (1966) with instrumented strain gauge prosthetics reported the forces at different speeds 0.9m/s to 1.4m/s with measured forces ranging between 1.59BW to 3.3BW.

Earlier studies conducted on hip joint contact forces show comparable results of muscle asymmetry being a possible factor to higher joint contact forces. A study conducted with two patients; Patient EB with bilateral replacement and Patient JB unilateral replacement and neuropathic disease. Force magnitudes in patient JB were higher than EB, which may be due to disturbed muscle function Patient EB had higher forces in the right joint compared to left

joint which may be a result of muscle asymmetry. Another reason could be the position of the right femur being more lateral and distal after the surgery. Muscle strength impacting the increase in joint contact forces has been identified by other literature as well.

A study conducted with 4 patients with unilateral surgery to measure joint loads in gait cycle. As observed in figure 1, contact forces are different in the four patients therefore individual muscle strength can impact joint loads. Average peak forces were between 211% to 285% BW similar to literature studies. Patient JB showed peak contact force at 409% during walking greater compared to the limits observed in the recent literatures. (Bergmann *et al*, 2001) Also indicating muscle dysfunction contributing to higher joint contact forces as joint moment substituted by other muscles with short lever arms hence, higher forces.

Figure has been removed due to Copyright restrictions.

Figure 7: Resultant HCF for 5 different patients for all cycles and average in normal walking -Reproduced from Bergmann et al. (2001)

Another study also showed the forces to be as high as 411% BW but in weight bearing exercises post-operative. This study was conducted to investigate the influence of weight bearing exercises on bone ingrowth. The initial phases of uncemented implants lacking stability, high loads may cause micromotions in the bone-stem-interface leading to

impairment of long-term fixation. Increased micromotion lead to decreased ingrowth into porous surface. The surface becomes dominated by the fibrous tissues instream od cancellous bone when the motion between the bone and implant increases.

Fatty degeneration indicated by fat ratio was present in all gluteal muscles and showed a strong correlation with forces during sitting down and standing up. Contralateral decrease in the lean muscle was also present indicating the impact by the unilateral hip implant. Direct lateral approach surgery leads to damage of gluteal muscle function. Tensor fasciae latae, gluteus medius and minimus are a part of the hip abductors that stabilise the hip joint during different movements. Atrophy of one muscle group can be compensated by hypertrophy of other part, also supported by the results of volume increases in tensor fasciae latae. Higher fat ratio can result in weakened gait cycle which corresponds to higher in vivo joint contact forces. High fat ratio has been clinically predicted to be a muscle function substitute probably by increasing stiffness of muscle hence, decreased forces. Joint contact forces can also be increased due to other muscle substituting for the impaired muscles. (Damm *et al.*, 2018)

Another similar study conducted with long term evaluation of the joint contact forces in THR patients compared to healthy individuals showed slower patients having lower contact forces. The hip contact forces also remained the same for both operated and non-operated hip throughout the gait cycle for both slow and fast speed walking. Measured Hip contact forces are also similar to the literature values. G Bergmann et al. (1993) showed peak HJF at 3.5BW at 0.83m/s. At faster walking speeds two studies have predicted first peak and second peak forces at 1.34m/s and 1.38m/s. First study estimated 4.3BW and 4.6BW while the second study showed 3.39 ± 0.45 BW and 4.61 ± 0.55BW. (O'Connor *et al.*, 2018)

2.4.2 Different Activities

Bergmann et al. (2004) conducted a study of the loads directions for stumbling compared to other activities. The data was collected with hip implants containing built-in sensors and telemetry. The results show the peak forces were twice a high for stumbling in comparison to other daily activities. The peak forces may be higher than 8.0BW. The direction of peak forces relative to the femoral bone show a constant trend with all the activities. Therefore, the muscle function and bone anatomy minimise the stresses created in the bone and muscle during different activities.

Table 2: Resultant peak HCF estimated by two studies; Bergmann et al. (2001) and Damm et al. (2018) for slow, normal, fast walking, stair up and down, standing up and sitting down.- Adapted from Bergmann et al. (2001); Damm et al. (2018)

Activity	**Peak HCF Range (%BW)**	
	Bergmann et al. (2001)	Damm et al. (2018)
Slow Walking	239 - 255	-
Normal Walking	211 - 285	209 - 301
Fast Walking	218 – 279	-
Up stairs	227 – 314	172 - 336
Down stairs	226 – 316	192 - 388
Standing up	182 – 220	109 – 277
Sitting down	149 – 199	103 - 355

Bergmann et al. (2001) conducted a study with 4 patients and Damm et al. (2018) study was conducted with 10 patients measuring in vivo HCF during different activities with instrumented hips (Table 2). Damm et al. (2018) load pattern for in vivo measured HCF show 2-peak profile for walking, stair up and down but one peak for stand up and sit down. Peak HCF for stair descend and ascend were for peak 2 were 2.56BW and 2.33BW respectively. Activities such as standing up and sitting down contributed to lower HCF of 1.95BW and 1.69BW, respectively. (Damm *et al*., 2018) The forces reported by both studies are within the similar range. The range reported by Damm et al. (2018) is wider for down stairs and standing up & down activity compared to Bergmann et al. (2001). This could be due to having a larger sample size of patients within the Damm et al. (2018) study. Also, Damm et

al. (2018) was conducted 3 months post THA whereas Bergmann et al (2011) were taken between 11 - 31 months post THA. However, one of the patients in the Bergmann et al (2011) had a replacement on the contralateral hip 10 years earlier.

Further recent studies with hip and knee joint loading have been conducted during vertical jumping and push jerking with musculoskeletal model. (Cleather *et al*., 2013) The study has measured peak loading forces in knee joint (6.9 -9.0BW), angle joint (8.9 -10.0BW) and hip joint (5.5 - 8.4 BW).

Other activities such as cycling has also been included in studies regarding hip joint loads. The study measures the cycling in vivo hip contact forces and pedal forces. The loads were measured in five patients with instrumented protheses. The results showed a strong correlation between joint loads & pedal forces and power. (Damm *et al*., 2017)

2.5 Musculoskeletal Modelling

Musculoskeletal Models (MSM) has been an increasing method to study joint mechanics in the recent years. It allows patient-specific models for approximation of individual HJF for daily activities. Musculoskeletal models have been used in studies for physiological loading, wheelchair propulsion, ergonomic evaluation and design optimization. (Weinhandl *et al*, 2019) Hip joint contact force studies have been conducted with various methods and daily activities. The loading on the hip joint can impact the bone structure and density. (Vainionpaa *et al*, 2007). Excessive hip joint contact loading may influence development of osteoarthritis in healthy individuals. (Felson, 2013). Although various in vivo studies have been conducted to measure the internal joint contact forces, it is difficult to achieve due to practical and ethical reasons. (Weinhandl *et al*, 2019) In vivo hip contact and muscle forces have been measured for THA patients through instrumented prosthetics in small sample size. (Bergmann *et al*, 2001, Bergmann *et al*, 1993, Schwachmeyer *et al*, 2013, Damm, 2010) Due to difficulty of in vivo measurements, musculoskeletal models have been developed to measure hip contact forces. Several studies have been conducted using three-dimensional modelling techniques of lower limb muscle forces. This method is non-invasive and can be performed without medical imaging therefore reduced subject risk and financial costs. (Weinhandl et al, 2019). This method also allows the study of normal healthy subjects as its

not available with in vivo studies. Technical problems with in vivo implants have also been encountered. Modelling also may be used for investigating the impact of different surgical methods on the joint contact forces with validated models. (Brand *et al*., 1994)

Musculoskeletal modelling software such as OpenSim (Delp *et al*., 2007) and AnyBody (Damsgaard et al.,2006) are widely used in studies for estimating joint contact forces. Wagner et al., (2013) reported that simple scaling was not sufficient to produce consistent muscle and knee joint contact forces between models. The consistency of various software models studies has been an ongoing research, but validation still remains unknown. Although some models such as Heller et al., (2001) and Modenese et al., (2011) have been backed up by results from instrumented prosthetics.

OpenSim is an open source software used to model and study neuromuscular coordination, musculoskeletal internal loading and performance of athletes. It can provide information to further assist in developing implants and treatments for disease such as osteoarthritis. (Delp *et al*., 2007) Anybody can be used to analyse musculoskeletal system of humans or animals. The models allow to provide boundary conditions through management of external objects, loading and motion specifications. (Damsgaard *et al*.,2006).

2.5.1 Lower Limb Modelling

Lower limb modelling has been studied with mainly knee and hip joint contact forces. Some studies use subject-specific models and use in vivo data to validate the estimate hip joint contact forces. Modenese et al., (2012) used in vivo contact forces from previous study conducted by Bergmann et al., (2001) with 4 patients with instrumented prosthetics. The musculoskeletal models were more accurate for slow speed walking. Although the study does suggest improving the geometrical modelling of gluteal muscles. Estimated of the hip contact forces require increase in accuracy of muscle layers. (Modenese *et al*., 2012)

Study by Heller et al. (2001) also attempted to validate the musculoskeletal model forces with in vivo hip contact forces. The cycle to cycle validation of the patients with THA showed a difference of 12% during walking and 14% during stair climbing. The study does have limitations as the musculoskeletal model has not been described accurately. Therefore, this

study can't be used to analyse the in vivo and model hip contact forces as it does not provide a valid comparison.

Similar earlier study has been analysed in vivo and musculoskeletal model forces in the same patient. There have been assorted studies conducted with mathematical models and instrumented implants. The estimation of mathematical models has consistently higher compared to instrumented implants also shown by the results in this study. The study does have limitations that have been discussed in the recent studies as well. The high measured forces by the model have been accounted for the physiological absence of muscle force boundaries i.e. max isometric forces. The study does state that the solutions may be more realistic if the unphysiological muscle forces are disallowed. (Brand *et al*., 1994). This is not an accurate study to validate the comparison as it didn't directly compare hip joint contact forces of measured and calculated at the same instant.

Musculoskeletal modelling studies has also been conducted with healthy individuals to calculate the hip joint forces at different speeds. The resultant second peak hip contact forces calculated for slow, normal and fast speeds were 4.41 to 4.61BW and 4.88 BW, respectively. While the second peak vertical hip contact forces were measured between 3.72 to 4.12 BW for slow and fast speeds. (Weinhandl *et al*., 2017) In comparison to similar studies conducted the forces measured in this study varied significantly based on sample size and methodology. Crowninshield et al. (1974) has reported similar calculated values for normal healthy subject of 3.3 to 5BW. The forces calculated with in vivo prosthesis by Rydell (1966) were lower (1.6 to 3.3BW) than calculated in this paper. The paper states that the calculated forces are consistent with Rydell's data as the forces in pain-free subjects are expected to be greater compared to prosthetic joint with reduced floor reaction forces. Studies conducted by Bergmann et al. (2001) also show the contact forces within the range of Rydell (1966).

Giarmatzis et al. (2015) shows higher forces compared to Weinhhandl et al. (2017) study. First peak 4.22 to 5.41BW and second peak between 4.37 to 5.74BW with speed ranging from 3 to 6km/h. This may be accounted for due to the methodology changes in Giarmatzis et al. (2015) study. The increased hip joint forces in Giarmatzis et al. (2015) may be due to additional muscle force distributed to gluteus medius as high hip abduction reserve actuator torque was indicated. (Weinhandl *et al*., 2017). However, the hip joint forces in both studies are higher than direct measured (Bergamnn *et al*., 2001) and estimated forces in older

subjects (Heller et al., 2001, Modenese et al., 2012). Although these studies also have discussed limitations for their estimation.

Heller et al., (2001) analysed hip loading during walking and stair climbing also similar to a study conducted later by Modenese et al., (2011). The patients used in study Modenese et al., (2011) has been previously studied by Heller et al. (2001) and subjects S1 and S2 Stansfield et al. (2003).

2.5.2 Muscle Asymmetry Studies

One of the few studies conducted with studying the impact of hip muscle weakness on the HCF were conducted by Valente et al., (2013) as a problematic failure analysis. The muscle asymmetry was introduced to gluteus medius, minimus and tensor fascia latae with different combinations of weakness. Latin hypercube sampling technique was used as a strategy to introduce the different combination between the abductor muscles of uniform weakness. Similar study conducted by van der Kroght et al. (2012) introducing muscle weakness to the muscles in healthy subjects for failure analysis. The muscle asymmetry was induced in gluteus medius, plantar flexor (gastrocnemius and soleus) and iliopsoas (iliacus psoas major). The asymmetry was introduced linearly from 0 to 100% with 20% increments for each model.

Most of different weakness combinations in Valente et al (2013) study were able to run due to muscle compensation (Thelen and Anderson, 2006). The unsuccessful kinematics for few weakness variation models were due to significantly high weakness. Van der Kroght et al. (2012) also had comparable results with models up to 80% to 100% weakness of individual or muscle groups were able to sustain the forces and normal gait kinematics. Weakness in the hip abductors, plantar flexors and hip flexors contributed to the greatest impact on the gait due to weakness could only be tolerated to a limited extent. Hence, lead to increased total muscle cost (capacity) due to other muscles compensating. Weakness may also result in patients altering their gait pattern to avoid overloading the affected hip therefore no compensation occurs. (van der Kroght *et al*., 2012)

Valente et al. (2013) and van der Kroght et al. (2012) both have focused on a common abductor muscle; medius and healthy young subjects. Also, both studies used OpenSim software and introduced asymmetry through maximum isometric forces but with different muscle groups.

2.6 OpenSim

OpenSim is an open-source musculoskeletal modelling software used to estimate resultant HCF and muscle forces. The software enables the development, analysation and visualisation of musculoskeletal system models. The models consist of joints connected to rigid body segments. These joints are spanned by the muscles and generate forces and motions. Musculoskeletal models in OpenSim have implemented Hill-type model that represents the physiological muscle-tendon unit (MTU). The software allows users to create custom studies to investigate the impact of musculoskeletal geometry, joint kinematics and muscle-tendon properties on the forces and joint moments produced by the muscles. (OpenSim, 2019)

2.6.1 Hip Replacement Modelling

Weinhandl & Bennett (2019) investigated four models generic and subject-specific models; gait2392 & Arnold Lower Limb Model and hip2372 & London Lower Limb, respectively. Data for the models was taken from Bergmann et al., (2001) study for subjects with instrumented prothesis. The study mainly focuses on the discussion of push-off peak error for the four models, but the results have been collected for hip contact forces. The Lower Limb Model estimated peak push-off forces with lower magnitude and timing error in contrast to the other three models. Hence, the Lowe Limb Model has been classified the most suitable for investigations as hip contact forces closely matched the in vivo data. The study does suggest an improvement of including individual muscle weighting values in the object function.

Modenese et al., (2011) used lower limb model (HIP98) from OpenSim to investigate the validation of hip contact force results with previous in vivo data. The study evaluated the muscle force impact on hip contact forces and muscle force estimation through a mathematical model. Power *p* of muscle synergism is changed which influences the load sharing hence, the muscle activation between recruited actuators is changed. The study further compares the EMG data that has been previously collected by Wootten et al.(1990). Agreement between EMG measurements and muscle forces has been validated to evaluate muscle force estimations.

Skalshøi et al. (2015) investigate hip contact forces and walking patterns using OpenSim model. The difference between this and other studies analysing hip contact forces is that the patients had hip dysplasia. The study found an increased hip abduction and external rotation torques. Although this study has not been conducted with OA patients but uses the same modelling methodology to calculate hip contact forces. The study further discusses the limitations of the method of different walking speeds of patients and controls. This could impact the hip contact forces due to pain caused by pressure therefore further investigation is required.

Wesseling et al. (2015) conducted a study with OpenSim model evaluating four different optimization techniques to calculate muscle forces. The optimization method computed muscle control (CMC) created the highest forces while SO2 created lower forces. The comparison with instrumented prostheses hip contact forces by Bergmann et al. (2001) were lower than values calculated with all optimization techniques. The overestimation from the modelling may be due to the different parameters before the optimization stages such as attachment points, number of muscles and muscle parameters. Therefore, the study suggests further research into the modelling techniques and the influence of different parameters on data. Other similar studies (Heller et al., 2001, Modenese and Phillips, 2012 and Stansfield et al., 2003) have calculated hip contact forces closer to the reported values but using different modelling software or methods.

2.6.2 Subject-Specific Modelling

Lenaerts et al. (2008) has calculated hip contact forces by a sensitivity analysis and 20 subjects with OA pre-operative. The first part of the study involved analysing effect of femoral neck-length (NL) and neck- shaft angle (NSA) on muscle activation and hip contact forces at the stance phase. Second part of the study included introducing abductor weakness by halving the maximal hip abductor force gluteus medius, minimus and tensor fasciae latae. The results show the contact forces were not affected due to the 50% weakness. However, the muscle activations increased in order to achieve the normal hip abduction moment. Although, differences in NL (41-74mm) and NSA (113 – 140 degrees) changed the hip contact forces by up to 3.0BW.

The hip contact forces can be greatly impacted by the scaling techniques used for subject-specific data. Previous studies (Bergmann *et al*., 2001) have shown an overestimation through modelling compared to in vivo data. Study conducted by Correa & Pandy. (2011) with two analysis; development of a method for scaling peak isometric muscle forces and determine effect of scaling method on muscle forces for normal gait cycle. The muscle size was measured through MR imaging to calculate the maximum isometric forces. There have been previous scaling methods with simple allometric laws in order to scale the isometric forces. Linear regression method has been used by some studies (Folland et al., 2008; Jaric, 2002) but assumption for equal growth rates for all muscle are present.

Folland et al., (2008): $\ln(y) = \ln(a) + b\ln(x)$
Jaric, (2002): $Log\ S = Log\ a + b \log m$

The Correa & Pandy. (2011) study has constructed a new method of scaling. l_{MT}^{scaled}represents muscle-tendon length calculated in the reference position and M^{scaled} represents total body mass for the scaled model.

Equation 1: Maximum isometric force scaling equation for subject specific forces

Figure has been removed due to Copyright restrictions.

The study found that body mass displayed a strong relationship with muscle volume. Although there are limitations to the study of only assessing 10 subjects and assuming bilateral symmetry as right leg muscle volume was applied to both legs.

Giarmatzis et al. (2015) study also using OpenSim model with 20 young healthy subjects. The method included application of Kalman smoothing algorithm to calculate the joint angles during movement. Weinhandl et al., (2017) also conducted a similar study with 10 healthy subjects, collecting EMG data with surface electrodes placed on lower limb muscles. Second peak of resultant hip contact forces ranged between 4.41 to 4.88 BW between slow to fast speeds. Giarmatzis et al. (2015) second peak range was higher between 4.22 to 5.74BW for slow to fast ranging speeds. This slight difference can be accounted by different

methodologies as Giarmatzis et al. (2015) showed larger hip abduction reserve actuator torque due to additional muscle force production by gluteus medius. Studies that used musculoskeletal modelling approach to predict contact forces showed slight variation between using Anybody and Opensim software. (O'Connor *et al.,* 2018)

2.7 Discussion

Recent studies conducted have overcome the limitations of earlier musculoskeletal modelling studies but still have limitations of measuring HCF. O'Connor et al. (2018) study discusses limitation around modelling the musculoskeletal model including isotropic scaling. Previous studies have used similar scaling and location of gait markers but can result in misplacing the joint centres. (Nolte *et al.*, 2016; Oberhofer, Lorenzetti and Mithraratne, 2019; Suwarganda *et al.*, 2019) Post THR the hip joint centre (HJC) location is often moved. Previous studies have also suggested to find the location of the joint using medical imaging or function method. (Zhang, Malcolm, *et al.*, 2014; Zhang *et al.*, 2016; Bahl *et al.*, 2019) Shift of the location does not significantly change the HCF magnitude, but it does affect the orientation of the force.

Wesseling et al. (2018) also suggests similar limitations of using generic musculoskeletal model. This study used generic scaled modelled due to absence of medical imaging compared to previous studies that used subject-specific models. There is a difference between measured hip contact forces of 0.47BW at the second peak. Most recent study by Peiri et al. (2019) also identified a limitation of generic scaled model with certain level of errors due to absence of subject-specific bone geometry and muscle physiology information.

Several studies discuss limitations of the method including the non-randomized sample size (Winther *et al*., 2016) and gait speed of OA patients. Louriero et al, (2018), identified OA patients exhibited lower hip joint loading and mechanics over reduced range of hip motion walking at their preferred speed compared to healthy control participants. The study needs to be conducted with larger sample for validation of two subgroups; unilateral and bilateral participants. Zacharias *et al*., (2016) study doesn't separate the fatty infiltrate and muscle volumes for analysing. Although some studies have overcome this limitation by segmenting fatty infiltrate of hip abductors, but the methodology has not been validated.

Kovalak et al. (2018) study reported the degree of FA on the operated side was not correlated to older age. However, this study contradicts as several studies reported the influence of age on FA. (Muller et al. 2011).

2.8 Conclusion

As seen in previous studies where muscle asymmetry is present in OA due to atrophy and fatty infiltration. (Arokoski *et al.*, 2002; Madsen *et al*., 1997; Rasch *et al*., 2007; Suetta *et al*., 2004; Loureiro et al., 2018; Zacharias et al., 2016) The scaling does not account for the asymmetry and this has been identified by various studies to conduct further research into muscle asymmetry.

The hip replacement prosthetics are designed with generic data collected from a group of healthy individuals but due to OA patients lose muscle and therefore affected HCF, the design of the prosthetics may not be valid. Although the study by Lenaerts, (2008) showed no change in the HCF through reduction of abductors muscles but the study did not specify whether there was an asymmetry introduced. Most studies also suggest to further look into muscle atrophy and asymmetry.

Although few studies have been conducted with introduce muscle asymmetry. A recent study has investigated it but within vivo prosthetics. (Damm et al, 2019) Furthermore, hip muscle asymmetry has been studied but with healthy subjects where walking symmetry is present. Mostly HCF have been calculated with in vivo after THA but limited data is available with a small sample size. Most musculoskeletal models only include generic scaled models which don't account for muscle asymmetry or subject specific geometry within OA population. There hasn't been a validated OpenSim scaled subject specific modelling technique to measure the HCF with introduction of muscle asymmetry. Although previous studies have validated their subject specific models with in vivo data.

As the studies show that muscle asymmetry can be present due to unilateral OA but does not further investigate the effect on the HCF. This study investigates the effect of creating the

muscle asymmetry on HCF and individual muscle forces through changing the max isometric force as it is directly proportional to the cross-sectional area in an OpenSim model.

Chapter 3

3 OpenSim Musculoskeletal Modelling

3.1 Introduction

The HCF and muscle forces were predicted using musculoskeletal modelling software; OpenSim 4.0. The main steps followed within the OpenSim were scaling, inverse kinematics, static optimization and analyse (Figure 9). Musculoskeletal models in OpenSim have implemented Hill-type model that represents the physiological muscle-tendon unit (MTU).

3.2 Data Collection

All the data used in the present study was collected as a part of a previous study (Bahl *et al*., 2019) for six patients awaiting for surgery for primary THA. 12 surface markers (12mm diameter) were place on the anatomical landmarks of the pelvis and lower limbs. Each thigh and shank were strapped with a cluster of four markers. Static trail pose was recorded for measurement of surface landmark positions. The dynamic data was captured with multiple walking trails on self-selected gait speed. The marker trajectories were captured using 10 Vicon V5 cameras (Vicon Motion Systems, Oxford, UK) at a frequency of 100Hz. Force plate data was collected using 4 plates in some trails while 2 plate in others. The data was visually assessed using Mokka (Version 0.6, Biomechanical Toolkit). (Barre and Armand, 2014) The raw static and dynamics data for six patients was manipulated with MATLAB into

appropriate files by Bahl et al., (2019) as well in order to be used in OpenSim for different steps (Figure 8).

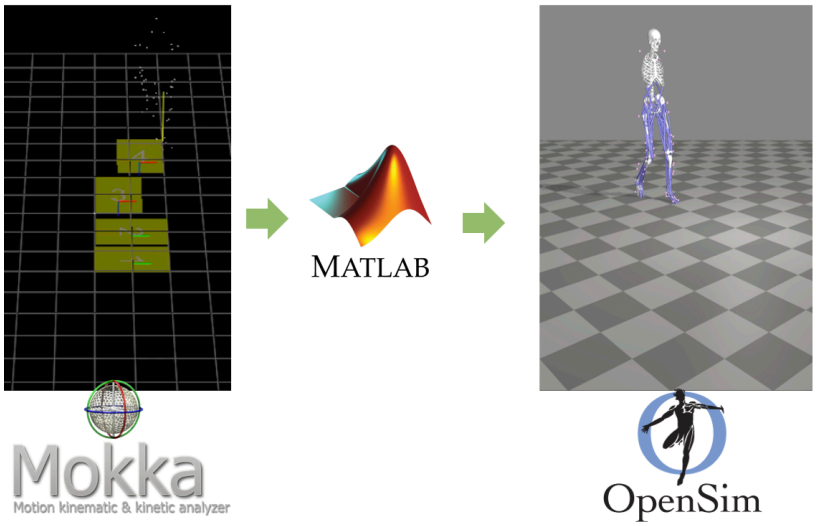

Figure 8: Kinematics and force plate data manipulated with Matlab to .trc and .mot files to be processed in Opensim

3.3 Subject Specific Maximum Isometric Force Scaling

Subject specific scaling is important as many several studies have shown that force predictions are sensitive to parameters such as optimal fibre length and tendon slack. (Heinen *et al*., 2016). Patient characteristics can strongly influence the HCF therefore subject-specific modelling is important and crucial step in the process for accuracy results. (Pieri *et al*., 2019). The maximum isometric force that is directly proportional to physiologic cross-sectional area (PCSA) is also affected by the subject specific scaling. (Morl *et al*., 2016, Groote et al., 2010, Scovil *et al.,* 2006 and Redl *et al*., 2007). Scaling step changes the model anthropometry to match the subject as much as possible through comparison of experimental and virtual marker data placed on the model (Section 4.2).

Equation 2: Linear scaling ratio for maximum isometric forces with generic model (G) and subject specific (SS) height and weight. The calculated scaling ratio was used to determine maximum isometric forces for muscles in each patient.

$$\frac{G_{Height} * G_{Weight}}{SS_{Height} * SS_{Weight}} * \text{Maxium Isometric Force}$$

The scaling of maximum isometric force was altered using a linear ratio with subject and generic model (OpenSim model) (Equation 2). The scaling ratio used is linear scaling as it is one of the common methods and also used in a previous study. (Ng *et al.*, 2018) This linear scaling ratio has been used for the present three phase study for subject specific maximum isometric forces to reflect each patient's maximum contractile force.

3.4 Gait Simulation

The main procedure followed to predict resultant HCF and muscle forces has been outlined in the flowchart (Figure 9).

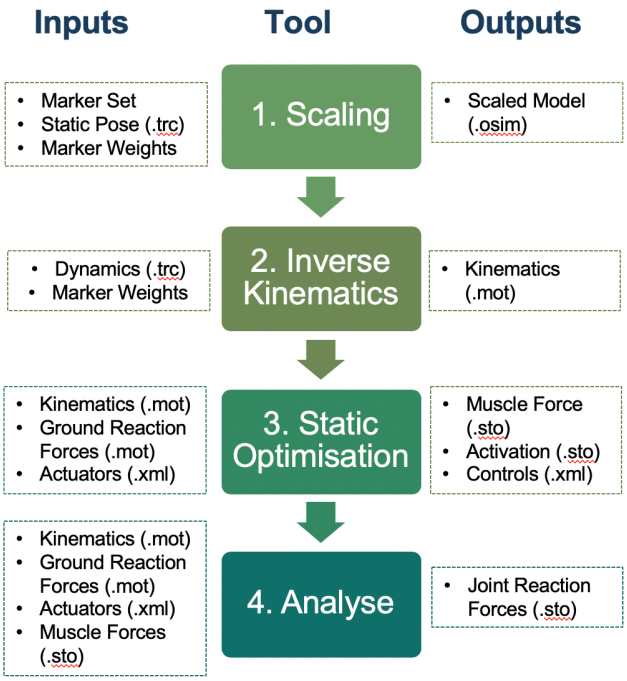

Figure 9: Overview of the workflow procedure for musculoskeletal modelling conducted to obtain HCF and individual muscle forces. The steps used were scaling, inverse kinematics, static optimisation and analyse tools within OpenSim.

The musculoskeletal model was scaled to the subject specific sizes with anatomical landmarks and functional joint centres. Inverse kinematics was used to reproduce gait patterns through tracking patient marker trajectories and obtain joint angles. Computed muscle control (CMC) designed by Bahl *et al*. (2019) was used in static optimization to estimate the muscle forces and activations. There were no constraints applied on the muscle

activations therefore any activation pattern could be taken by the patients. The resultant and directional HCF are predicted with CMC actuators in analyse tool. (Ng *et al.*, 2018; O'Connor *et al.*, 2018)

3.4.1 Scaling

Scaling was implemented on the model through combinations of measured distances between the marker locations (x-y-z) and specified scale factors of the subject. The scale factors were calculated based on the distance between experimental markers and virtual markers. The scaling factors can be defined through the measurement-base scaling or manual scaling procedures. The marker locations were obtained during the data collection through motion capture (Section 3.2). Virtual markers on the unscaled model were placed in the same anatomical locations as the experimental markers. The marker locations were used to scale the dimensions of segments to match the subject. (Delp *et al.*, 2007; Valente *et al*., 2013)

The scaling tool is a multi-stage process involving:

Step 1: Computing scale factors

1. Measurement based scale factors were computed by comparison of experimental and virtual markers. One scale factor can be computed using one or multiple marker pairs.
2. Manual scaling factors were specified for segments if they are known or determined using alternative algorithms.

Step 2: Scaling model geometry

3. The computed or manually defined scale factors were used to scale joint frame locations, mass centre location, force application points as well as muscle attachment points. Positions were scaled using the scale factors for the corresponding body as each object is defined in a specified body frame.

Step 3: Scaling mass and inertial properties

4. Segment masses were scaled using the previously scaled factors, target massed and preserve mass distribution.

Step 4: Scaling muscle and length components

5. Components involving length and distance such as ligaments and muscle actuators were scaled. Furthermore, a scale factor ratio was computed based on

length prior to scaling to the length after scaling. The resultant ratio was used to scale length dependent properties of the components.

The maximum isometric forces computed using the linear scaling ratio (Equation 2) were manually modified in the XML file of the scaled model.

3.4.2 Inverse Kinematics

IK step was implemented with the same marker weights and scaling factors as the previous scaling step. Each time frame in the experimental data (dynamics) was stepped through by the IK tool to position the model to best match the experimental markers and coordinate data for every time step. The best match pose was critical to minimise sum of weighted squared errors of markers and coordinates. The IK tool computes generalised coordinate trajectories (joint angles and translations) in motion file. (University Standford, 2013; Valente *et al.*, 2014)

3.4.3 Static Optimization

SO computed the individual muscle forces in each time frame by minimising the sum of squared muscle activations. The tool used the known motion defined by positions, velocities and accelerations to solve the equations of motion for generalised unknown forces. The ground reaction forces captured from the force plates were associated to the right and left foot applied to the calcaneus expressed in the ground. CMC files computed previously (Bahl *et al*., 2019) were added to append forces. (Valente *et al.*, 2014)

3.4.4 Analyse

Analyse step was used to compute hip joint reaction loads (hip contact forces) between the femur and pelvis. The CMC and external loads applied were same as SO step as well as individual muscle forces computed by SO. The reaction loads were calculated as forces and moments required to constraint the body motions for joint satisfaction. The joint centres for both hips were defined as parent and child bodies. (Valente *et al.*, 2014)

3.4.5 Data Analysis

The HCF converted into Body weight (BW) and used available muscle maximum isometric force capacity percentage also known as muscle cost (force capacity) were computed for all patients. All the calculations for both equations were done using excel or MATLAB for all patients for tabulated and graphed results. All patients were analysed for the full gait cycle for both hips. Throughout this present study, patient's used force of the potentially available maximum isometric force was referred to as force capacity.

Equation 3: Body weight (BW) calculation for patient HCF with gravity and patient weight

$$BW = \frac{Hip\ Joint\ Contact\ Force\ (N)}{Patient\ Weight\ (kg) * 9.81\ (N)}$$

Equation 4: Used muscle force predicted by SO of the available maximum isometric force percentage (capacity %) or muscle cost percentage

$$Capacity\ \% = \frac{Muscle\ Force\ (N)}{Maximum\ Isometric\ Force\ (N)} * 100$$

Chapter 4

4 Study One: Linear Scaling Versus Statistical Shape Scaling

4.1 Introduction

Mathematical models have become a common way to analyse HCF in patients due to being complex and too invasive to be measured using in vivo methods. It is fundamental method to study the joint function, injury and diseases such as hip OA. However, every musculoskeletal model holds uncertainty due to various parameters associated with subject specific scaling. (Valente *et al.*, 2014; Navacchia *et al*., 2015) Studies have shown scaling step is very critical aspect as factors such as determining the location of the HJC, optimal fiber length and tendon slack length can propagate into the muscle forces and HCF calculations. (Scovil and Ronsky, 2006; Navacchia *et al*., 2015; Carbone *et al.*, 2016) Generally models are altered from generic to subject-specific by linear scaling of segment anthropometries. (Kainz *et al.*, 2017; Ng *et al.*, 2018; O'Connor *et al.*, 2018; Bahl *et al.*, 2019) Studies have shown this method is not appropriate for OA patients, obese and elderly subjects. Statistical shape modelling has been predicted as a solution for increasing the accuracy in capturing the anatomical and geometrical variations. (Zhang *et al.*, 2016)

The objective of this phase was to test the impact of different scaling methods and maximum isometric forces on the resultant HCF and individual muscle forces within two similar models. This study will use two models; statistical shape scaled model (Bahl model) developed in a previous study (Bhal *et al*., 2019) and OpenSim lower limb extremity (gait2392 model) (Delp *et al*., 2007; Delp *et al*., 1990). The aim of this study was to conduct a sensitivity test on the influence of scaling factors and select one model for the asymmetry modelling.

4.2 Methodology

There were two models evaluated in study one; gait2392 and Bahl model. This study was only conducted with Patient009 RH with different maximum isometric forces for gait2392 and Bahl Model (Table B.1). Bahl model was developed as a part of previous study with subject-specific scaling step fully conducted with predefined maximum isometric forces by Bahl et al. (2019). The differences between the two models were the scaling methods of skeletal anatomical sites and maximum isometric forces. The Bahl model's maximum isometric forces approximately 3 times higher for every muscle compared to the Gait2392. For both models HCF and individual muscles forces were predicted by following IK, SO and analyse steps (Section 3.4.2-3.4.4). However, gait2392 was scaled from generic to subject specific model (Section 3.4.1) but Bahl model was already scaled (Figure 10).

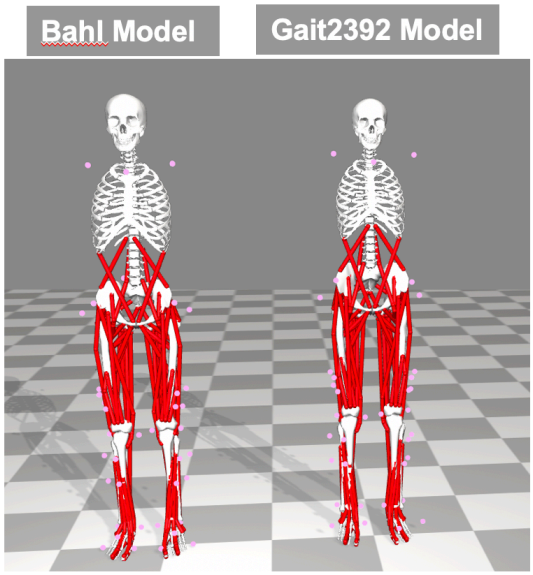

Figure 10: Scaled Bahl model and gait2392 model in OpenSim

4.3 Bahl Model – Statistical Shape Scaled Model

Shape Modelling and PC Fit

Bahl model was designed with statistical shape modelling by Bahl et al. (2019) where the HJCs from shape modelling, functional and regression methods were implemented into the OpenSim gait2392 model (Delp *et al.*, 2007; Delp *et al*., 1990). The Musculoskeletal Atlas Project client (MAPClient) was used for morphing individualised meshed for every patient. (Zhang *et al.*, 2014b) Experimental motion capture trail was used to register the anatomical landmarks to the pelvis, left and right femurs, tibias, fibulas and patellae in the shape model. Patient's bone shape and size was captured by rigid-body translation, rotations and deformations along the PCs in the registration.(Zhang *et al.*, 2014a; Zhang *et al.*, 2016) Furthermore, the model pose was set by attaching the experimental landmarks to the anatomical landmarks located on the pelvis, femurs and tibias.

Shape Modelling and PC Fit with Medical Imaging

The shape modelling + PC fit was used for further morphing in order to segment pelvis surface using the computed tomography (CT) images data. The CT data was also collected by Bahl et al. (2019) of full pelvis in a supine position using dual-energy Siemens SOMATOM Definition Flash (Siemens, Erlangen, Germany). Segmentation of the pelvis 3D geometry using semi-automatic threshold-based approach in the ScanIP module (version 5.0, simpleware UK). Smoothing to the reconstructed 3D surface model was applied by a recursive Gaussian Filter.

CT data was used to further modify the shape modelling and PC fit:

1. Alignment of morphed pelvis mesh to target segmented pelvis
2. Host mesh fitting: non-rigid morphing of pelvis mesh to target point cloud
3. Mesh integrity maintained by host mesh constraining the deformations of pelvis mesh
4. Distance between pelvis mesh and target minimisation by least-squares optimisation

5. RMS error reduction between source and target points through host mesh iterations
6. Pelvic mesh fine-scale fitting to remove host mesh constraint for independent adjustment of pelvis mesh control points.

Scaling was implemented by using virtual makers to match the experimental markers and manually defining the scale factors and weights. Furthermore, HJC location and estimation was conducted by Bahl et al. (2019) as well. Segmented acetabulum using CT data was fitted by centre of sphere least-squares-fitted to define the HJC for the reference. For the shape model, centre of least-squares sphere-fit to the acetabular vertices of shape model mesh was calculated.

4.4 Gait2392 – Linear Scaled Model

Gait2392 model was an open source with 23-degree-of-freedom, 92 musculotendons actuators representing 76 muscles in the lower extremities and torso modelling the ball and socket joints. (Delp, 1990) The general unscaled model had a height of 1.8m with 75.16kg weight. The virtual marker sets used in present study were from a previous study used to validate musculoskeletal models (Correa *et al*., 2011) and scaling marker weights were not modified. Scale factors were computed automatically by the scaling tool (Section 3.4.1). The maximum isometric forces were also predefined in the model that were further scaled for patient009 RH.

4.5 Data Analysis

The analysis for this phase was based on the HCF and individual muscle forces for the two differently scaled models. The comparison was conducted between the peak gluteal minimus and medius forces as well to evaluate the difference between the forces. The data was evaluated on the right hip which was the contralateral hip (unaffected). The stance phase (60%) of the gate cycle was analysed. The data was processed in excel and plotted in MATLAB (Section Data Analysis MATLAB).

4.6 Results

The gait2392 and Bahl model followed the same general trend in the predicted forces with two peak profile. The first peak was very similar force prediction however, Bahl model predicted slightly higher forces for the second peak. Furthermore, there was a spike present in the Bahl model at 95% of the stance phase. The results showed the Bahl Model (6.58 BW) having a higher HCF compared to the gait2392 (3.26 BW) model with linear scaling (Figure 11). The Bahl model has a high peak contributing to the higher force at the end of the stance phase. Neglecting the random spike as an outlier or error in the modelling reduced the HCF (4.34 BW).

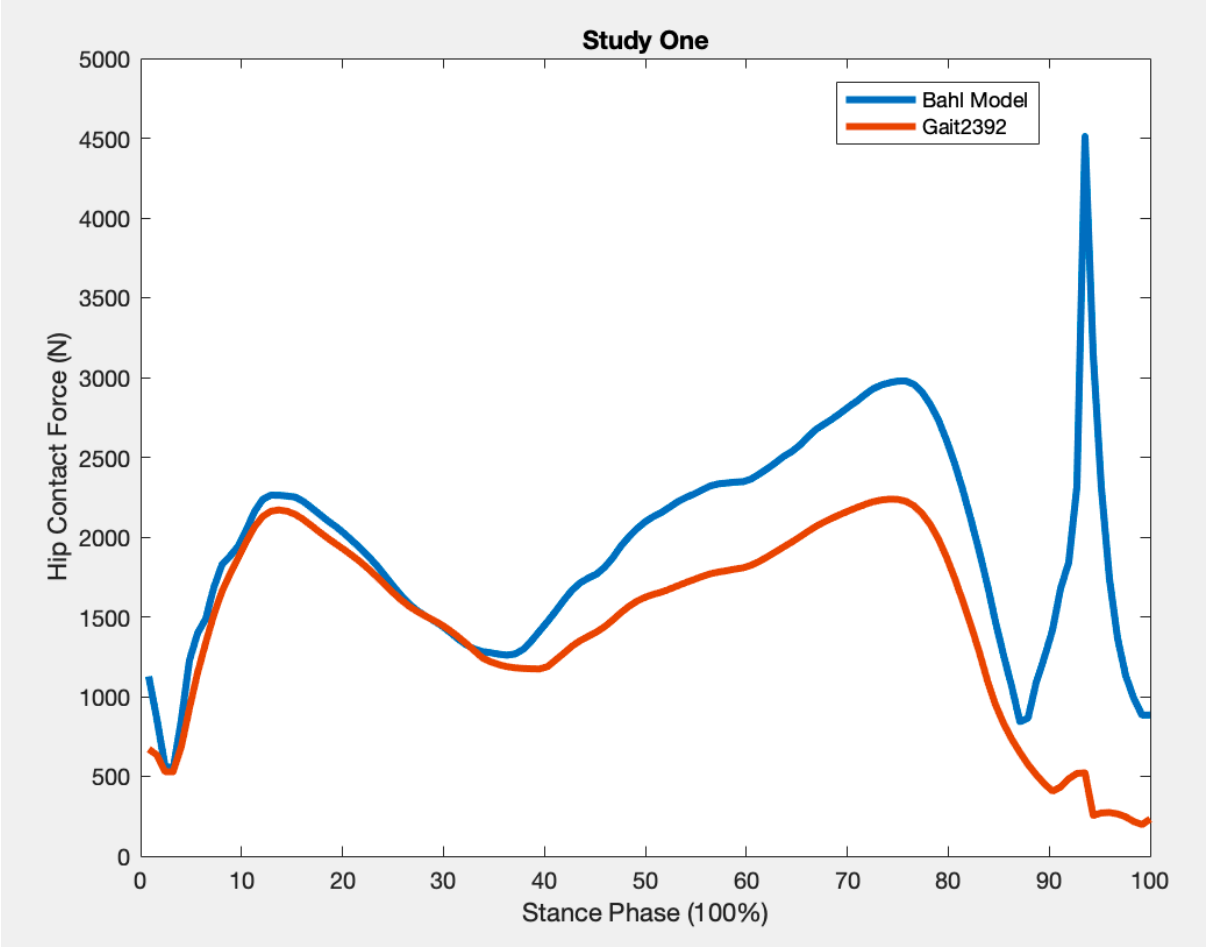

Figure 11: Resultant HCF for Bahl model (blue) and gait2392 model (red) over the 100% stance phase for linear vs statistical shape scaling.

The primary flexors and internal extensors muscles were the major groups that resulted in high peak force in the Bahl model. Resultant muscles forces such as iliopsoas, rectus femoris

and quadratus femoris were as high as of the gait2392. Individual muscle forces showed random spikes occurring in the stance phase at various locations in the Bahl model. (Appendix B). The gluteus medius and minimus muscle capacity was approximately 3 times higher for gait2392 compared to the Bahl model (Table 3). However, the muscle forces were similar for both medius and minimus for both models. This was also the case with the maximum isometric forces difference between the two models (Appendix B).

Table 3: The muscle capacity (%) and muscle forces (N) for gluteus medius and minimus for gait2392 linear and Bahl model for linear vs statistical shape scaling.

Model	Gluteus Medius		Gluteus Minimus	
	Capacity (%)	Force (N)	Capacity (%)	Force (N)
Bahl	15	785	7	156
Gait2392	52	620	26	132

4.7 Discussion

Study one was conducted to analyse the impact of different scaling methods on the resultant HCF. The percentage of the force capacity reached by gluteus medius and minimus was also evaluated. Furthermore, the individual muscle forces were also compared to analyse the difference between the two models.

The resultant HCF from both models were similar therefore the maximum isometric forces didn't significantly influence the resultant HCF. Musculoskeletal modelling reported forces by previous studies for healthy subjects ranging between 3.0 to 6.0BW. (Weinhandl *et al*., 2017, Giarmatzis *et al*., 2015, Crowninshield *et al*., 1974) were within the range for gait2392 and Bahl model HCF as well. The force capacity for the Bahl model was lower for the medius and minimus due to the assumed maximum isometric (contractile) force of individual muscles being set extremely high. While, muscle forces (Table B.1) for both models were similar however, spikes were present in some muscle in the Bahl model.

Both models were appropriate for this study however, Bahl et al. (2019) reported statistical scaling using shape modelling + PC fit with medical imaging produced considerably closer predictions of the HJC location in comparison to the linear scaling methods. Also, Bahl et al.

(2019) study further showed conventional HJC estimation for linear scaling of the pelvis in modelling is not appropriate for larger BMI and limited hip ROM patients. Furthermore, previous studies reported statistical shape scaling and medical imaging of the anatomical sites was more accurate for musculoskeletal modelling. (Nolte *et al.*, 2016; Oberhofer, Lorenzetti and Mithraratne, 2019; Suwarganda *et al.*, 2019)

The Bahl model with statistical shape scaling was evaluated to be the most applicable choice for this study. Even though the forces for Bahl model were slightly higher but that was greatly impacted by maximum isometric forces set high. As level gait is sub-maximal task in normal healthy individuals in which muscle maximal isometric forces are not likely to be reached hence, it is not critical to define their boundaries. However, in pathological situations such as hip OA where muscle weakness is present, this may result in a significant impact on the individual muscle force and resultant peak HCF. (Arokoski *et al*., 2002; Madsen *et al*., 1997; Rasch *et al*., 2007; Suetta *et al*., 2004; Loureiro *et al*., 2018; Zacharias *et al*., 2016) However, since present study involves introducing abductor muscle weakness, it may impact the forces more significantly. Therefore, further study was needed to assess the impact of different maximum isometric forces reported by previous literature.

Chapter 5

5 Study Two: Influence of Maximum Isometric Forces on the Resultant HCF and Individual Muscle Forces

5.1 Introduction

In study one, significant variation was observed in maximum isometric forces for the muscles. Therefore, impact of maximum isometric forces on the resultant HCF needed to be further studied. Hence, the aim of study two was to assess the influence of maximum isometric forces on the resultant HCF and muscle forces using the Bahl model (Section 4.3). There have been numerous studies conducted to calculate the isometric forces for individual muscles. (Delp, 1990; Anderson and Pandy, 1999) The maximum isometric forces from gait2392 were modelled again from study one which, have been adopted from the Anderson and Pandy (1999) study. Hence, gait2392 maximum isometric forces were modelled using the Bahl model hence, statistical shape scaling. Delp (1990) maximum isometric forces were based on strengths based on cadaver muscle cross-sections.

5.2 Methodology

Bahl model was used to implement the maximum isometric forces for all muscles from four different studies (Appendix C). This study was only conducted with Patient009 RH (Table B.1) with the Bahl model (Section 4.3) for the contralateral (unaffected) right hip.
The four different maximum isometric forces modelled were taken from previous studies (Table 4):

- Bahl et al. (2019) – Bahl
- Carhart and Yamaguchi (2000) - Carhart
- Delp (1990) - Delp
- Anderson and Pandy (1999) – Gait2392

Table 4: Gluteus medius and minimus unscaled maximum isometric forces (N) for Bahl (Bahl et al., 2019), Carhart (Carhart and Yamaguchi, 2000), Delp (Delp 1990) and Gait2392 (Anderson and Pandy, 1999).

Literature Study	**Maximum Isometric Force (N)**	
	Gluteus Medius	Gluteus Minimus
Bahl	5113	2196
Carhart	1363	585
Delp	1365	585
Gait2392	2045	878

5.2.1 Data Analysis

Data analysis for study two consisted of observing the resultant HCF and individual muscle forces for the four different reported maximum isometric force data. The peak forces for gluteus medius and minimus were also analysed to evaluate the effect of change in maximum isometric forces on muscle forces between the models. The data was processed in excel and plotted in MATLAB (Appendix C).

5.3 Results

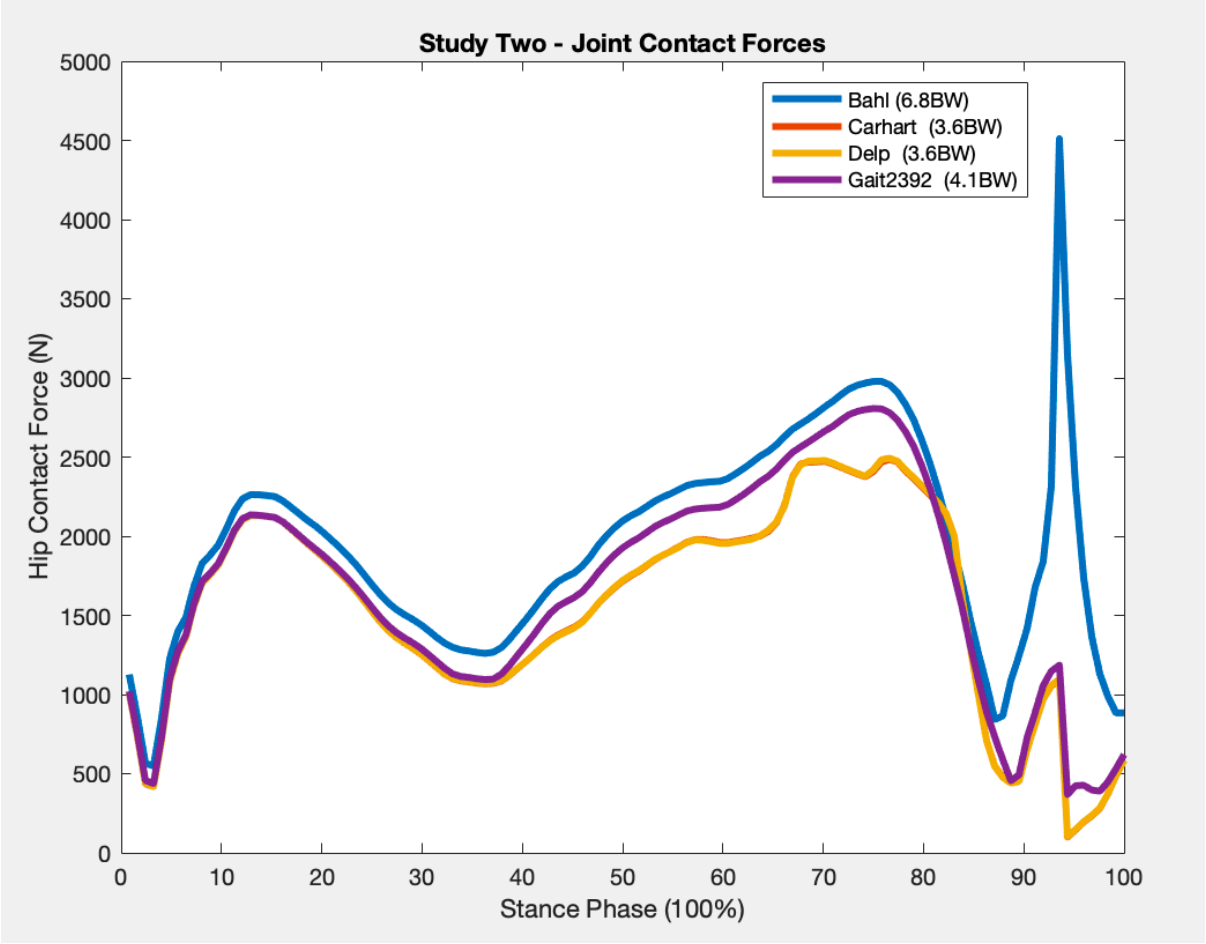

Figure 12: Resultant HCF for Bahl = 6.8BW (blue), Carhart = 3.6BW (red), Delp =3.6BW (Yellow) and gait2392 = 4.1BW (purple) models

The results show the highest peak resultant HCF (6.8BW) for the Bahl Model and lowest for Delp and Carhart model (3.6BW). The shape of the second curve for the Delp and Carhart model is like the Bahl and gait2392 model but with slight fluctuations. The graphs of Delp and Carhart model overlaps each other therefore only one is evidently seen. The first peak of the stance phase (15%) occurred at the same force for the Delp, Carhart and gait2392 models but second peak (78%) was higher for gait2392 model at 4.1BW. The peak present in Bahl model was previously discussed in study one (Section 4.7). In all models the peaks are very consistent in terms of occurrence in the gait cycle with very distinctive first and second peak.

Table 5: Muscle forces (N) and force capacity (%) for gluteus medius and minimus for Bahl (Bahl et al., 2019), Carhart (Carhart and Yamaguchi, 2000), Delp (Delp 1990) and Gait2392 (Anderson and Pandy, 1999).

Model	Gluteus Medius		Gluteus Minimus	
	Capacity (%)	Force (N)	Capacity (%)	Force (N)
Bahl	15	785	7	156
Carhart	53	717	78	454
Delp	52	716	78	455
GaIT2392	64	750	28	139

The Carhart and Delp model reached a higher force capacity (78%) for gluteus minimus compared to Bahl (7%) and gait2392 (28%). Gait2392 model reached the highest force capacity (64%) in comparison to the other model for gluteus medius. The Carhart and Delp model had same force capacity and forces of 78%. The Bahl and gait2392 models had similar forces but varied in force capacity of 7% and 28%, respectively. The varied force capacity is due to the difference in maximum isometric forces.

5.4 Discussion

The objective of study two was to assess the impact of maximum isometric forces on the resultant HCF and individual muscle forces. The percentage of the muscle capacity reached by gluteus medius and minimus was also evaluated. Furthermore, the individual muscle forces were also compared to analyse the difference between models.

The difference between the forces show that there is an influence of maximum isometric forces on the resultant HCF but do not reach their full force capacity in each model. Although the forces for all models were similar for gluteus medius with an average of 742 N. Conversely, gluteus minimus varied between the four models being significantly higher in muscle forces (454 N) compared to Bahl and gait2392 model. This may be due to the comparatively lower maximum isometric forces in the two models for all the muscles in the lower limb extremity. Therefore, gluteus minimus might be compensating for some of the other muscles as well resulting in higher muscle forces and force capacity. (Thelen and Anderson, 2006)

OA and elderly patients have muscle atrophy due to fatty infiltration and muscle volume reduction resulting in decreased contractile forces. (Arokoski *et al*., 2002; Madsen *et al*., 1997; Rasch *et al*., 2007; Suetta *et al.*, 2004; Loureiro *et al*., 2018; Zacharias *et al*., 2016) As there is a direct correlation between the maximum isometric forces and cross-sectional area hence, muscle volume. (Knarr *et al*., 2013) Delp (1990) forces were chosen as the most appropriate for this study due to representing the lowest maximum isometric forces for the end-stage OA patients.

Chapter 6

6 Study Three: Influence of Muscle Asymmetry on Resultant, Directional HCF and Individual Muscle Forces

6.1 Introduction

From previous study one and two, a scaling method and set of maximum isometric forces were chose; Bahl model (Bahl *et al*., 2019) with Delp study maximum isometric forces (Delp, 1990). The objective of study three was to introduce muscle asymmetry in the abductors within six patients. All the patients were end-stage OA patients awaiting surgery with three patients with previous hip replacement.

Study three aims:

1. Study the impact of abductor muscle asymmetry on the predicted peak resultant HCF, individual muscle forces and anterior - posterior directional forces
2. Impact of gait speed on the gait & muscle patterns and resultant HCF
3. Comparison of result HCF and muscle patterns between patients with contralateral THA and patient without THA
4. Resultant HCF of affected case hip and contralateral hip comparison

6.2 Methodology

Six subjects were pre-operational THA with end-stage OA were modelled using the Bahl model (Section 4.4) using maximum isometric forces selected from study two (Delp, 1990), following gait simulation method (Section 3.4.2-3.4.4). The methodology used for modelling and scaling was the linear scaling ratio (Equation 4) for all muscles within the lower limb extremity. Every model was evaluated using OpenSim tools and XML setup files were created for each tool.

6.2.1 Patient Specific Data

Table 6: Anthropometric data for six patients with maximum isometric force scaling ratio. Three patients with THA on the contralateral hip, three case hips on left leg and three right case hips.

Patient ID	Contralateral THA	Case Hip	Subject Weight [kg]	Subject Height [m]	BMI [kg/m^2]	Scaling Ratio
009 RH	Yes	LEFT	62.92	1.67	22.6	1.159
014 SP	Yes	LEFT	88.60	1.75	28.9	0.873
016 AF	Yes	RIGHT	108.4	1.70	37.5	0.734
044 JS	No	LEFT	80.92	1.68	28.7	0.995
046 BA	No	RIGHT	85.59	1.85	25	0.854
051 JO	No	RIGHT	88.78	1.80	27.4	0.846

There were multiple walking trails collected for each patient and the most appropriate were selected based on factors such as all markers on the force plate. The full gait cycle for each hip was selected within different trails (Appendix A-1).

6.2.2 Abductor Muscle Asymmetry

The muscle volume and strength decrease were created with reducing maximum isometric forces. As previous studies have reported, there is a direct correlation of maximum isometric forces with muscle volume (Knarr *et al*., 2013). The key abductor muscles gluteus medius and minimus were reduced. As seen in Table 7, the maximum isometric force reduction for patient009 RH were also performed on the other 5 patients (Appendix D). The gluteus medius and minimus are divided into three separate fibres in OpenSim having their own maximum isometric forces. The asymmetries were created at 20%, 40% and 60% reductions of the maximum isometric forces.

Loureiro et al. (2018) study reported 5-30% volume reductions in the OA patients for most muscle groups except gluteus medius. The medius results were not statistically significant in their study therefore 20% reduction was introduced as one of the models in this present study. The 20% reduction was designed within the range reported by both Loureiro et al. (2018) and Arokoski et al. (2002) studies with only accounting for volume reductions.

The 40% model was modelled for volume and fatty infiltration that would be caused from further strength deficits also to be close to previous upper range (37%) value (Arokoski et al., 2002). The upper range for Arokoski et al. (2002) was increased to 40% due to Loureiro et al (2018) reporting muscle atrophy contributing to muscle weakness and strength was 4% higher compared to the muscle reduction. Therefore the 40% model represented upper range, muscle volume & strength reduction and fatty infiltration. The third model 60% was simulated to evaluate worst-case scenario whereas 20% and 40% covered the range of the literature reviews. It was also designed to see the major change within the model hence, assessing the hypothesis of how much reduction would be required to see change in joint contact forces.

Table 7: Gluteus medius and minimus maximum isometric force reductions for Patient009 RH used in OpesnSim to create the asymmetry with three individual fibres.

Patient009 RH – Abductor Muscle Asymmetry in Left hip				
Muscle	**Maximum Isometric Force**			
	Base (N)	**20% (N)**	**40% (N)**	**60% (N)**
glut_med1_l	475	380	285	190
glut_med2_l	327	262	196	131
glut_med3_l	375	300	225	150
glut_min1_l	155	124	93	62
glut_min2_l	164	131	98	66
glut_min3_l	186	149	112	74

6.2.3 Data Analysis – Study Three

Study three analysis the impact of asymmetry on the HCF and individual muscle forces. The force capacity of each muscle was analysed to evaluate the muscles compensating for the reduction of gluteus medius and minimus. The anterior - posterior forces were also analysed to check the impact on forces and change in direction. The contralateral HCF capacity was compared to the affected OA hip and muscle asymmetry. The forces were evaluated over the full gait cycle (100%). The walking pattern and gait speed was also analysed for each patient to assess the impact on the resultant HCF. The data was processed in excel and plotted in MATLAB.

6.3 Results

The walking observations made was visualised in Mokka of all walking trails for each patient with the data provided by Bahl et al. (2019).

Patient009 RH was limping on contralateral unaffected right leg therefore unloading the affected hip.

Patient014 SP had no evident limping and therefore equal distribution of loading on each hip was assumed.

Patient016 AF was limping on the contralateral unaffected left leg and barely walking on the affected case right leg. Therefore, unloading the affect hip.

Patient044 JS had more weight towards the unaffected right leg hence, limping towards the contralateral hip.

Patient046 BA had slight limping on the contralateral unaffected left leg but mainly equal distribution on both hips.

Patient051 JO was limping on the contralateral unaffected left leg therefore unloading the affected hip.

6.3.1 Patient009 RH

Hip Joint Contact Forces

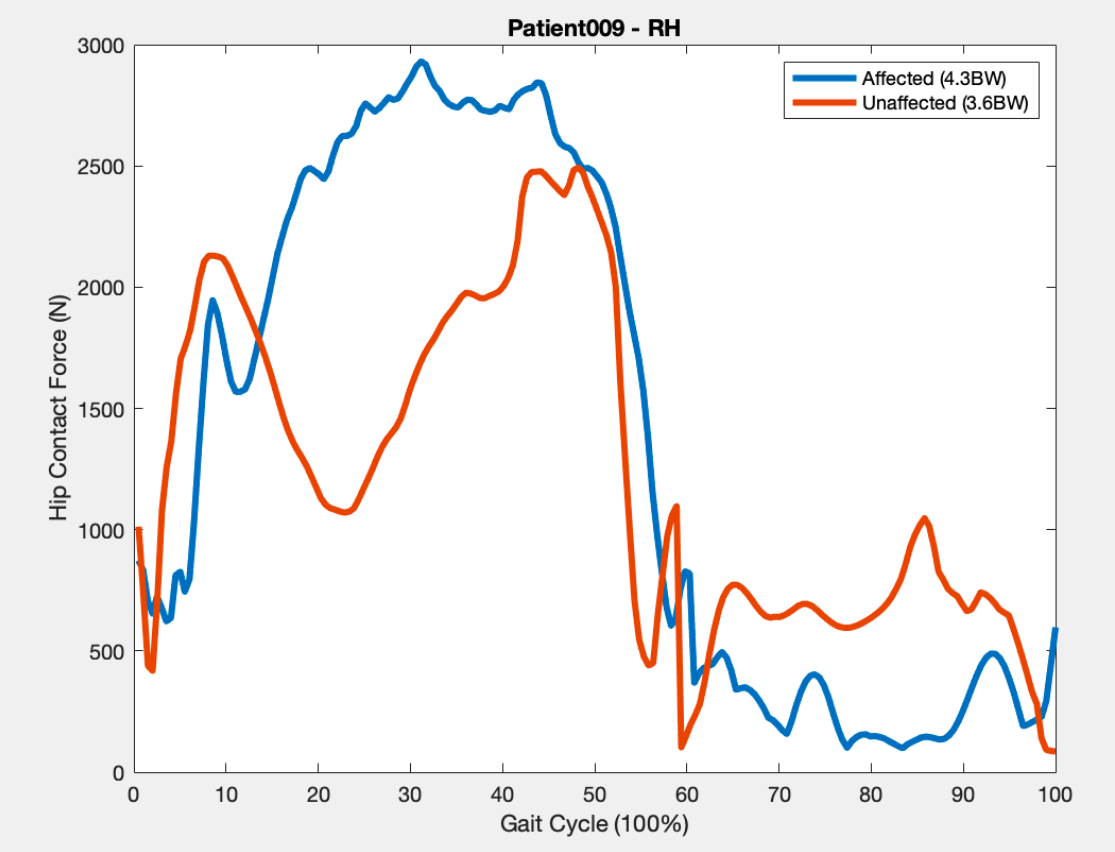

Figure 13: Resultant HCF (N) for affected left case hip (blue) and contralateral right hip (red) with peak BW for Patient009 RH. Affected Case Hip = 4.3 BW and contralateral unaffected hip = 3.6BW.

The results for patient009 RH show a two-peak profile with distinctive first and second peak for the contralateral right leg both lower than affected left hip (4.3BW). The first peak is lower (3.1BW) compared to the second peak (3.6BW). The trend of the affected hip graph didn't show clear first and second peak. However, the small spike during loading response (10%) in the gait cycle was assumed as first peak and second peak was identified between 13% to 60%. The forces during the swing phase between 60% to 100% of gait cycle were higher for the contralateral hip compared to affected case hip having a peak resultant HCF of 1.5BW and 0.71BW, respectively.

Muscle Force Capacity

Table 8: Base (left affected hip), contralateral hip (right unaffected hip) and muscle asymmetry (left affected hip); 20, 40 and 60% muscle force capacities for all hip muscles for patient009 RH. Muscle reaching capacity with increased abductor muscle asymmetry (green) and high capacity base or contralateral hip (yellow).

Patient009 RH Muscle	**Peak Muscle Capacity (%)**				
	Contralateral Hip	**Base Model**	**Muscle Asymmetry**		
			20%	**40%**	**60%**
Gluteus Medius	73	77	89	97	109
Gluteus Minimus	90	37	54	98	108
Semimembranosus	45	6	6	6	34
Semitendinosus	53	11	9	9	8
Biceps Femoris	75	20	21	21	26
Sartorius	99	44	66	55	99
Adductor Longus	110	18	19	17	18
Adductor Brevis	9	4	4	4	3
Adductor Magnus	32	1	1	1	1
Tensor Fasciae Latae	100	52	82	104	112
Pectineus	99	3	3	3	3
Gracilis	105	4	4	4	4
Gluteus Maximus	49	15	18	30	44
Iliacus Psoas Major	117	43	51	46	47
Quadratus Femoris	64	11	16	16	16
fixme gem	21	8	9	12	11
Piriformis	67	39	51	59	71
Rectus Femoris	104	45	48	59	119
Vastus Medialis	6	2	2	1	1
Vastus Intermedius	7	2	3	2	2
Vastus Lateralis	9	3	1	1	1

The gluteus medius and minimus increased to over force capacity as the muscle asymmetry was increased. The medius for base model with no induced muscle asymmetry had slightly higher force capacity (+4%) compared to contralateral hip. The 60% muscle asymmetry (worst case) was reaching over capacity for medius, minimus, tensor fasciae latae and rectus femoris. Muscles from major groups; flexors and adductors such as adductor longus, pectineus, gracilis and iliopsoas were reaching force capacity for the contralateral hip. Comparison between the affected case hip and contralateral hip shows muscle forces and force capacities were higher for the contralateral hip but the resultant HCF were higher for the affected case hip. The forces between the midstance (23%) to end of terminal stance (50%) for both hips were lower for the contralateral hip. Hence, the HCF were higher for the affected case hip having a peak force of 4.3BW during that phase.

The high capacity peak forces for the contralateral hip occurred between the initial swing (60%) and mid terminal swing phase (95%). Which contributed to the higher individual capacity forces on the contralateral hip. The muscle force capacity within the stance phase was higher for the affected case hip which also resulted in higher resultant HCF (Figure 13) during the stance phase (60%). It was seen in the graphs for individual muscles, the occurrence of high peaks in the gait phase for the contralateral and affected hip (Appendix D-1.1).

The muscle forces were higher in the contralateral hip in comparison to the affected hip for majority of the muscles. The contralateral muscles including, adductor longus, tensor fasciae latae, pectineus, gracilis, and rectus femoris were reaching capacity or over. An increasing trend was seen in piriformis, maximus and rectus femoris as the muscle asymmetry was increased. Contralateral hip muscles forces were also high as well as being close to the maximum isometric forces.

The medius and minimus both had an increasing trend in force capacity from the base model. Contralateral hip medius capacity was lower (-16%) compared to the 20% reduction model however for minimus capacity was higher (+36%) and nearly reaching capacity.

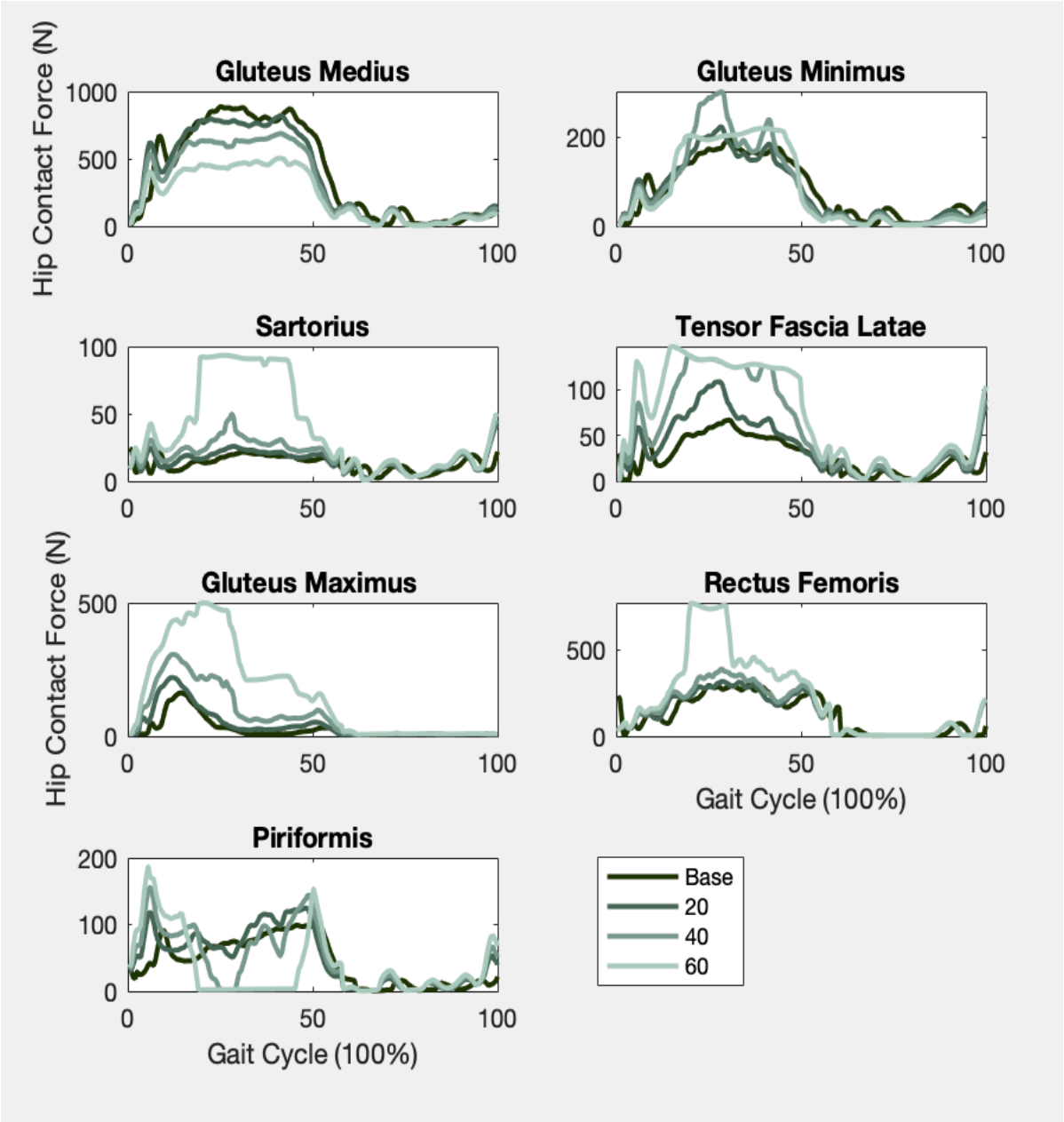

Figure 14: Patient009 RH base model (dark green) to 60% muscle asymmetry (light green) for the main muscles influenced by abductor muscle asymmetry.

The major changes were seen for the 60% muscle asymmetry models for sartorius, maximus, rectus femoris and piriformis. These muscles showed an increasing trend in their peak forces although the shape of the graph remains the same for 20 and 40% asymmetry models. The medius showed a clear trend of muscle force decrease as muscle asymmetry was decreased. However, minimus showed a fluctuation within the different asymmetry models.

6.3.2 Patient014 SP

Hip Joint Contact Forces

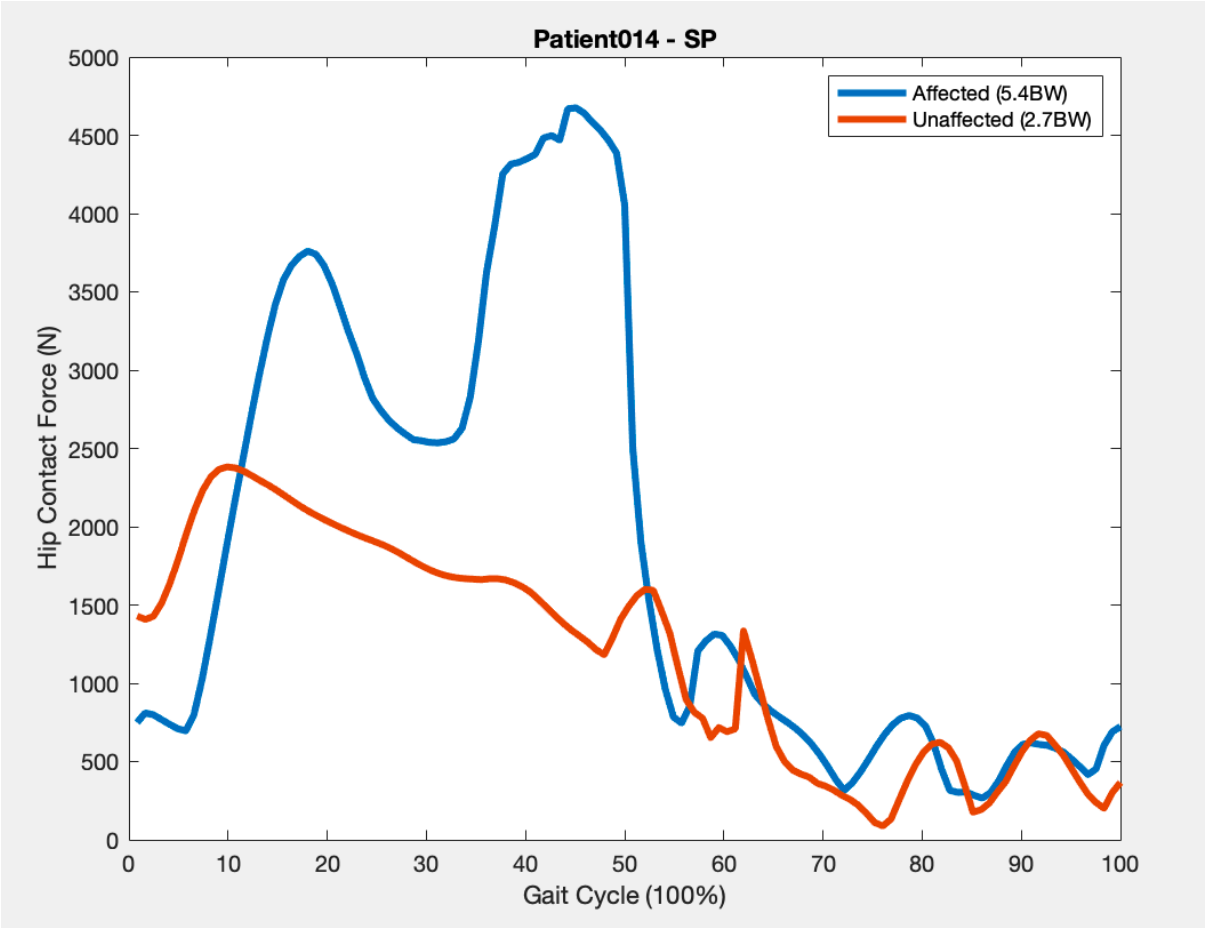

Figure 15: Resultant HCF (N) for affected left case hip (blue) and contralateral right hip (red) with peak BW for Patient014 SP. Affected case hip = 5.4 BW and contralateral unaffected hip = 2.7BW.

The results for affected left hip displayed a two-peak profile with first peak at 4.3BW and second peak 5.4BW. The first peak occurred between 10% to 27% and second peak between 35% to 50% of the gait cycle. The unaffected contralateral right hip didn't have two distinct peaks. The first peak is assumed to be at 10% gait cycle at 2.7 BW and second peak at 53% at 1.8BW. During the swing phase (60%), both hips peaked with similar resultant HCF and gait cycle locations. The resultant HCF were very high for the affected hip compared to the unaffected contralateral hip. As there was not much change in the walking pattern it was assumed there was equal weight distribution between the two hips. However, 014 SP did have a right hip replacement on the contralateral hip.

Muscle Force Capacity

Table 9: Base (left affected hip), contralateral hip (right unaffected hip) and muscle asymmetry (left affected hip); 20, 40 and 60% muscle force capacities for all hip muscles for patient014 SP. Muscle reaching capacity with increased abductor muscle asymmetry (green) and high capacity base or contralateral hip (yellow).

Patient014 SP Muscle	**Muscle Capacity (%)**				
	Contralateral Hip	**Base Model**	**Muscle Asymmetry**		
			20%	**40%**	**60%**
Gluteus Medius	57	62	69	71	84
Gluteus Minimus	77	87	98	99	101
Semimembranosus	42	38	38	38	42
Semitendinosus	24	93	93	93	93
Biceps Femoris	55	57	55	55	55
Sartorius	50	100	100	104	104
Adductor Longus	57	104	73	91	11
Adductor Brevis	15	8	5	14	2
Adductor Magnus	26	4	4	5	1
Tensor Fasciae Latae	45	98	104	112	117
Pectineus	15	100	100	100	100
Gracilis	16	103	103	95	95
Gluteus Maximus	23	1	4	13	23
Iliacus Psoas Major	66	104	104	104	104
Quadratus Femoris	27	45	31	17	19
fixme gem	10	6	6	71	6
Piriformis	27	19	21	21	21
Rectus Femoris	28	36	37	37	39
Vastus Medialis	13	1	3	2	1
Vastus Intermedius	13	1	4	2	2
Vastus Lateralis	20	1	4	1	1

The majority of the muscle capacity is higher for the affected left hip as the peak resultant HCF (5.4BW) was higher. The base model (affected hip) were reaching muscle capacity and higher than contralateral hip for extensor; semimembranosus, flexors; sartorius, iliopsoas, adductor longus & tensor fascia latae and adductors; pectineus & gracilis. Quadratus femoris part of the external rotator muscle group was higher for the affected hip compared to contralateral. Although tensor fasciae latae, pectineus and gracilis are smaller muscle with low contractile forces (Appendix D-1.2) but still were reaching maximum force capacity.

The impact of asymmetry on the muscle capacities did not increase significantly for the medius and minimus in comparison to the base model. But there was an increasing trend in the force capacity as the muscle asymmetry increased with small increments in force capacities. Comparison of the asymmetry and contralateral hip showed a significant difference for both medius and minimus. The contralateral hip medius and minimus are 57% and 77%, respectively compared to 60% muscle asymmetry being 84% and 101%, respectively. Observing the 20% muscle asymmetry, gluteus medius had an increase of +7% and +12% from the affected and contralateral hip, respectively. Similarly, in gluteus minimus with 20% muscle asymmetry, an increase of +21% and +11% was present in force capacity from the contralateral and affected hip, respectively.

There is also an increasing trend seen in tensor fasciae latae with increasing asymmetry for both hips. With a significant increase between contralateral hip and 20% muscle asymmetry of +59% in force capacity. Similar trend was present in the smaller muscles such as pectineus and gracilis with an increase of +85% between the contralateral and 20% muscle asymmetry.

Vastus medialis, intermedius and lateralis were higher for contralateral hip compared to the affected hip but only for small force capacity. These muscles have higher maximum isometric forces therefore the force capacity wasn't very high but the muscle forces (N) were within the same range as other hip muscles (Appendix D-1.2). Similar trend was also seen with adductor brevis and magnus as capacity was low for affected hip and asymmetry.

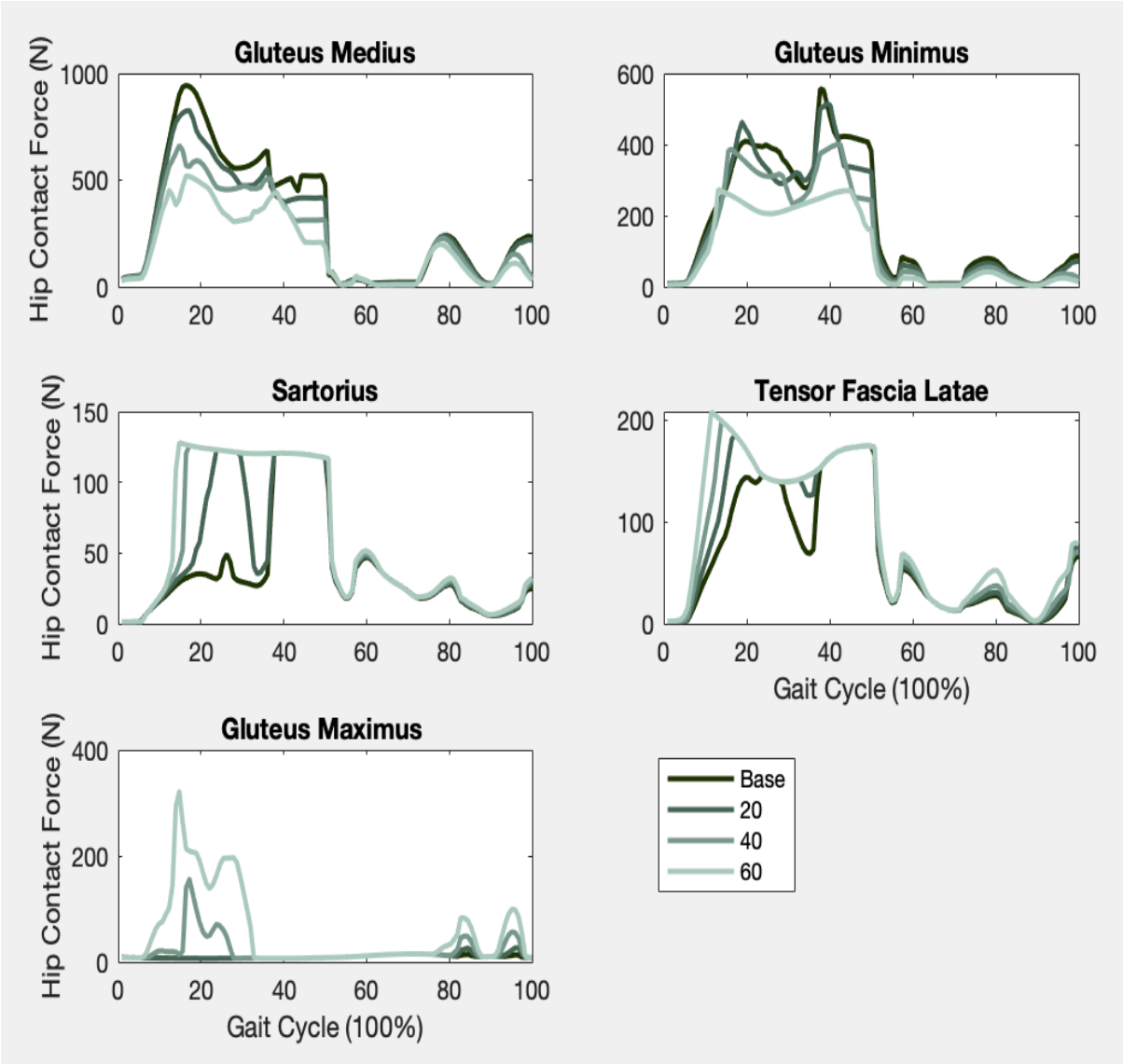

Figure 16: Patient014 SP base model (dark green) to 60% muscle asymmetry (light green) for the main muscles influenced by abductor muscle asymmetry.

There was an evident decrease present in both medius and minimus as the muscle asymmetry was increased. Sartorius, tensor fascia latae and maximus showed a corresponding decrease to increasing muscle asymmetry. There were different patterns present within all muscles due to abductor muscle weakness.

6.3.3 Patient016 AF

Hip Joint Contact Force

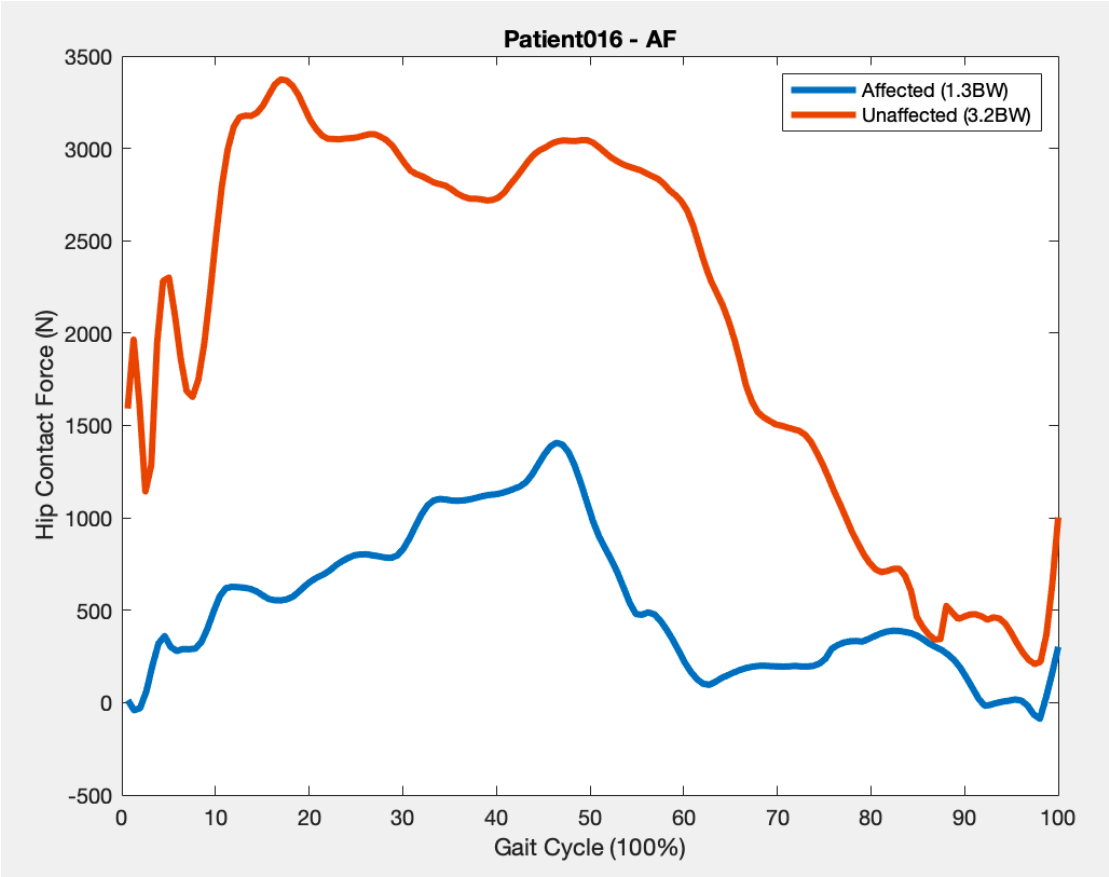

Figure 17: Resultant HCF (N) for affected case right hip (blue) and contralateral left hip (red) with peak BW for Patient016 AF. Affected case hip = 1.3BW and contralateral unaffected hip = 3.2BW.

There were slightly distinctive peaks in the unaffected contralateral left hip. First peak (3.2BW) was higher compared to second peak (2.9BW). There was only one distinctive peak in the affected right hip at 1.3BW which was identified as the second peak. First peak was assumed between 10% to 30% of the gait cycle at 0.59BW. In the swing phase (60% -100%), the HCF for unaffected contralateral hip remained higher than affected hip. The peak forces between during the swing phase were 1.3BW and 0.37BW for contralateral and affected hip, respectively. There was an increase in both hips with a similar trend from 98% to 100%. There were also two small spikes in the start of the gait cycle in the contralateral unaffected hip at 1% and 4% during the loading response.

Muscle Force Capacity

Table 10: Base (left affected hip), contralateral hip (right unaffected hip) and muscle asymmetry (left affected hip); 20, 40 and 60% muscle force capacities for all hip muscles for patient016 AF. Muscle reaching capacity with increased abductor muscle asymmetry (green) and high capacity base or contralateral hip (yellow).

Patient016 AF Muscle	**Muscle Capacity (%)**				
	Contralateral Hip	**Base Model**	**Muscle Asymmetry**		
			20%	**40%**	**60%**
Gluteus Medius	27	26	27	27	23
Gluteus Minimus	7	5	5	6	6
Semimembranosus	64	10	10	10	11
Semitendinosus	22	1	1	1	1
Biceps Femoris	49	26	27	28	28
Sartorius	70	52	49	49	51
Adductor Longus	16	1	1	1	1
Adductor Brevis	14	1	1	1	1
Adductor Magnus	18	1	1	1	1
Tensor Fasciae Latae	17	26	26	28	28
Pectineus	3	1	1	1	1
Gracilis	12	1	1	1	1
Gluteus Maximus	39	24	27	31	36
Iliacus Psoas Major	27	26	26	26	26
Quadratus Femoris	23	65	62	61	58
fixme gem	20	40	40	40	40
Piriformis	44	92	102	112	124
Rectus Femoris	24	26	26	26	26
Vastus Medialis	10	2	2	2	2
Vastus Intermedius	12	2	2	2	2
Vastus Lateralis	16	3	3	3	3

The gluteus medius and minimus were similar capacity for both hips and the muscle asymmetry. There was no major change between the muscle asymmetry models and contralateral & affected hip. Majority of the hip muscles were higher for the contralateral hip compared to affected hip, contributing to the higher resultant HCF. Semimembranosus (+54%), sartorius (+18%) and biceps femoris (+23%) reaching higher capacity for contralateral hip than affected side. Although some of the affected hip muscles such as quadratus femoris, fixme gem and piriformis were higher with a difference of +48%, +42% and +20%, respectively. But these muscles had small contractile force therefore didn't contribute to as much to the resultant HCF.

Vastus medialis, intermedius and lateralis were higher for contralateral hip compared to the affected hip but only for small muscle capacity. These muscles have higher maximum isometric forces therefore the force capacity wasn't very high but the muscle forces (N) were within the same range as other hip muscles (Appendix D-1.3). Similar trend was also seen with adductor brevis, longus and magnus as capacity was low for affected hip and asymmetry (1%). Pectineus, gracilis and semitendinosus also have higher muscle capacity and muscle forces (Appendix D-1.3) for contralateral hip compared to the affected hip as they are hardly activating.

The increasing trend for the asymmetry was only apparent in gluteus maximus and piriformis. The difference between 20% reduction and contralateral hip in the piriformis is +58% increase for the reduced affected hip and over capacity (+28%) for 60% muscle asymmetry hip. The gluteus maximus contralateral hip and 20% muscle asymmetry had a decreased force capacity (-12%) but there was a slight increasing trend between the affected hip to the 20% muscle asymmetry (+3%). There was also a slight decreasing trend observed in base affected model to muscle asymmetry of quadratus femoris (-7%), but the contralateral hip was lower by -40% than 20% reduction. The tensor fasciae latae was also consistent in force capacity for the muscle asymmetry although a small change was observed between contralateral and affected hip being higher (+9%).

In patient016 AF, muscle weakness of medius and minimus did not impact the asymmetry models. The only secondary abductor muscle impacted was gluteus maximus for the asymmetry.

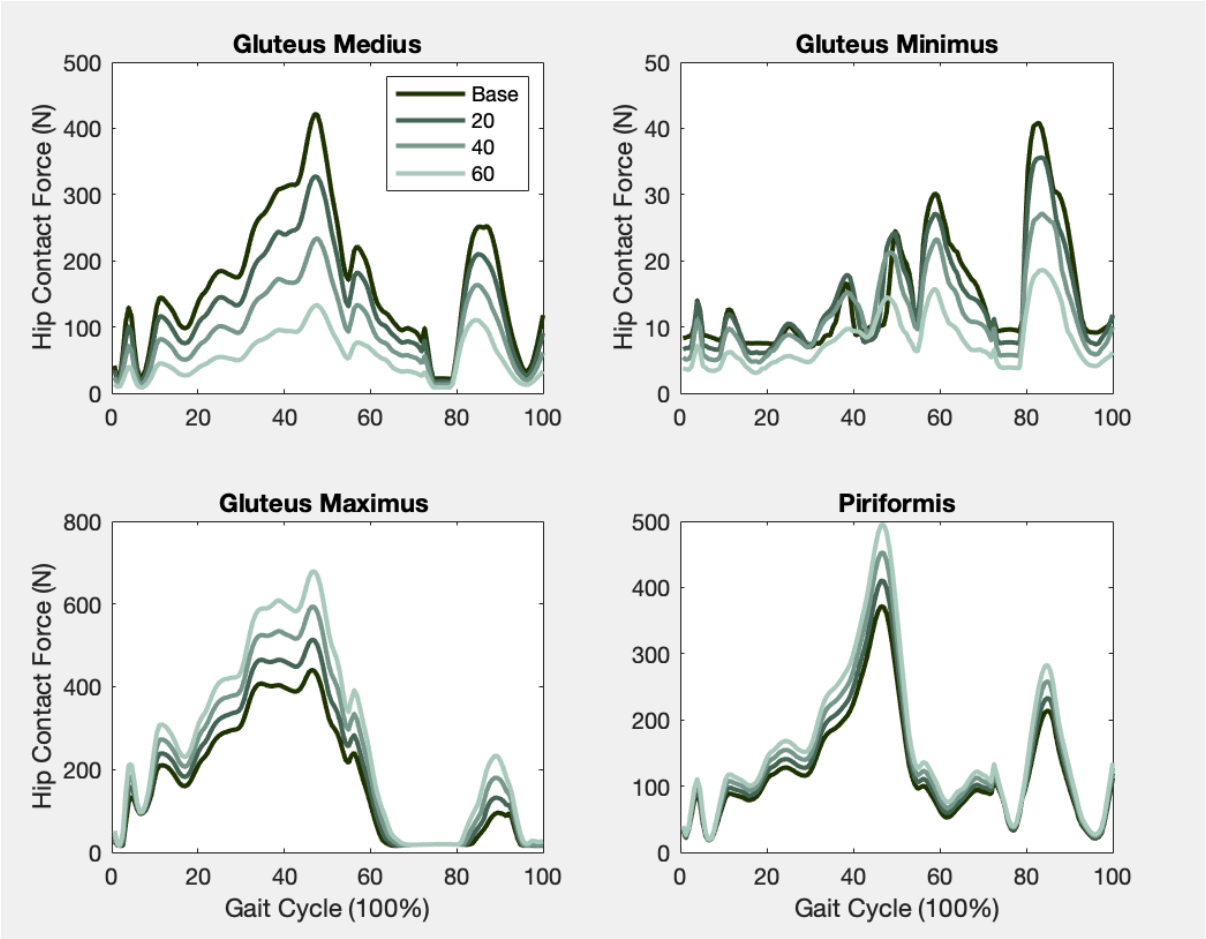

Figure 18: Patient016 AF base model (dark green) to 60% muscle asymmetry (light green) for the main muscles influenced by abductor muscle asymmetry.

There were clear decreasing trends present in both medius and minimus as the muscle asymmetry increased. Corresponding increase in maximus and piriformis as a result of the abductor weakness with same patterns within all asymmetry models.

6.3.4 Patient044 JS

Hip Joint Contact Forces

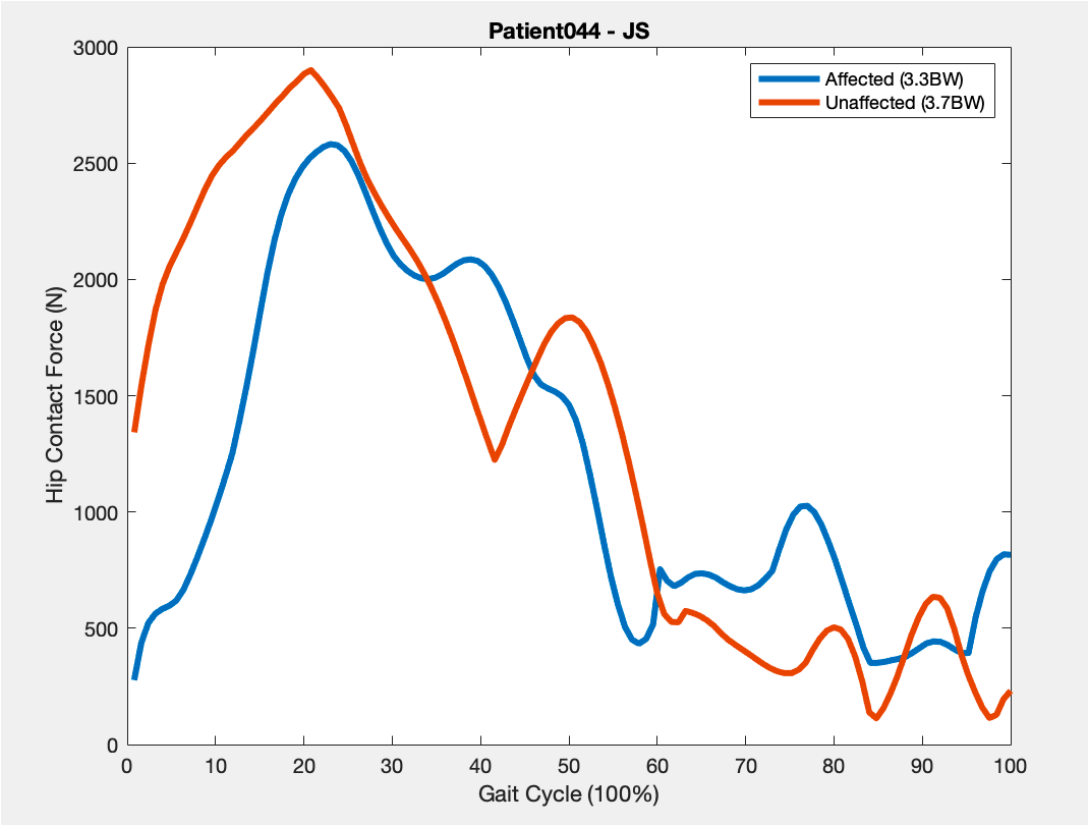

Figure 19: Resultant HCF (N) for affected case left hip (blue) and contralateral right hip (red) with peak BW for Patient044 JS. Affected case hip = 3.3 BW and contralateral unaffected hip = 3.7 BW.

The unaffected contralateral hip showed more distinctive first and second peak compared to the affected hip. Although both hips had a first higher and second lower peak. For contralateral and affected hip, the first peak occurred at 3.7BW and 3.3BW, respectively followed by the second peak at 2.3BW and 2.6BW, respectively. The peak resultant HCF for both hips were moderately close for the two peaks. The first peak for both hips occurred in the similar gait cycle phase (25%). However, second peak occurred later in gait cycle for the contralateral hip (40% - 60%) compared to the affected hip (35% to 45%). In the swing phase affected hip had a higher peak compared to the contralateral hip. Walking pattern of the patient044 showed more inclination towards to the unaffected right hip. Although this didn't majorly impact the peak resultant HJF for the contralateral hip.

Muscle Force Capacity

Table 11 Base (left affected hip), contralateral hip (right unaffected hip) and muscle asymmetry (left affected hip); 20, 40 and 60% muscle force capacities for all hip muscles for patient044 JS. Muscle reaching capacity with increased abductor muscle asymmetry (green) and high capacity base or contralateral hip (yellow).

Patient044 JS Muscle	**Muscle Capacity (%)**				
	Contralateral Hip	**Base Model**	**Muscle Asymmetry**		
			20%	**40%**	**60%**
Gluteus Medius	73	53	69	77	79
Gluteus Minimus	86	30	48	95	111
Semimembranosus	58	22	22	23	43
Semitendinosus	90	5	5	5	5
Biceps Femoris	51	27	27	28	28
Sartorius	28	30	33	35	103
Adductor Longus	30	24	24	24	23
Adductor Brevis	9	4	4	4	3
Adductor Magnus	27	7	7	7	7
Tensor Fasciae Latae	96	38	58	109	128
Pectineus	6	5	5	5	5
Gracilis	8	5	5	5	3
Gluteus Maximus	25	10	12	16	30
Iliacus Psoas Major	38	42	42	42	42
Quadratus Femoris	7	5	5	5	5
fixme gem	4	5	6	6	6
Piriformis	19	24	24	25	26
Rectus Femoris	77	51	51	48	77
Vastus Medialis	6	17	17	17	17
Vastus Intermedius	6	20	20	21	21
Vastus Lateralis	9	26	26	26	26

Gluteus medius and minimus was higher +20% and +56%, respectively for the contralateral hip compared to affected hip. Comparison between the contralateral hip and 20% reduced affected hip show a decreased trend for both medius (-4%) and minimus (-36%). However, base affected model to the 20% reduction had an increasing trend for both medius (+16%) and minimus (+18%). The increase trend was seen in all asymmetry affected hip models and 60% (worst case) was over capacity for minimus (+11%). Other muscles over capacity were tensor fascia latae (+28%) and sartorius (+3%) for 60% reduction. Between the affected base model and 60% reduction, an increase of 81% capacity for minimus as well as moderate increment of 26% within the medius muscle capacity.

Contralateral hip has higher capacity compared to affected leg for majority of the muscles such as extensors; gluteus maximus (+15%), adductor magnus (+20%), biceps femoris (+24%), semitendinosus (85%) and semimembranosus (+36%). Secondary abductor muscle group including sartorius, tensor fasciae latae, maximus and rectus femoris all showed increasing trends from the base model to the incremental reductions. The tensor fascia latae (+58%) and rectus femoris (+26%) were also higher for the contralateral hip compared to base affected hip.

The 20% reduction and base model comparisons showed an increase of +20% in tensor fasciae latae. The 60% reduction affected hip was higher than contralateral hip (32%) as well as being over capacity by +28%. There was also a significant increase (+90%) in the muscle capacity between the base affected and 60% reduction hip. There was very minor difference in maximus and rectus femoris between affected base hip and 20% reduction model.

Vastus medialis, intermedius and lateralis were higher for affected base hip compared to the contralateral hip but only for small muscle capacity (~+20%). These muscles have higher maximum isometric forces therefore the force capacity wasn't very high but the muscle forces (N) were within the same range as other hip muscles (Appendix D-1.4). Similar trend was also seen with adductor brevis and magnus as capacity was low for affected hip and with no change in asymmetry models.

Pectineus, gracilis, quadratus femoris and fixme gem were activating at low muscle capacity and muscle forces (Appendix D-4) for both muscles. Iliopsoas and piriformis remained constant in capacity for all models including asymmetry.

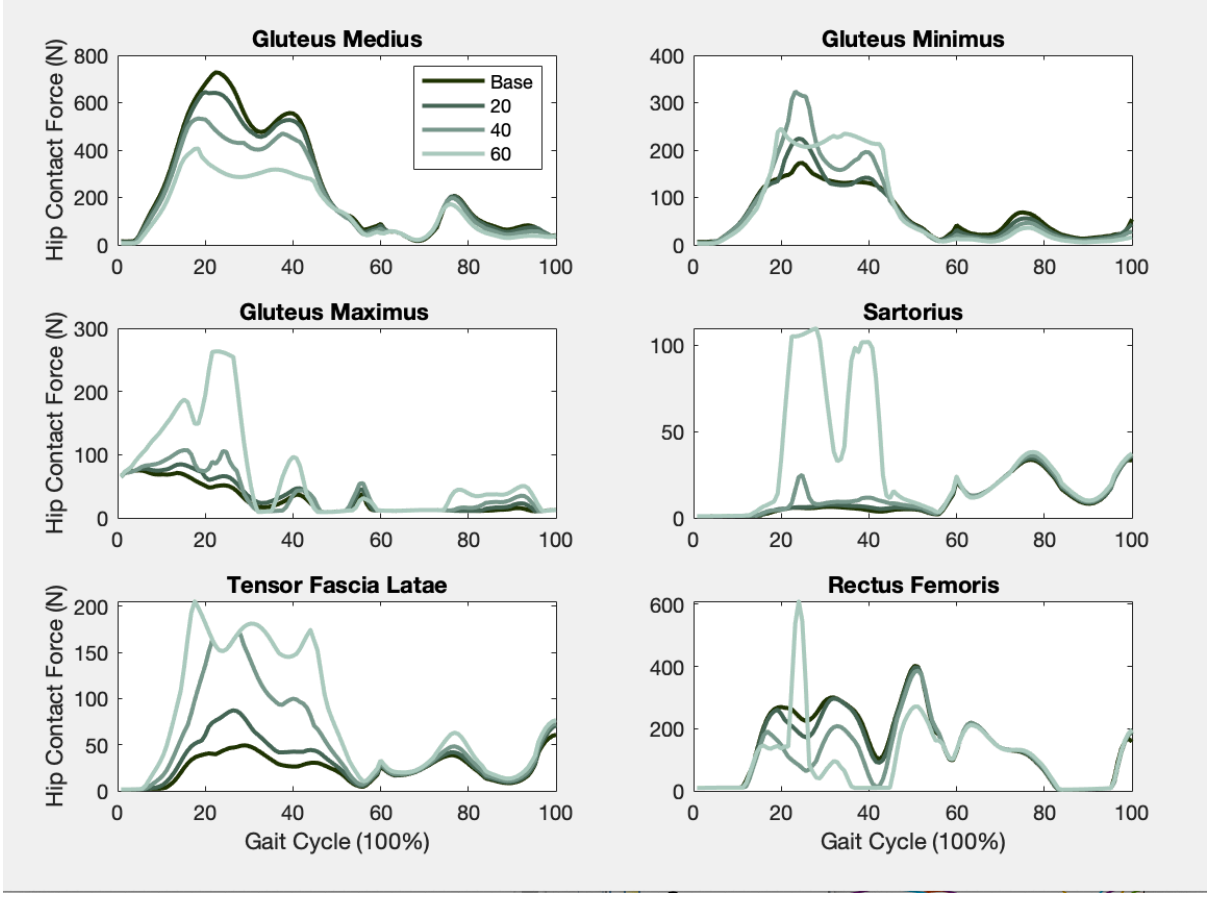

Figure 20: Patient044 JS base model (dark green) to 60% muscle asymmetry (light green) for the main muscles influenced by abductor muscle asymmetry.

The gluteus medius represented a clear decreasing trend as the muscle asymmetry was increased. However, fluctuations were present in the minimus as there as an increase from base to 40% followed by a decrease in 60% muscle asymmetry model. Although, maximus, sartorius, tensor fascia latae and rectus femoris increased with increasing muscle asymmetry but 60% model was peaking with higher spikes.

6.3.5 Patient046 BA

Hip Joint Contact Forces

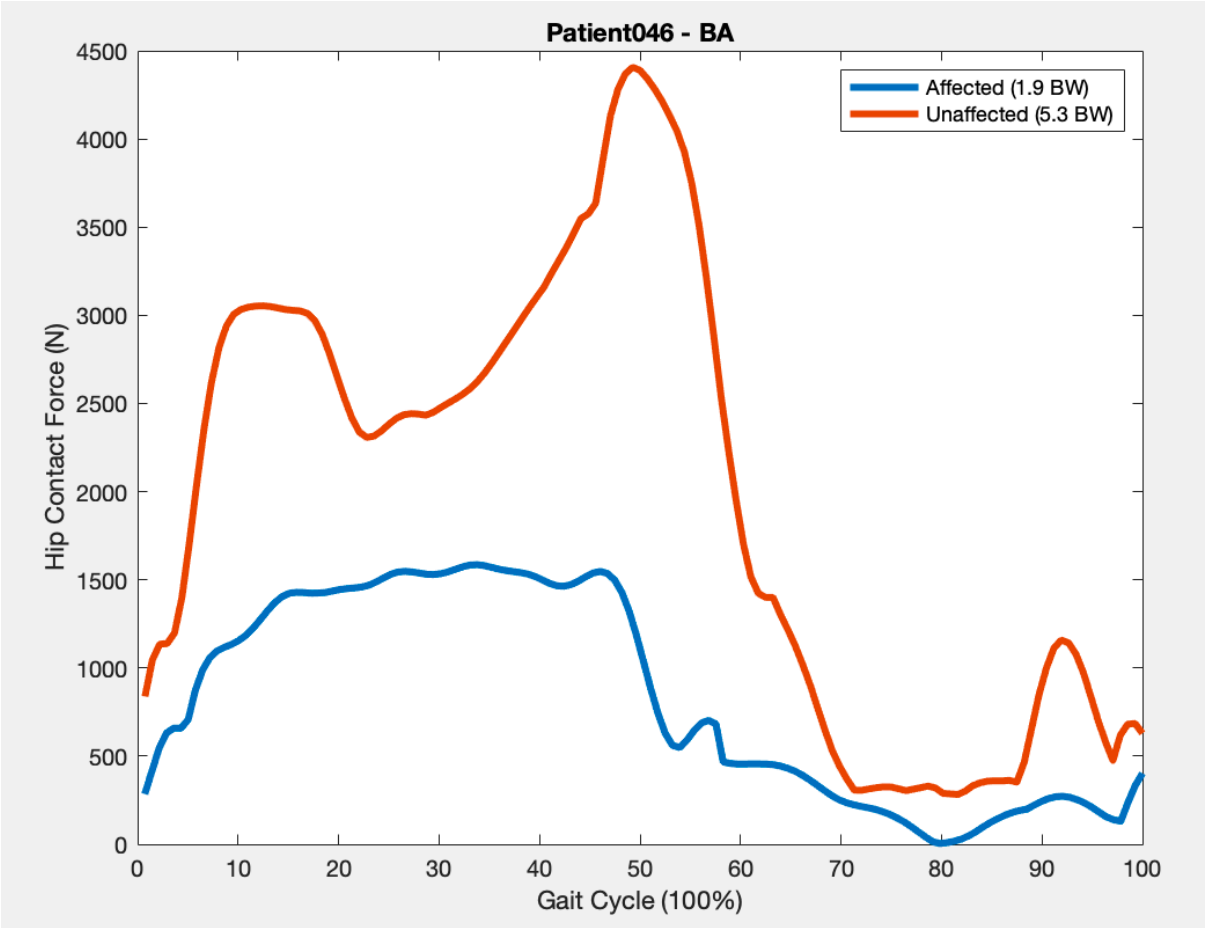

Figure 21: Resultant HCF (N) for affected case right hip (blue) and contralateral left hip (red) with peak BW for Patient046 BA. Affected case hip = 1.9BW and contralateral unaffected hip = 5.3 BW.

There were clear distinctive peaks in the unaffected contralateral hip with the second peak being higher (5.3BW) than first peak (3.6BW). There was an absence of two peak profile in the affected right hip with only one constant peak reaching and maintaining 1.9BW between mid-stance to terminal stance (10% to 48%) gait cycle. There was also a constant force maintained within the first peak of contralateral hip for approximately 8% of the gait cycle during the mid-stance. During the swing phase (60%-100%), contralateral hip remained higher with a peak (1.4BW) during terminal phase compared to affected leg (0.34BW). Walking pattern of the patient was slight limping on the unaffected contralateral hip.

Muscle Force Capacity

Table 12: Base (left affected hip), contralateral hip (right unaffected hip) and muscle asymmetry (left affected hip); 20, 40 and 60% muscle force capacities for all hip muscles for patient046 BA. Muscle reaching capacity with increased abductor muscle asymmetry (green) and high capacity base or contralateral hip (yellow).

Patient046 BA Muscle	**Muscle Capacity (%)**				
	Contralateral Hip	**Base Model**	**Muscle Asymmetry**		
			20%	**40%**	**60%**
Gluteus Medius	54	36	43	52	63
Gluteus Minimus	74	18	20	24	32
Semimembranosus	33	22	23	23	23
Semitendinosus	12	7	6	6	6
Biceps Femoris	53	22	22	22	22
Sartorius	98	24	24	23	28
Adductor Longus	91	6	4	3	3
Adductor Brevis	3	1	1	1	1
Adductor Magnus	13	3	3	3	3
Tensor Fasciae Latae	110	36	39	44	77
Pectineus	27	3	2	2	2
Gracilis	25	3	3	3	2
Gluteus Maximus	27	9	10	13	15
Iliacus Psoas Major	48	45	43	43	42
Quadratus Femoris	4	3	3	2	3
fixme gem	2	4	3	2	3
Piriformis	14	20	23	26	26
Rectus Femoris	16	52	51	51	53
Vastus Medialis	1	9	9	9	10
Vastus Intermedius	1	10	9	9	9
Vastus Lateralis	1	14	14	14	14

Gluteus medius and minimus was higher +18% and +56%, respectively for the contralateral hip compared to affected hip. Comparison between the contralateral hip and 20% muscle asymmetry affected hip show a decreased trend for both medius (-9%) and minimus (-54%). However, base affected model to the 20% muscle asymmetry had a minor increasing trend for both medius (+7%) and minimus (+2%). The increase trend was seen in all muscle asymmetry affected hip models but only with small increments. Difference between base affected model and 60% muscle asymmetry had an increase for both medius (+27%) and minimus (+14%).

The minimus capacity for 60% muscle asymmetry (worst case) remained significantly lower (-42%) than contralateral hip. However, medius had a slight increase (+9%) for the 60% muscle asymmetry compared to contralateral hip.

Tensor fascia latae was significantly higher (+74%) for the contralateral hip compared to the affected hip as well as being 10% over capacity. Between the base model and 20% muscle asymmetry, only a minor increase (+3%) was present but the 60% muscle asymmetry had a significant increase (+41%). Although the contralateral hip still remained higher (+33%) compared to the 60% muscle asymmetry affected hip. The maximus also showed an increasing trend from the base model to 60% muscle asymmetry but with minor increments in the muscle capacity. The contralateral hip was higher in muscle capacity by +15% compared to affected hip and also remained higher (~+10%) than 20% and 40% muscle asymmetry. However, 60% muscle asymmetry affected hip was higher with a minor increase in muscle capacity (+5%) than contralateral hip.

Comparison between affected hip and contralateral hip showed an increase within biceps femoris (+31%), sartorius (+74%), adductor longus (+85%) for the unaffected side. Majority of the muscles were higher for the contralateral hip although by only small force capacity. However, rectus femoris was higher (+40%) for the base model as well as vastus medialis, intermedius and lateralis but with minor muscle capacity increase (~10%). These muscles have higher maximum isometric forces therefore the force capacity wasn't very high but the muscle forces (N) were within the same range as other hip muscles (Appendix D-1.5). Iliopsoas and piriformis remained constant in capacity for all models including asymmetry.

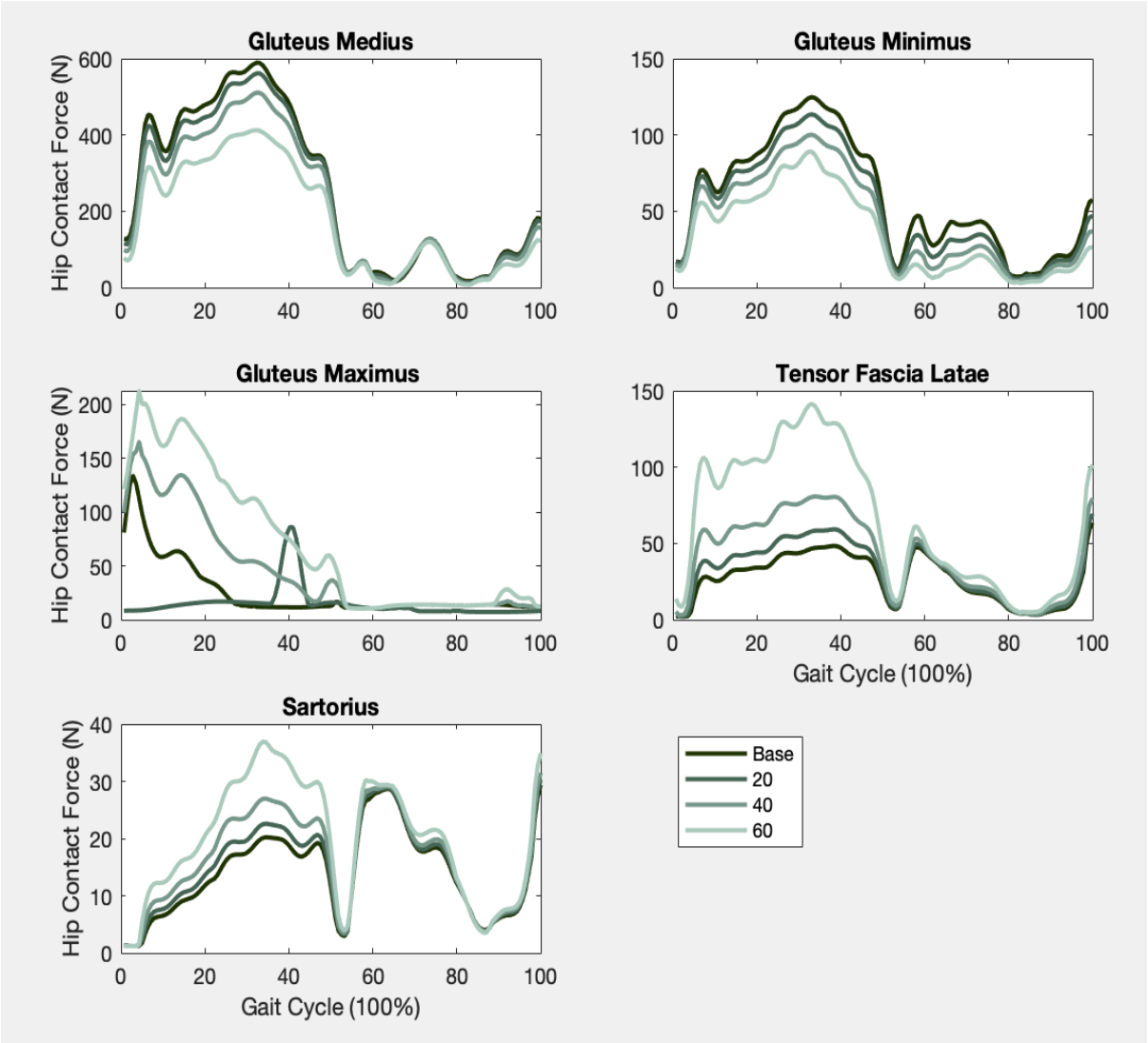

Figure 22: Patient046 BA base model (dark green) to 60% muscle asymmetry (light green) for the main muscles influenced by abductor muscle asymmetry.

There were clear decreasing trends present within both medius and minimus as the muscle asymmetry increased. Corresponding increase in maximus, tensor fascia latae and sartorius as a result of the abductor weakness with same patterns within all asymmetry models.

6.3.6 Patient051 JO

Hip Joint Contact Forces

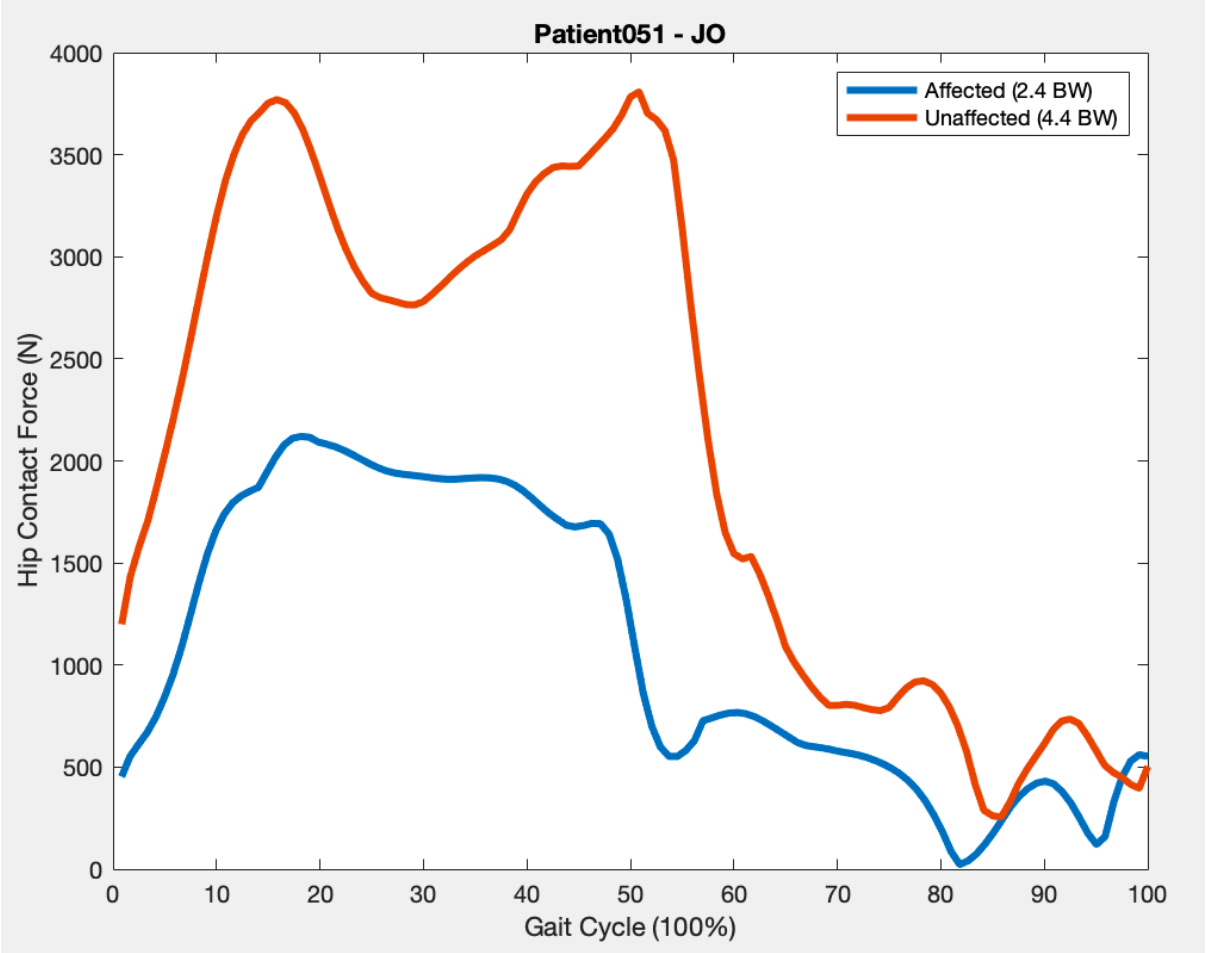

Figure 23: Resultant HCF (N) for affected case right hip (blue) and contralateral left hip (red) with peak BW for Patient051 JO. Affected case hip = 2.4BW and contralateral unaffected hip = 4.4BW.

There were clear distinctive peaks in the unaffected contralateral hip, both peaks at the same peak force (4.4BW). There was a slight pattern seen for the two peaks in the affected hip where first peak occurred during midstance (15% to 25%) followed by lower second peak terminal stance (30% to 40%). Both peaks for affected hip were similar force; first peak (2.4BW) and second peak (2.2BW). During the swing phase (60%-100%), contralateral hip remained higher with a peak (1.1BW) during terminal phase compared to affected leg (0.83BW). Walking pattern of the patient was slight limping on the unaffected contralateral hip.

Muscle Force Capacity

Table 13: Base (left affected hip), contralateral hip (right unaffected hip) and muscle asymmetry (left affected hip); 20, 40 and 60% muscle force capacities for all hip muscles for patient051 JO. Muscle reaching capacity with increased abductor muscle asymmetry (green) and high capacity base or contralateral hip (yellow).

Patient051 JO Muscle	**Muscle Capacity (%)**				
	Contralateral Hip	**Base Model**	**Muscle Asymmetry**		
			20%	**40%**	**60%**
Gluteus Medius	69	72	80	81	102
Gluteus Minimus	74	49	78	107	110
Semimembranosus	33	30	30	30	30
Semitendinosus	14	9	8	8	9
Biceps Femoris	47	25	25	26	27
Sartorius	105	30	30	105	105
Adductor Longus	30	38	37	36	35
Adductor Brevis	4	3	3	2	2
Adductor Magnus	15	8	7	7	7
Tensor Fasciae Latae	96	66	104	112	126
Pectineus	17	10	10	10	9
Gracilis	12	12	12	12	12
Gluteus Maximus	21	17	20	37	38
Iliacus Psoas Major	106	55	54	54	54
Quadratus Femoris	9	23	24	24	23
fixme gem	8	8	7	7	8
Piriformis	20	37	37	46	52
Rectus Femoris	92	62	65	62	58
Vastus Medialis	24	25	26	28	27
Vastus Intermedius	27	25	26	27	27
Vastus Lateralis	36	38	39	41	41

Contralateral hip for gluteus medius muscle capacity was slightly lower (-3%) but higher for minimus (+25%). In both muscles, an increasing trend was present from the base model to the 60% muscle asymmetry. The 20% muscle asymmetry model was also higher than contralateral hip for medius (+11%) and minimus (+4%). For 60% muscle asymmetry case, both muscles were above force capacity.

There was also a slight increasing trend present in gluteus maximus and contralateral hip (+4%) was also higher compared to base affected hip. There was also an increasing trend present in tensor fascia latae from the base model to each asymmetry model. There was an increase of +38%, +46%, +60% within muscle capacity for 20%, 40% and 60% muscle asymmetry, respectively from the base model. Sartorius was over capacity and higher than base model for contralateral, 40% and 60% muscle asymmetry model by +75%. for the contralateral hip Iliopsoas (51%) and rectus femoris (+30) were also reaching capacity and higher compared to affected base hip.

There was also a slight increase between base model and 20% muscle asymmetry in rectus femoris followed by a decreasing trend to 60% muscle asymmetry model. Vastus medialis, intermedius and lateralis were firing consistently for all models with a medium force capacity but higher forces (Appendix D6).

Majority of the other muscles were also higher for the contralateral hip compared to affected hip except for quadratus femoris and piriformis. There was also a slight increasing trend seen in piriformis between the base & contralateral hip and the muscle asymmetry models.

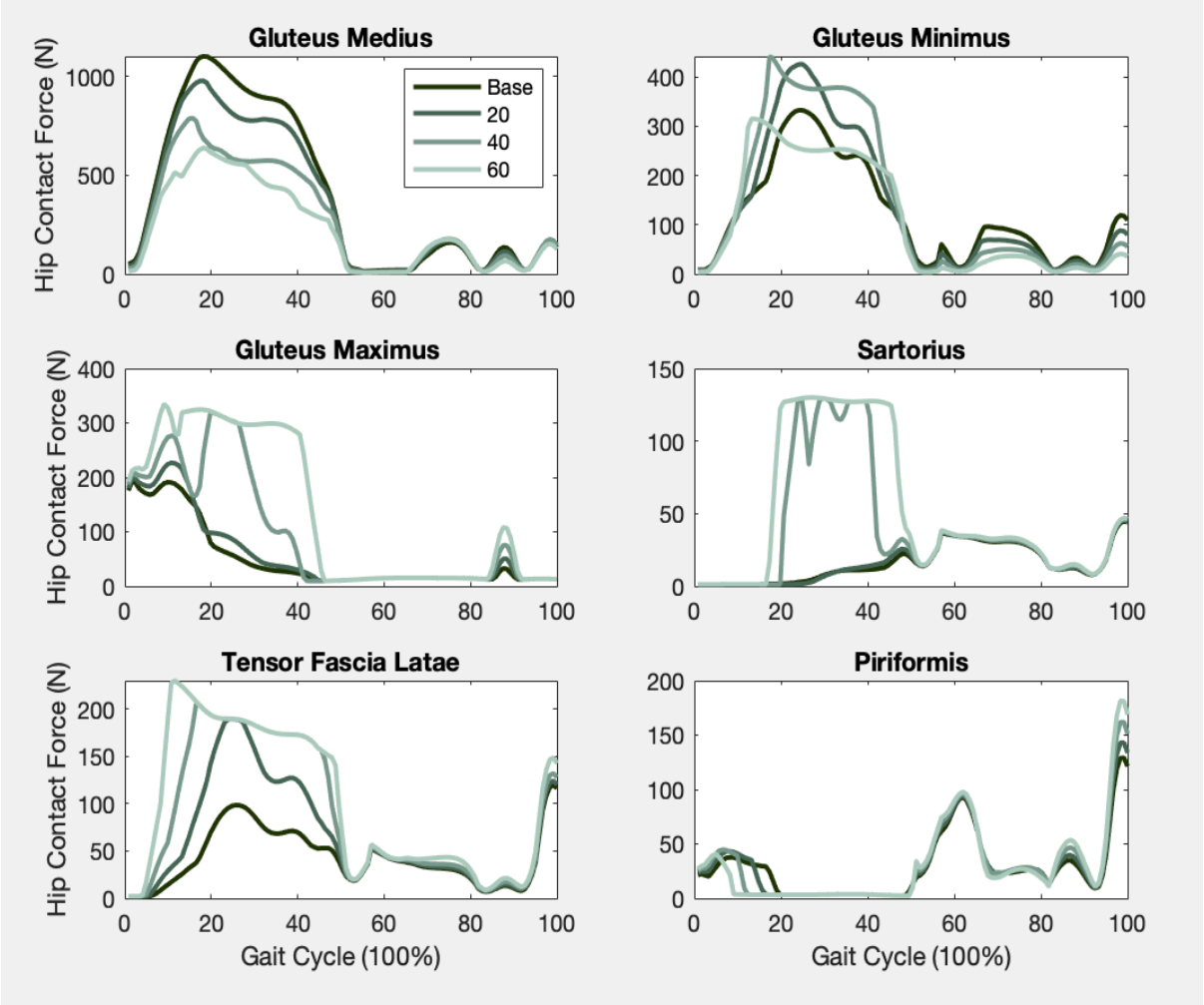

Figure 24: Patient051 JO base model (dark green) to 60% muscle asymmetry (light green) for the main muscles influenced by abductor muscle weakness.

The gluteus medius represented a clear decreasing trend as the muscle asymmetry was increased. However, fluctuations were present in the minimus as there as an increase from base to 40% followed by a decrease in 60% muscle asymmetry model. Although, maximus, sartorius, tensor fascia latae and piriformis increased with increasing muscle asymmetry, but 60% model was peaking with higher spikes and different activation pattern.

6.3.7 Anterior - Posterior HCF

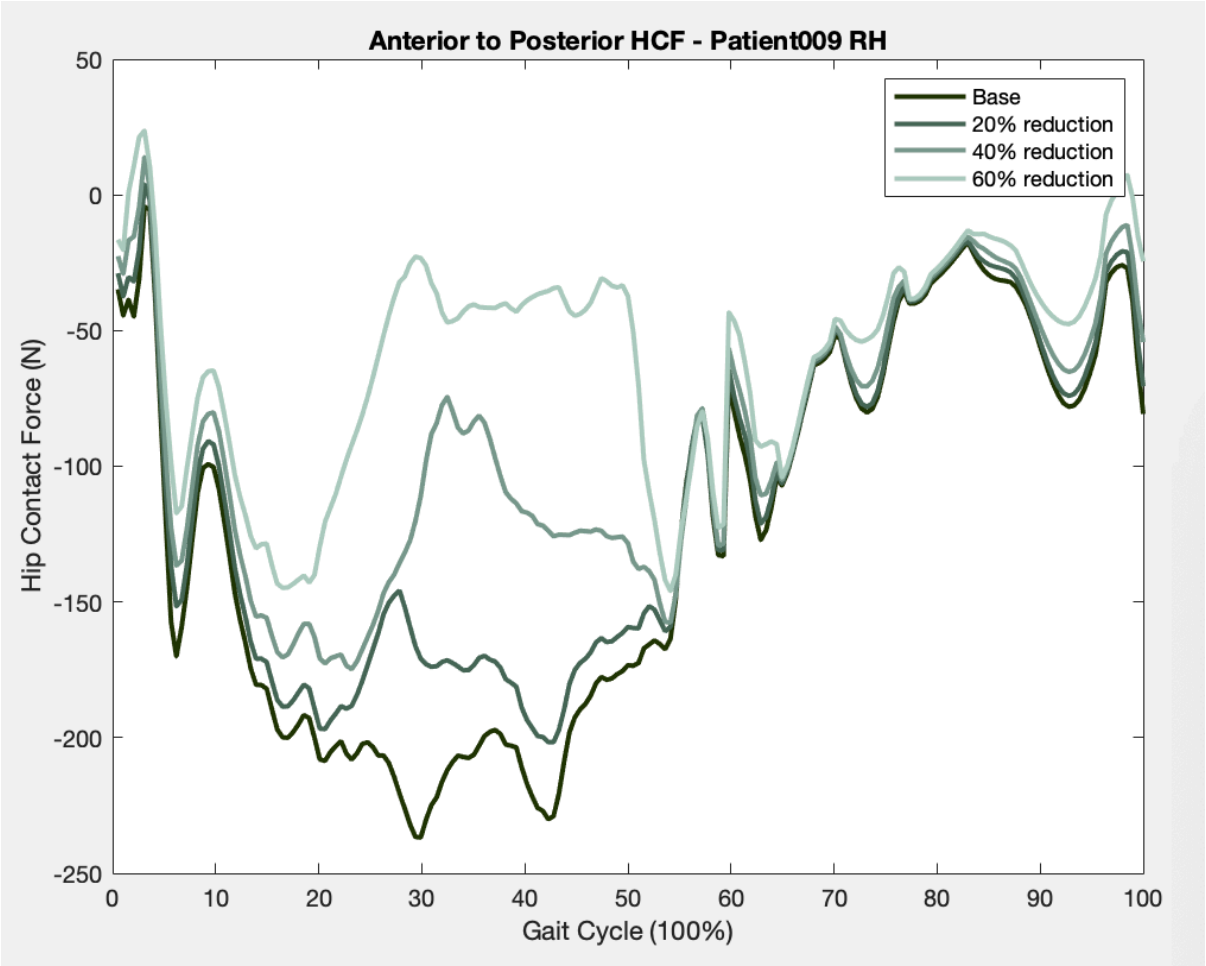

Figure 25: Anterior to Posterior left hip HCF for patient009 RH with Base model (dark green) to 60% muscle asymmetry (light green)

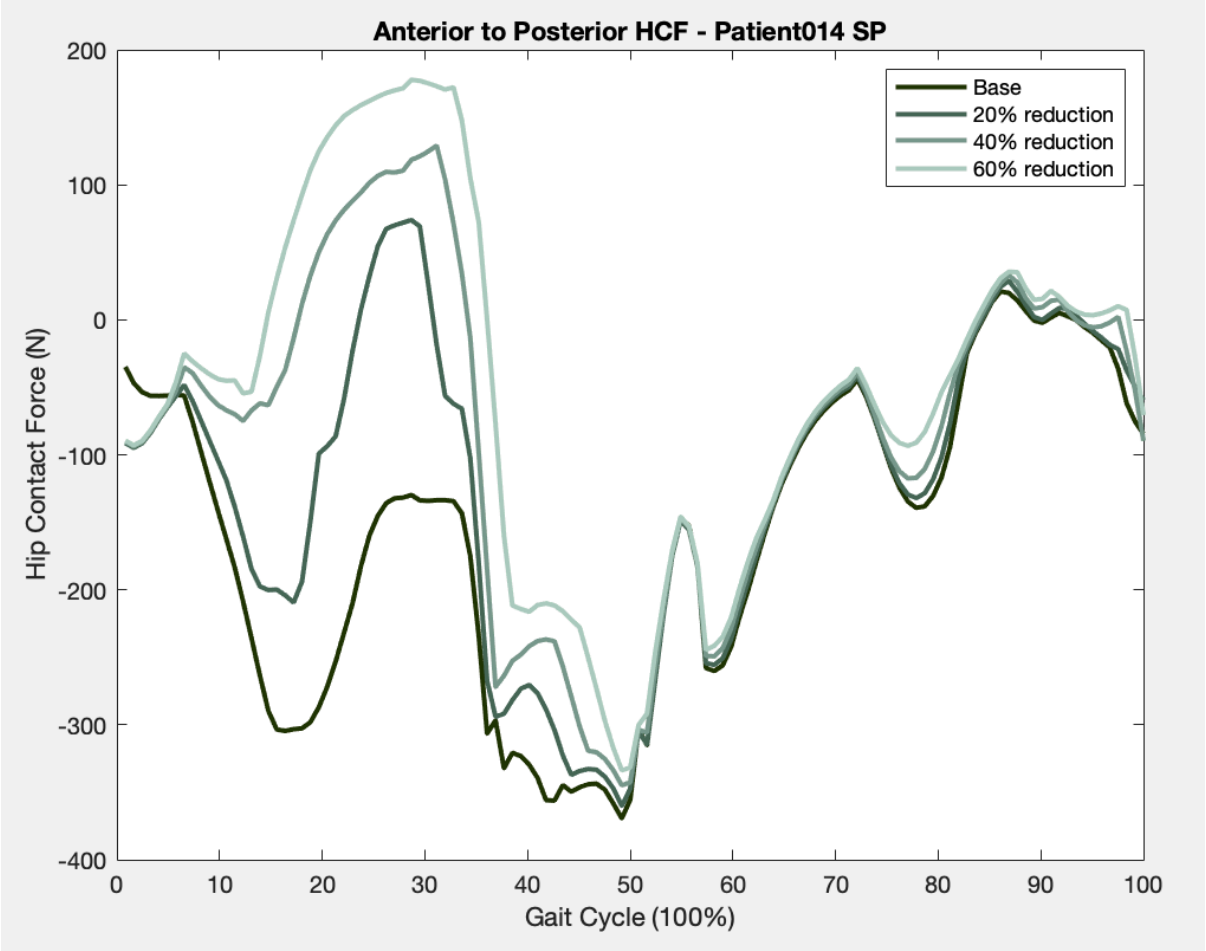

Figure 26: Anterior - Posterior left hip HCF for patient014 SP with Base model (dark green) to 60% muscle asymmetry (light green)

The anterior to posterior HCF is seen to increase to the positive anterior direction as the asymmetry is increased in both patients. These patients had the most significant impact within the anterior to posterior force compared to other patients. Additionally, patient014 SP had a change in direction from negative (posterior) to positive (anterior). The major increase for patient009 RH occurred between mid-stance to end of pre-swing (20 – 55%). Whereas, for patient014 SP it was from the mid-stance to end of terminal stance (10% to 40%). The pattern and shape for both patients was different.

6.3.8 Comparison of Patient Results

Table 14: The peak resultant HCF forces (BW) for affected case hip and contralateral unaffected hip with gait speed for six patients. Peak resultant HCF for abductor muscle asymmetry for affected case hip: 20%, 40% and 60% with mean and standard deviation (SD) forces for all models.

Patient ID – Case Hip	THA	Gait Speed (m/s)	Unaffected (BW)	Affected (BW)	Muscle Asymmetry (BW)		
					20%	40%	60%
009 RH – Left	Yes	0.64	3.63	4.27	4.45	4.45	5.71
014 SP – Left	Yes	0.98	2.74	5.38	4.89	4.37	4.20
016 AF – Right	Yes	0.30	3.17	1.32	1.36	1.41	1.50
044 JS – Left	No	0.75	3.65	3.25	3.23	3.15	4.09
046 BA – Right	No	0.92	5.25	1.89	1.89	1.89	1.89
051 JO – Right	No	0.91	4.37	2.43	2.52	2.74	2.74
Mean ±SD			3.80 ± 0.89	3.09 ± 1.53	3.06 ±1.40	3.00 ±1.25	3.35 ±1.60

Influence of Asymmetry on resultant HCF

There were only slight differences for the resultant HCF in affected hip models 20 to 60% muscle asymmetry (Table 14). However, Patient014 SP had a major decrease (1.2BW) between the base affected model and 60% muscle asymmetry. The resultant peak HCF were fluctuating between the base model and muscle asymmetry. There was a small increment in resultant HCF between the base affected case hip and 20% muscle asymmetry model. The change in muscle asymmetry models (20 – 60%) was very case dependent as peak resultant HCF increased in some patients (009 RH & 016 AF) while the others fluctuated or decreased (014 SP). The trend between unaffected contralateral hip and 20% muscle asymmetry peak resultant HCF was the same as in the individual muscle forces. Patient009 RH and 014 SP had higher forces for the 20% muscle asymmetry compared to contralateral hip. However, for other patients the HCF for 20% muscle asymmetry remained lower than contralateral hip. There was a small increment in resultant HCF between the base affected case hip and 20%

muscle asymmetry for some patients. However, major change was seen in patient009 RH and patient044 JS with 1.44BW and 0.84BW increase, respectively between the base model and 60% muscle asymmetry.

Two patients (009 RH & 014 SP) with contralateral right hip THA had higher resultant peak HCF on the affected hip than the contralateral THA hip. Whereas, patient016 AF also with contralateral THA but on left hip showed lower forces on the affected right hip compared to contralateral. The affected hip resultant HCF and gait speed ranged between 1.3 to 5.4BW and 0.3 to 0.98m/s, respectively. The slow gait speed (0.3m/s) was associated with lower peak HCF (1.3BW) and similarly faster gait speed (0.98m/s) with higher peak HCF (5.4BW).

Patients with replaced contralateral hips, all have different gait patterns. Only patient009 RH displays a very clear first peak and second higher peak pattern. While, patient016 AF also displayed two slight peaks but with not much difference.

First and second peak wasn't seen in the affected legs compared to contralateral without THA was only seen in patient044 BA but not very distinctively. The speed was higher (+0.17m/s) for the patients without clear affected hip gait peaks. In all patients' contralateral hips displayed two peaks except for Patient014 SP. All affected case hips had one peak during the stance phase (60%) excluding patient 014 SP having two distinctive peaks. Patient046 BA had comparatively high resultant HCF (5.25BW) to all other contralateral hip patients. This patient (BA) also had low resultant HCF on the affected side (1.89BW).

Individual Muscle Forces

Contralateral peak muscle capacities are higher compared to affected case hip for majority of the muscles and patients. Patient014 SP have higher forces for their base model, and this was also reflected by the resultant HCF (Table 14). The main muscles contributing to the higher contralateral muscle capacity were abductors, flexors and extensors. A common trend in contralateral hip was high force capacity was achieved by flexors and extensors when the medius and minimus had high force capacity. Vastus medialis, intermedius and lateralis were at a similar muscle capacity for all other patients except for patient051 JO had a comparatively higher capacity for both hips and muscle asymmetry models.

For most of the patients, adductor longus, brevis and magnus were not significantly active for the affected hip compared to the contralateral hip. Semitendinosus was active with higher forces for the contralateral hip for most of the patients except patient014 SP. For Patient016 AF, the muscle forces (N) were like all other patients but due to the scaled maximum isometric forces (Appendix D-1.3) being higher the force capacity percentage is low.

The gluteus medius and minimus muscle forces decreased (Appendix D) as asymmetry increased but the force capacity increased. In most of the patients medius, minimus, tensor fascia latae, maximus and sartorius are reaching or over the force capacity as the muscle asymmetry increased to the 60% muscle asymmetry model. These muscles are part of the primary and secondary abductor muscle group. Most common pattern seen in patients for 60% muscle asymmetry was abductors reaching force capacity. The increasing trend between capacity and muscle asymmetry was observed in medius, minimus, sartorius and tensor fascia latae. Although there was not a linear trend between the increase of capacities and muscle asymmetry. When the medius and minimus were over or close to maximum force capacity, tensor fascia latae and sartorius maxed out as well as a minor increasing trend was seen in gluteus maximus.

6.3.9 Level Gait Muscle Activity

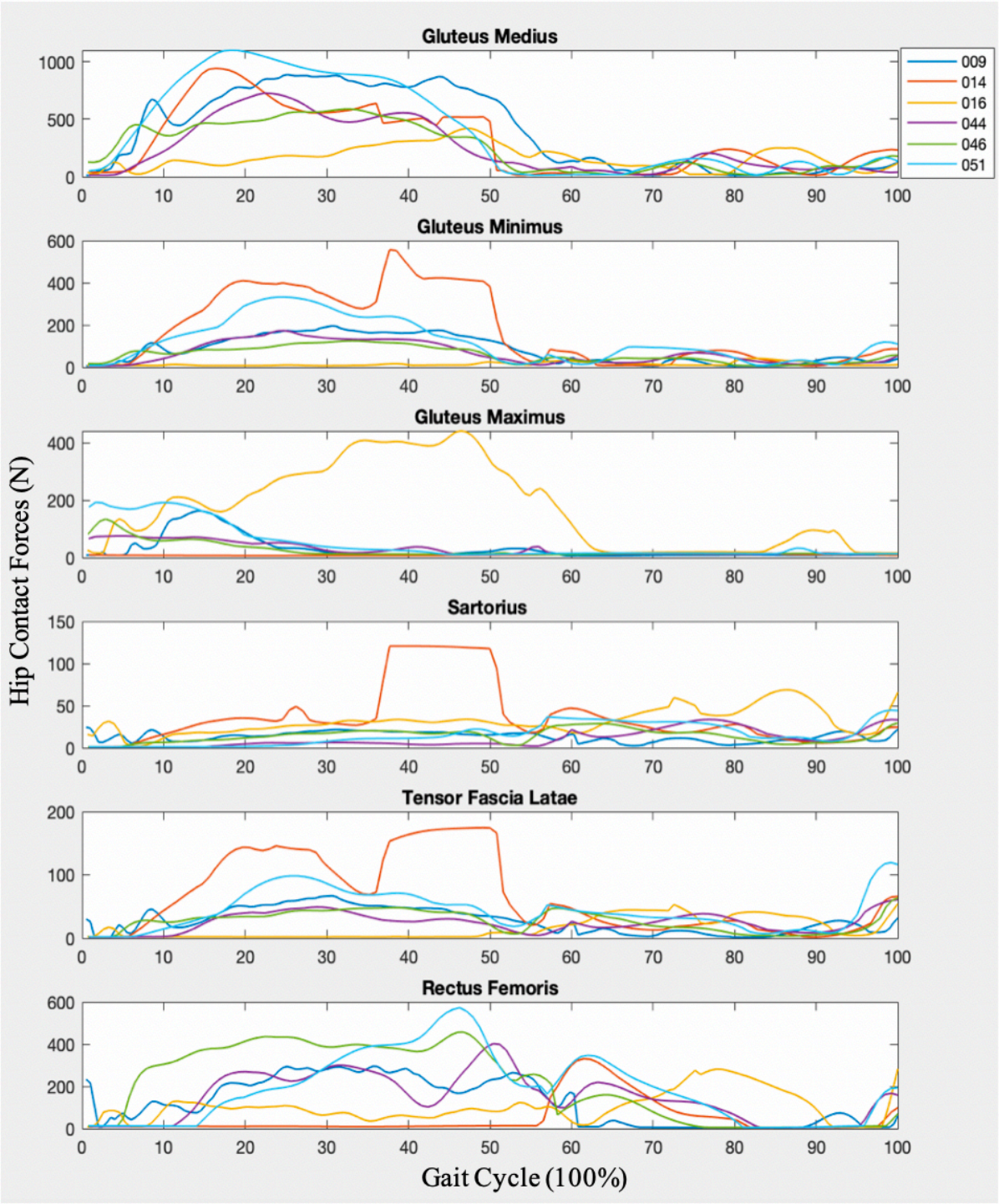

Figure 27:Activation patterns and muscle forces (N) over 100% gait cycle for gluteus medius, minimus, maximus, sartorius, tensor fascia latae and rectus femoris for patient009 RH (dark blue), 014 SP (orange), 016 AF (yellow), 044 JS (purple), 046 BA (green) and 051 JO (light blue) for affected case hip.

All patients do have different patterns but all peaking around the same phase. For the iliopsoas, minimus and medius, all patients followed a similar trend to the study peaking with different forces. (Thelen and Anderson, 2006) The graph shape and pattern remained the same for all the patients of the but the resultant HCF varied. Although there were no consecutive trends between the patients. The muscle forces did significantly vary between patients for all muscle in Figure 27. The main difference of muscle activation patterns and forces were present in patient014 SP and 016 AF. Patient014 SP had higher muscle forces for minimus, sartorius and tensor fascia latae. Additionally, patient016 AF had a major pattern different between 20% to 60% of the gait cycle and high peak force (400 N) compared to other patients.

6.4 Discussion

The objective of this study was to analyse the impact of asymmetry on the resultant HCF, directional and individual muscle forces for each patient for affected and contralateral hip.

6.4.1 Comparison of Contralateral versus Affected Case Hip

Resultant HCF

All six patients had higher resultant HCF on the contralateral hip compared to the affected case hip except for patients; 009 RH and 014 SP. These two patients had previous THA replacement on the contralateral hip. Although, patient016 AF also had THA but had lower HCF on the affected hip compared to contralateral. All three THA patients had similar resultant peak HCF on the contralateral hip. The contralateral hip peak resultant ranged between 3.80 ± 0.89BW also similar to affected hip with 3.09 ± 1.53BW. Patient046 BA had comparatively high resultant HCF (5.25BW) to all other contralateral hip patients. This patient (046 BA) also had comparatively low resultant HCF on the affected side (1.89BW).

Gait Patterns

All affected case hips had one peak during the stance phase (60%) excluding patient 014 SP having two distinctive peaks. In majority of the cases two peak profile were seen in the contralateral hip excluding patient014 SP. Which shows that if a two peak profile was present in one hip then the opposite hip only had one peak occurring in the stance phase of the gait cycle. One peak profile could have been due to slow speed or the walking pattern (limping). Equivalent results have been seen in the O'Connor et al. (2018) study, in the slow walking speed subjects, there weren't two clear peaks. The speed was higher (+0.17m/s) for the patients without clear affected hip 2 peak profile. Furthermore, high fatty infiltration in the gluteal muscles can result in impaired gait cycles (Daguet *et al.*, 2011) but was not measured in the present study.

The slow gait speed (0.3m/s) was associated with lower peak HCF (1.3BW) and similarly faster gait speed (0.98m/s) with higher peak HCF (5.4BW). However, there is a significant variation between the patient resultant HCF due to their walking patterns and speed. The

results showed the gait speed only impacted the affected hip as the increase in gait speed between different patients did not influence the contralateral replaced hip.

In some cases, even though patients were limping on the contralateral leg, the affected hip peak HCF still remained higher (Patient009 RH).

Individual Muscle Percentage Used of Available Force Capacity

Contralateral hip used higher available muscle force capacity compared to affected case hip for majority of the muscles and patients. Patient014 SP had the highest peak resultant HCF on the affected hip, out of the six patients (Figure 13). Which was also evident in their muscle forces as higher available muscle capacity was used compared to other patients. The different trend and high force in iliopsoas for patient016 AF can be explained by the extremely high affected forces (5.4BW) and other muscles also maxing out. The different trend in maximus for patient016 AF could be due to the minimus and medius hardly contracting resulting in maximus taking over. This is known as the compensatory effect designed for the OpenSim further discussed in Section 6.4.3.

The main muscles contributing to the higher contralateral force capacity were abductors, flexors and extensors. A common trend in contralateral hip was high force capacity was achieved by flexors and extensors when the medius and minimus had high force capacity. Vastus medialis, intermedius and lateralis were at a similar muscle force capacity for all other patients except for patient051 JO had a comparatively higher used capacity for both hips and asymmetry models.

For most of the patient adductor longus, brevis and magnus were not significantly active for the affected hip compared to the contralateral hip. Semitendinosus was active with higher forces for the contralateral hip for most of the patients except patient014 SP.

6.4.2 Impact of Muscle Asymmetry on Resultant HCF

The results fluctuated predicted for all the asymmetry models and were very case dependent. Only a minor change was evident within the 20% and 40% muscle asymmetry for all patients. The minor change present in all patients could be due to 20% muscle asymmetry

being very insignificant to be able to cause a distinctive trend or change in the resultant HCF. The major impacts were evident within the 60% muscle asymmetry but only for some patients. For example, patients 009 RH and 044 JS had a major increase of approximately 1.0BW from the base model to 60% muscle asymmetry. There was an increase in compensating muscle forces that contributed to major differences in peak resultant HCF in patient009 RH and 044 JS. Patient009 RH and 044 JS had a high random peak appearing in the stance phase (Appendix D-1.7) that contributed to the high HCF may be due to the method of programming OpenSim further discussed in Section 6.4.3. Furthermore, a decrease was also present for patient014 AF from base to 60% a muscle asymmetry model.

The higher peak resultant HCF in the 60% abductor muscle asymmetry in patient009 RH and 014 SP was majorly caused by rectus femoris as well as sartorius and piriformis reaching force capacity. The gait speed for these patients was also similar and in the mid-range compared to other patients. The gluteus medius and minimus used available force capacities for the base model were also like other patients. Although patient009 RH had a previous replacement on the contralateral hip that might have led to higher peak resultant HCF. There was limping on the contralateral hip for both patients; 009 RH and 044 JS. The major decrease in peak resultant HCF in patient014 SP (-1.0BW) in the 60% muscle asymmetry was correlated to the decrease in used muscle capacities of adductor longus, quadratus femoris, fixme gem and fluctuations within other smaller muscles. The gait speed for pateint014 SP was also comparatively the highest (0.98 m/s) with no difference seen in the walking patterns. There was no apparent reason for the increase or decrease in resultant HCF as other patients also showed the same properties. There could have been multiple factors resulting in the significant change that were not measured during this study.

Patient 016 AF, 046 BA and 051 JO were able to sustain the high abductor weakness more efficiently than others (009 RH, 014 AF & 044 JS) also reported by previous studies. Van der Kroght et al. (2012) reported 100% gluteus medius weakness was only tolerated by some adolescent healthy subjects. Furthermore, Valente et al. (2013) study also showed few unsuccessful models with high muscle weakness. Further indicating patients with abductor weakness are very case dependent, hence the variation in present study OA patients. Furthermore, patient016 AF and 046 BA used available muscle capacity was low for 60% model. However, patient051 JO used available muscle capacity for abductors was over but didn’t highly impact the peak resultant HCF.

Walking patterns and gait speed are first order effects and muscle atrophy is defined as second order effects. The first order effects were assessed with comparison between peak resultant HCF of affected hip and contralateral unaffected hip. The second order effects were assessed based on base affected model and 60% muscle asymmetry. The results showed major impact of gait speed and walking asymmetry in some patients while in other muscle asymmetry made more impact on the resultant HCF. Patient009 RH was greatly impacted by both first and second order effects (Figure 14).

Table 15: first and second order effects for all patients; increase (↑), decrease (↓) and minor or no change (=). Change of 0.5 to 1BW (orange), 1 to 2BW (blue) and 2 – 3BW (yellow) and 3 – 4BW (green).

Patient ID – Case Hip	First Order Effect: Gait speed and pattern	Second Order Effect: Muscle Asymmetry
009 RH – Left	↑	↑
014 SP – Left	↑	↓
016 AF – Right	↓	=
044 JS – Left	=	↑
046 BA – Right	↓	=
051 JO – Right	↓	=

Anterior – Posterior Component HCF

The impact of muscle asymmetry on the anterior - posterior component of the HCF was very case dependent, with different patterns seen in every patient. Patient009 RH and Patient014 SP increased significantly from the base model to the 60% muscle asymmetry (Figure 25 & Figure 26). Patient014 SP changed direction with reaching positive forces (200N). The other patients only had minor increases in HCF as the muscle asymmetry increased.

Anterior - posterior changed direction for patient014, indicating there might be increased risk of implant failure due to anterior dislocation. Also indicates that other factors can highly impact the HCF in order to sustain the implant and high loads. This patient also had a

contralateral THA and there was an absence of two peak profile in the gait cycle. The forces for the affected hip were also significantly high (5.4BW) and increased pattern in the peak resultant HCF for increasing muscle asymmetry. This could also impact the change in force direction as well as affected hip sustaining more loads as the contralateral HCF were lower (2.7BW). There was no visible change in their walking pattern with no limping on the either hip. Therefore, the possible contributing factors to high HCF on the affected hip could have been further weakness in the muscles resulting in higher loads. Another factor could be problems or diseases in the affected or contralateral hip in the other joints.

The peak anterior - posterior HCF occurs within the stance phase but at different location of the gait cycle ranging between mid-stance and terminal stance (20 – 50%). The pattern remained the same for all the muscle asymmetry models for each patient.

6.4.3 Impact of Muscle Asymmetry on Muscle Patterns and Forces

For Patient016 AF, the muscle forces (N) were like all other patients but due to the scaled maximum isometric forces (Appendix D-3) being higher the available used capacity percentage was low. The gluteus medius and minimus muscle forces decreased (Appendix D) as asymmetry increased but the used muscle capacity increased (Table 8-Table 13). However, for gluteus maximus, patients displayed a similar trend to a previous study (Thelen and Anderson, 2006) except patient016 AF peaking for 60% of the gait phase. Iliopsoas was higher compared to all other patients with a slightly different trend.

The increased trend present in medius as the muscle asymmetry increased was also reported by (Van Der Krogt et al., 2012). In most of the patients medius, minimus, tensor fascia latae, maximus and Sartorius are reaching or over the capacity as the muscle asymmetry increases to the 60% muscle asymmetry. These muscles are part of the primary and secondary abductor muscle group. Most common pattern seen in patients for 60% muscle asymmetry was abductors reaching force capacity. The increasing trend between capacity and muscle asymmetry was observed in medius, minimus, sartorius and tensor fascia latae. Although there was not a linear trend between the increase between the capacities and reductions. When the medius and minimus were over or close to maximum capacity, tensor fascia latae and sartorius maxed out as well as a minor increasing trend was seen in gluteus maximus.

Compensatory Action by Surrounding Muscles

In order to compensate for the abductor weakness created in the medius and minimus, other muscles especially secondary abductors were peaking with high forces for small durations. (Damm et al., 2018). This is caused due to the compensatory synergistic action by other muscles such as flexors and extensors spanning the hip. Valente et al. (2013) reported for the first peak, concurrent induction of hip forces may result from marked compensatory actions for the anterior and medial gluteus maximus compartments to act as back up forces for weak abductors. As maximus is part of the extensors resulting in their increased action further contributing to increased action by the flexors. More flexor force is required in order restore the muscular balance during the gait cycle at the weight bearing hip joints in the sagittal plane. From the flexor muscle group, rectus femoris was recruited by the optimization criterion. However, Valente et al. (2013) also reported a decrease in iliopsoas which was not seen in the present study. The compensation of hip abductor muscle weakness is conducted with assumptions of motor control strategy optimal conditions in muscle force calculations. (Thelen and Anderson, 2006). Furthermore, movement alterations can be caused in the lower extremity due to end-stage OA at various lower extremity joints resulting in compensatory gait mechanics. (Schmitt et al., 2015)

6.4.4 Comparison to Literature Review

The mean resultant peak HCF on the affected hip was 3.09 ± 1.53BW which was also close to the subject-specific simulation by Fischer et al. (2018) of 2.71BW ±0.33BW for OA patients. Furthermore, comparison to in vivo data from instrumented implants for the same patients were lower HCF; 2.55BW ±0.27BW (Fischer *et al.*, 2018). Indicating that musculoskeletal modelled results are higher compared to in vivo data. Patients with contralateral hip THA had a mean HCF of 3.2BW also being close to Fischer et al., (2018) in vivo and modelled forces.

Musculoskeletal modelling forces by previous studies for healthy subjects have been ranging between 3.0 to 6.0BW. (Weinhandl et al., 2017, Giarmatzis et al., 2015, Crowninshield et al., 1974). For most patients, forces measured in this study both hips were within that range but for other patients (AF & BA) were lower for affected hip.

As different patients had varying speeds between 0.3m/s to 0.98m/s, this could have been an influence on the varying resultant HCF. A previous study conducted by Rydell (1966) with instrumented strain gauge prosthetics reported the forces at different speeds 0.9m/s to 1.4m/s with measured forces ranging between 1.59BW to 3.3BW. In this study, the slow gait speed (0.3m/s) was associated with lower peak HCF (1.3BW) and similarly faster gait speed (0.98m/s) with higher peak HCF (5.4BW). Although, in comparison to Rydell (1996) study HCF, patients RH & SP and BA & JO had higher forces for affected and contralateral hip, respectively by approximately 1.0BW – 2.0BW. However, the results from present study for most of the patients was within the range for varying gait speeds reported by the Weinhandl et al. (2017) study. The resultant second peak hip contact forces calculated for slow, normal and fast speeds were 4.41 to 4.61 and 4.88 BW, respectively for musculoskeletal modelling. (Weinhandl et al., 2017)

Measured HCF from this study were also similar to the other literature values for both in vivo and modelling. G Bergmann et al. (1993) showed peak HCF at 3.5BW at 0.83m/s compared to 2.98BW at 0.72m/s with a musculoskeletal modelling approach by O'Connor et al. (2018).

Previous studies also have shown that impaired gait cycles are associated with higher in vivo HCF (Bergmann et al., 2001, Bergmann et al.,1993; Schwachmeyer et al., 2013). However, this is only true for some patients as impaired gait cycle also resulted from limping on the contralateral leg. In the patient014 SP case, this statement could be true as there was not much change in the gait pattern, but the peak resultant forces were still high (5.38BW).

Individual Muscle forces

The reported muscle forces for healthy subjects were within the same range (Van Der Krogt et al., 2012). The mean muscle force average for six patients show a good correlation with the reported data for medius (777N), minimus (225N), maximus (167N) and iliopsoas (451N). The reported value was higher were medius (1000N) and iliopsoas (800N) but the same for minimus (200N) and maximus (220N). The force variation could be due to present study conducted with end stage OA patients. The pattern of the muscle activation (Appendix D-8) during gait cycle varied between patient and between present study and Van Der Krogt et al. (2012) study. Iliopsoas was higher compared to all other patients with a slightly different trend but peaking close to the same force (1000N) as Van Der Krogt et al. (2012) study.

Valente et al. (2013) reported abductor weakness with healthy subjects mean peak hip force; first peak 4.21BW and second peak at 4.64BW. All asymmetry models resultant HCF were peaking approximately close to the reported values (Valente et al., 2013). Although some models (patient 016 AF and 046 BA) were as low as 1.4 to 1.9BW for resultant HCF.

Chapter 7

7 Discussion

The objective of this thesis was to develop a method to predict the resultant HCF for introducing abductor muscle asymmetry. The muscle asymmetry was created through manipulating the maximum isometric forces for gluteus medius and minimus. The impact was also analysed on the directional forces (anterior – posterior) as well as individual muscle forces. The study was conducted in three phases analysing scaling methods, maximum isometric forces followed by impact of muscle asymmetry on resultant HCF.

First two studies showed there was an influence of different scaling methods and maximum isometric forces. Furthermore, the maximum isometric forces also influence the resultant HCF and individual muscle forces. The resultant peak HCF gait2392 model from study one (Section 4.6) which was linearly scaled were lower (3.3BW) compared to gait2392 model (4.1BW) which was statistically scaled in study two. Observing the gait2392 model force capacity and muscle forces from study one (Section 4.6) were slightly lower compared to statistical gait2392 model for both gluteus medius and minimus. Further indicating the difference between the two different scaling methods influencing the resultant HCF and muscle forces. The first study results showed higher resultant HCF for the Bahl model compared to gait2392. But further research conducted into the Bahl model showed it was more accurate and suited for this study. The first two studies led to using the Bahl model (Bahl et al., 2019) with maximum isometric forces reported by Delp (1990).

The final study showed that influence of abductor muscle asymmetry on the patients is very case dependent where increase, decrease and no change was present within different patients.

Although data was variable across different patients some supporting conclusions could be made. The main compensating muscles due to increased muscle asymmetry were secondary abductors. While some patients where medius and minimus reached over force capacity, extensors and flexors were also compensating. There were also a significant impact of gait patterns and speed on resultant HCF seen in some patients. This showed first and second order impacts on each patient was different.

7.1 Muscle Fatigue

Muscle fatigue can be defined as reduction in maximal isometric force in response to the muscle contractile activity (Gandevia, 2001). Failure at sites along the force production pathway of central nervous system to the contractile apparatus can cause fatigue during muscle contraction (Davies et al, 1986) The gluteal medius provides stability on the mediolateral (ML) side (Winther *et al.*, 2016) as well as maintenance of centre of mass (COM) during single limb supporting in the gait cycle. It is also responsible for initiation and execution of weight transfer (Pai et al., 1994). Damage to the function of medius influence the hip abduction movement and can lead to poor postural control as well as hip external rotation (Cichanowski et al., 2007). In the late stance phase of the gait cycle, gluteus medius pulls the COM back inwards when it tries to move outwards due to gravity hence, restoring the postural control.

Hip abductor fatigue leads to decrease in postural control ability hence, compensation takes place for neuromuscular adaption. Therefore, for the patients that are reaching capacity for their abductor muscles might go through fatigue further resulting in instability and difficulty performing daily activities. As hip abductors are related to quality of balance as well as gait patterns. (Wan *et al.*, 2017) Loss of muscle strength and central activation failure can further cause decreased proprioceptive acuity and muscular output.(Edwards, 1981)

Impairment of gait control in the ML direction may be a consequence of hip abductor weakness.(Arvin *et al.*, 2015) ML balance control impairment and hip abductor weakness may also be a possible reason for hip fractures from sideway falls in older adults (Greenspan *et al.*, 1998) As OA patients have fatty infiltration and muscle atrophy, there may be a higher risk of possible dislocation of implant as a result of the side fall. Arvin et al. (2015) study reported hip joint repositioning decrease resulted in an increased absolute error due to fatigue further suggesting muscle spindle afferents dysfunction. Arvin et al. (2015) further reported healthy subjects with increased stride variability, ML symmetry decrease and lower peak ML trunk velocity in the fatigued leg.

Present study showed for majority of the 60% muscle asymmetry cases the primary and secondary abductor muscles were reaching or over capacity. This may result in fatigue of the muscles therefore patients getting tired more easily. This will also result in patients only being able to conduct daily activities for short span of time also reducing stability. These factors should be considered while conducting balance and gait training after the THA (Wan et al., 2017). Furthermore, increased load on the muscles can also lead to muscle damage. Which can also lead to further muscle weakening and increased compensations by other muscles. (van der Kroght et al., 2012)

7.2 Affected OA Hip THA

Nielsen & Ortenblad (2013) compared early stage THA with age matched control subjects. The THA patients had slow gait speed, shortened stride length, decreased cadence and trunk lateral displacement increase. Hence, THA patients walk using compensation due to hip abductor weakness and limited mobility. Therefore, post THA in present study patients may still have impaired or further impairment of gait cycle might also results in comparison to end stage preop. Furthermore, gait remains abnormal one year after THA (Foucher et al., 2007; Foucher & Wimmer, 2012) therefore the gait cycle post one year of THA in the affected hip may still not recover.

Temporiti et al., (2019) reported longer stance and shorter swing phase for bilateral compared to unilateral THA patients. This could be due to reduction in push off during the pre-swing phase of the contralateral THA hip. In comparison to the unilateral patients, unaffected

contralateral hip propulsion influenced the stance phase duration on the affected THA hip. The propulsion reduction of THA hip may last for several year (Kubonova et al., 2016). The bilateral hip also restored more physiological pelvic kinematics. (Temporiti et al., 2019). The same trend may be seen in the present study post THA where some patients (009,014 & 016) will be bilateral and other (044, 046 & 051) will be unilateral hip replacement.

Damm et al (2018) reported higher in vivo HCF post 3 months due to gluteal muscle damage. As gluteal minimus lean muscle volume decrease was strongly correlated with high in vivo joint contact forces in all daily activities. It can be predicted; present study patients could have higher HCF due to further gluteal muscle damage post THA.

7.3 Muscle Volume & Strength

As there is further damage to muscles during THA especially to abductor muscle using certain surgical methods such as DLA. In the worst-case scenario (60%), risk of implant failure may be increased with higher resultant HCF. The reduction in volume of certain hip muscles can continue according to previous studies. Rasch et al. (2009) reported reduction in cross-sectional area of iliopsoas (7%). There was a persistent muscle atrophy post 2 years of THA in the hip muscles (Rasch *et al*., 2009). Reported 6% muscle weakness compared to contralateral healthy hip. Furthermore, preoperatively deficits were 18% compared to 6 months preoperative of 12% deficit. Hence, although muscle weakness was improved but deficits remained. Volume reduction (CSA) was 8.4% for abductors post 2 years of THA compared to the healthy hip. (Rasch *et al.*, 2009) Similar studies conducted to measure the hip muscle strength post long term THA have reported, there was muscle recovery, but strength remained lower compared to pre-operational and unaffected contralateral hip. (Fukumoto *et al*., 2013; Rasch *et al*., 2010).

The patients undergoing THA may reduce further in abductor muscle strength, however recovery can occur, but pre-operative muscle strength may not be achieved. The impact of further reduction post THA can be representative of the 60% model. As discussed in Section 6.5.1, majority of the patients were impacted significantly by the 60% reduction in medius and minimus.

7.4 Implant Dislocation

Hip instability is one of the main complications resulting from THA and common causes of early revision. (Eftekhar, 1976; Lindberg *et al.*, 1982) One of the reasons for dislocation and revision THA is weakness in hip abductors reported in studies (Brooks, 2013; Zahar, Rastogi and Kendoff, 2013)

As for one of the patients, a directional change in anterior to posterior was present due to abductor weakness. This can also increase the dislocation probability as it is one of the most common result to implant failure. Some of the patients already have a THA on the contralateral hip. There might be higher risk of dislocation of these patients as there is abductor weakness on both sides with bilateral THA.

Chapter 8

8 Limitations

The study also had limited number of patients (6 patients) with variations in BMI and age. Also, some patients had hip replacement on the contralateral hip therefore that was assumed as unaffected hip. As discussed in section 6.5.1, there are variations between the resultant HCF between patients. Further information regarding other diseases in the leg was not accessible about the patients which could have resulted in high HCF.

Another limitation to the study was both gluteus medius and minimus were scaled with the same uniform scaling ratio. Another limitation regarding the scaling was linear scaling for used with an assumption of accuracy and best method. The anatomical statistical scaling was also assumed to be an accurate method. The patients were end stage OA patient, they already had weakness in their hip muscles either through fatty infiltration, volume deficit and further strength reduction due to limited mobility caused by pain. Therefore, additional asymmetry was added but the previous muscle weakness wasn't accounted for.

The gait speed for all patients varied due to being self-selected. Moreover, it has been reported by various studies there is an influence of gait speed on HCF (Rydell, 1996). Therefore, in this study conclusions about the data trend could not be made.

Another major limitation was only gait level was modelled therefore other daily activities could not be analysed. Although the impact of other daily activities on resultant HCF and muscle activity were discussed and predicted (Section 7.3).

Decreased loading of the hip also induced overloading of the knee. (Van Der Kroght et al. 2012). Hip joint loading was analysed in the present study, but the effect of abductor weakness was not evaluated in the knee joint. This could have been the case for Patients 014 (Section 6.4.2) where a decrease was present as the abductor weakness was increased.

One of the main assumptions set by OpenSim of the direct correlation between muscle strength and muscle volume could also be a limitation. This is due to the impact of muscle training can results in increased muscle strength without the change in muscle volume. This should be considered if future studies are carried out with directly measuring the patient muscle volume and converting it to muscle strength. Surveys should be conducted with the patients regarding their previous physical activities and muscle training.

Chapter 9

9 Conclusion

9.1 Summary of Findings

This study has been one of the few to model muscle asymmetry using musculoskeletal modelling to predict resultant HCF and individual muscle forces. The aim of this thesis was to analyse the impact of abductor asymmetry on the peak resultant HCF, individual muscle and directional forces in osteoarthritis. The abductor muscle asymmetry was introduced through changing the maximum isometric forces in OpenSim assigned to each muscle. The focus key muscles for muscle weakness were gluteus medius and gluteus minimus. This thesis comprised of three phase study to analyse the appropriate scaling methods, maximum isometric forces and impacts of abductor asymmetry on the resultant HCF.

Study one results showed higher forces for the statistical shape Bahl model but after further analysing it was chosen for the other phases. Followed by study two conducted with Bahl model with four different maximum isometric forces reported by studies were analysed. The most appropriate model was Delp model which was used in study three to evaluate with induced muscle weakness.

The results for the resultant peak HCF in some patients were not significantly affected due to increase in abductor muscle asymmetry. There was a significant increase (+1.0BW) for

patient009 RH and 044 JS from the base model to 60% reduction. While, major decrease was present in peak resultant HCF of patient 014 SP (-1.0BW) in the 60% comparison to base model. This was due to compensation by the individual muscles taking over for the weak abductors. The results suggest, only some patients were able to withstand the muscle weakness due to compensation by other muscles. The available used force capacity increased in gluteus medius, minimus, maximus and tensor fascia latae in all the patients with increase in muscle asymmetry.

There were minor correlations seen within some patients between gait speed and resultant peak HCF but could not draw firm conclusions. The slower speeds were associated with lower peak HCF, but this was only true for some patients. There were many other factors that could have impacted the change in the HCF (Section 8.0). There was correlation between results from previous and present study showing the flexors and extensors compensating in majority of the patients as an impact of abductor weakness.

The significance of this study was a contribution to the method for introducing asymmetry in OpenSim musculoskeletal modelling software. This study has shown the need to assess OA patients individually with introducing abductor muscle asymmetry as resultant HCF were case dependent. The present study has also shown the requirement to further assess patient specific muscle volume and fatty infiltration for accurate estimation of resultant HCF and muscle forces. Additionally, this study can be used to design and study resultant HCF in end-stage OA patients awaiting to undergo hip replacement.

9.2 Future Recommendations

1. Effect of Asymmetry

Present study modelled 20, 40 and 60% abductor muscle asymmetry that represented mid-range, upper range and worst case of that in the reported values. In the future work, asymmetry can be analysed between 12 to 20% (Arokoski et al., 2002; Rasch et al., 2007; Ikeda et al., 2005) for every 2% in volume reduction increments. This CSA volume reduction range could also be tested with logarithmic increments. Further sensitivity tests can involve 90 to 95% reduction in maximum isometric forces for medius and minimus. Valente et al. (2013) also tested combinations of muscle weakness within medius, minimus and tensor fascia latae for healthy individuals. Therefore, this could also be incorporated within future studies as all abductor muscles will not have a linear muscle weakness.

2. Muscles Surrounding the Hip

Diverse studies have reported other muscles such as flexors and extensors also undergo muscle atrophy during OA. Therefore, future study can include also introducing muscle asymmetry within other muscles surrounding the hip. Van der Kroght et al. (2012) reported muscle cost (capacity) increased with weakness of plantar flexors, medius and iliopsoas. Significant variability of the muscle cost was also found influenced by the muscle reduced. Weakness in the iliopsoas resulted in an increased rectus femoris activation further led to increased knee flexor activation. (van der Kroght et al., 2012). Loureiro et al. (2018) measured muscle asymmetry within the flexors and extensors showing muscle volume and strength reduction across other knee and hip muscles as well. Further tests for future studies can include asymmetry models with primary; medius and minimus and secondary abductor muscles; tensor fascia latae, maximus, rectus femoris to analyse compensatory effects by other muscles.

3. Knee and Ankle Resultant Contact Forces

Various studies have investigated hip and knee contact forces while investigating hip muscle weakness. Van Der Kroght et al. (2012) results showed compensation of biceps femoris and gastrocnemius forces for maintenance of balance at the knee. The decrease of hip joint loading resulted in increased overloading at the knee joint (section 8.0). Also, gastrocnemius forces increase induced ankle force magnitude increase but balanced by a decrease in soleus force. As the abductor weakness also influences the knee and ankle loading, it should be evaluated in the future studies.

4. **Patient Specific Volume and Fatty Infiltration**

Future studies should be conducted with patient specific fatty infiltration and muscle volume captured by CT scans for the calculation of maximum isometric forces. (Zacharias *et al.*, 2016) As it has been discussed by previous studies and present study (6.5.1). The affected of muscle reduction on the individual and resultant forces. Therefore, it is very important to have individual patient muscle volume calculation for accuracy. Damm et al. (2018) observed a positive trend within gluteal muscles with increase fat ratio correlating with increased joint contact forces. Rahemi et al. (2015) and Daguet et al. (2011) have described high fat ratio as a clinical substitute predictor for muscle function. This could be due to increase in muscle stiffness resulting in decreasing forces. Fatty infiltration is also impacted by age, physical activity and obesity. Most of the patients are overweight and one being obese therefore this may impact the HCF highly. Therefore, these factors need to be evaluated correctly in order to conduct an accurate evaluation.

5. **EMG Data Correlation**

EMG data for the muscles could be conducted in the future studies to compare the musculoskeletal model data with the collected. The muscle activations were compared with previous studies, but the patients were different. In order to draw firmer conclusions, muscle activation need to be comparison need to be conducted with the modelled data.

6. **Daily Activities Models**

Present study only had data modelled for level gait where resultant HCF were not greatly impacted for majority of the patients even with 60% reduction. Even though prediction based

on previous studies was made in section 7.3.1 for all patients. Activities such as sitting, standing and stair climbing are most commonly conducted therefore resultant HCF need to be measured to analyse the influence of abductor asymmetry on different activities. There might also be increased dislocation risk in activities such as stair climbing compared to walking.

7. Measurement of Fatigue and Pain Pre-operative and Post-operative THA

In future studies, measurement of fatigue and pain through different methods such as surveys should be conducted. Both pre-operative and post-operative data of fatigue and pain might assist in making stronger conclusions about each patient. Some of the patients in the present study had a different trend to reported data therefore fatigue and pain might be the reason for impaired gait cycle and high HCF.

8. Gait Speed Data

One of the limitations of this study was variations between patients gait speed as it was self-selected. Future studies need to be carried out with collecting a larger sample size where similar speeds can be achieved to make firm correlations with the resultant HCF and gait speed.

10 References

A. Navacchia, C. Myers, P.J. Rullkoetter, K. B. S. (2015) 'Prediction of In Vivo Knee Joint Loads Using a Global Probabilistic Analysis', *Journal of biomechanical engineering*, 138(3), p. 4032379. doi: 10.1115/1.4032379.

Adolphson, P. *et al.* (1993) 'Bone and muscle mass after hip arthroplasty: A quantitative computed tomography study in 20 arthrosis cases', *Acta Orthopaedica*. doi: 10.3109/17453679308994566.

Amaro, A. *et al.* (2008) 'Gluteus Medius Muscle Atrophy is Related to Contralateral and Ipsilateral Hip Joint Osteoarthritis', *International journal of sports medicine*, 28, pp. 1035–1039. doi: 10.1055/s-2007-965078.

Andary, M. T. *et al.* (1998) 'Neurogenic atrophy of suboccipital muscles after a cervical injury', *American Journal of Physical Medicine and Rehabilitation*. doi: 10.1097/00002060-199811000-00019.

Anderson, F. C. and Pandy, M. G. (1999) 'A dynamic optimization solution for vertical jumping in three dimensions', *Computer Methods in Biomechanics and Biomedical Engineering*. doi: 10.1080/10255849908907988.

Anderson, F. C. and Pandy, M. G. (2003) 'Individual muscle contributions to support in normal walking', *Gait and Posture*. doi: 10.1016/S0966-6362(02)00073-5.

Arnold, C. M. and Faulkner, R. A. (2010) 'The effect of aquatic exercise and education on

lowering fall risk in older adults with hip osteoarthritis', *Journal of Aging and Physical Activity*. doi: 10.1123/japa.18.3.245.

Arokoski, M. H. *et al.* (2002) 'Hip muscle strength and muscle cross sectional area in men with and without hip osteoarthritis', *Journal of Rheumatology*.

Arvin, M. *et al.* (2015) 'Effects of hip abductor muscle fatigue on gait control and hip position sense in healthy older adults', *Gait and Posture*. doi: 10.1016/j.gaitpost.2015.08.011.

Associates., T. O. (2019) *Hip Joint Preservation*. Available at: https://www.towsonortho.com/specialties/joint-preservation-center/hip-joint-preservation/.

Attum, B. and Varacallo, M. (2018) *Anatomy, Bony Pelvis and Lower Limb, Thigh Muscles*, *StatPearls*.

Bahl, J. S. *et al.* (2018) 'Biomechanical changes and recovery of gait function after total hip arthroplasty for osteoarthritis: a systematic review and meta-analysis', *Osteoarthritis and Cartilage*, 26(7), pp. 847–863. doi: https://doi.org/10.1016/j.joca.2018.02.897.

Bahl, J. S. *et al.* (2019) 'Statistical shape modelling versus linear scaling: Effects on predictions of hip joint centre location and muscle moment arms in people with hip osteoarthritis', *Journal of Biomechanics*. doi: 10.1016/j.jbiomech.2019.01.031.

Barre, A. and Armand, S. (2014) 'Biomechanical ToolKit: Open-source framework to visualize and process biomechanical data', *Computer Methods and Programs in Biomedicine*. doi: 10.1016/j.cmpb.2014.01.012.

Berchtold, M. W., Brinkmeier, H. and Müntener, M. (2000) 'Calcium Ion in Skeletal Muscle: Its Crucial Role for Muscle Function, Plasticity, and Disease', *Physiological Reviews*. American Physiological Society, 80(3), pp. 1215–1265. doi: 10.1152/physrev.2000.80.3.1215.

Bergmann, G. *et al.* (1988) 'Multichannel strain gauge telemetry for orthopaedic implants', *Journal of Biomechanics*, 21(2), pp. 169–176. doi: https://doi.org/10.1016/0021-9290(88)90009-7.

Bergmann, G. *et al.* (1995) 'Influence of shoes and heel strike on the loading of the hip joint', *Journal of Biomechanics*, 28(7), pp. 817–827. doi: https://doi.org/10.1016/0021-

9290(94)00129-R.

Bergmann, G. *et al.* (1997) 'Hip joint forces during load carrying', *Clinical orthopaedics and related research*, (335), p. 190—201. Available at: http://europepmc.org/abstract/MED/9020218.

Bergmann, G. *et al.* (2001) 'Hip contact forces and gait patterns from routine activities', *Journal of Biomechanics*, 34(7), pp. 859–871. doi: https://doi.org/10.1016/S0021-9290(01)00040-9.

Bergmann, G. *et al.* (2016) 'Standardized loads acting in hip implants', *PLoS ONE*. doi: 10.1371/journal.pone.0155612.

Bergmann, G., Graichen, F. and Rohlmann, A. (1993) 'Hip joint loading during walking and running, measured in two patients', *Journal of Biomechanics*, 26(8), pp. 969–990. doi: https://doi.org/10.1016/0021-9290(93)90058-M.

Bergmann, G., Graichen, F. and Rohlmann, A. (1995) 'Is staircase walking a risk for the fixation of hip implants?', *Journal of Biomechanics*, 28(5), pp. 535–553. doi: https://doi.org/10.1016/0021-9290(94)00105-D.

Bergmann, G., Graichen, F. and Rohlmann, A. (2004) 'Hip joint contact forces during stumbling', *Langenbeck's Archives of Surgery*, 389(1), pp. 53–59. doi: 10.1007/s00423-003-0434-y.

Bertocci, G. E. *et al.* (2004) 'Isokinetic Performance after Total Hip Replacement', *American Journal of Physical Medicine and Rehabilitation*. doi: 10.1097/01.PHM.0000098047.26314.93.

Bijlsma, J. W. J., Berenbaum, F. and Lafeber, F. P. J. G. (2011) 'Osteoarthritis: an update with relevance for clinical practice.', *Lancet (London, England)*. England, 377(9783), pp. 2115–2126. doi: 10.1016/S0140-6736(11)60243-2.

Bonnefoy-Mazure, A. and Armand, S. (2015) 'Normal gait', in *Orthopedic Management of Children with Cerebral Palsy: A Comprehensive Approach*. doi: 10.1016/b978-075068883-3.50007-6.

Brooks, P. J. (2013) 'Dislocation following total hip replacement: causes and cures', *The*

bone & joint journal. doi: 10.1302/0301-620X.95B11.32645.

Byrne, D., J. Mulhall, K. and Baker, J. (2010) 'Anatomy & Biomechanics of the Hip', *The Open Sports Medicine Journal*, 4. doi: 10.2174/1874387001004010051.

Carbone, V. *et al.* (2016) 'Sensitivity of subject-specific models to Hill muscle-tendon model parameters in simulations of gait', *Journal of Biomechanics*. doi: 10.1016/j.jbiomech.2016.04.008.

Carhart, M. and Yamaguchi, G. (2000) 'Biomechanical analysis of compensatory stepping: implications for paraplegics standing via functional neuromuscular stimulation', *Annals of Biomedical Engineering*.

Castaño-Betancourt, M. C. *et al.* (2013) 'Bone parameters across different types of hip osteoarthritis and their relationship to osteoporotic fracture risk', *Arthritis and Rheumatism*. doi: 10.1002/art.37792.

Chi, A. S. *et al.* (2015) 'Prevalence and pattern of gluteus medius and minimus tendon pathology and muscle atrophy in older individuals using MRI', *Skeletal Radiology*. doi: 10.1007/s00256-015-2220-7.

Chiu, S. L., Lu, T. W. and Chou, L. S. (2010) 'Altered inter-joint coordination during walking in patients with total hip arthroplasty', *Gait and Posture*. doi: 10.1016/j.gaitpost.2010.09.015.

Cichanowski, H. R. *et al.* (2007) 'Hip strength in collegiate female athletes with patellofemoral pain', *Medicine and Science in Sports and Exercise*. doi: 10.1249/mss.0b013e3180601109.

Cleather, D. J., Goodwin, J. E. and Bull, A. M. J. (2013) 'Hip and knee joint loading during vertical jumping and push jerking', *Clinical biomechanics (Bristol, Avon)*. 2012/11/10, 28(1), pp. 98–103. doi: 10.1016/j.clinbiomech.2012.10.006.

Colgan, G. *et al.* (2016) 'Gait analysis and hip extensor function early post total hip replacement', *Journal of Orthopaedics*, 13(3), pp. 171–176. doi: https://doi.org/10.1016/j.jor.2016.03.005.

Constantinou, M. *et al.* (2014) 'Spatial- Temporal gait characteristics in individuals with hip

osteoarthritis: A systematic literature review and meta- Analysis', *Journal of Orthopaedic and Sports Physical Therapy*. doi: 10.2519/jospt.2014.4634.

Correa, T. A. and Pandy, M. G. (2011) 'A mass–length scaling law for modeling muscle strength in the lower limb', *Journal of Biomechanics*, 44(16), pp. 2782–2789. doi: https://doi.org/10.1016/j.jbiomech.2011.08.024.

Cucchiarini, M. *et al.* (2016) 'Basic science of osteoarthritis', *Journal of experimental orthopaedics*. 2016/09/13. Springer Berlin Heidelberg, 3(1), p. 22. doi: 10.1186/s40634-016-0060-6.

Daguet, E. *et al.* (2011) 'Fat content of hip muscles: An anteroposterior gradient', *Journal of Bone and Joint Surgery - Series A*. doi: 10.2106/JBJS.J.00509.

Damm, P. *et al.* (2017) 'In vivo hip joint loads and pedal forces during ergometer cycling', *Journal of Biomechanics*, 60, pp. 197–202. doi: https://doi.org/10.1016/j.jbiomech.2017.06.047.

Damm, P. *et al.* (2018) 'Gluteal muscle damage leads to higher in vivo hip joint loads 3 months after total hip arthroplasty', *PLoS ONE*. doi: 10.1371/journal.pone.0190626.

DAVIES, C. T. M., THOMAS, D. O. and WHITE, M. J. (1986) 'Mechanical Properties of Young and Elderly Human Muscle', *Acta Medica Scandinavica*. doi: 10.1111/j.0954-6820.1986.tb08954.x.

Davy, D. T. *et al.* (1988) 'Telemetric force measurements across the hip after total arthroplasty', *Journal of Bone and Joint Surgery - Series A*. doi: 10.2106/00004623-198870010-00008.

Delaunay, C. *et al.* (2013) 'What are the causes for failures of primary hip arthroplasties in France?', in *Clinical Orthopaedics and Related Research*. doi: 10.1007/s11999-013-2935-5.

Delp, S. L. (1990) *Surgery Simulation: A computer graphics system to analyze and design musculoskeletal reconstructions of the lower extremity*, *Ph.D. Dissertation*. Stanford University.

Delp, S. L. *et al.* (2007) 'OpenSim: Open-Source Software to Create and Analyze Dynamic Simulations of Movement', *IEEE Transactions on Biomedical Engineering*, 54(11), pp.

1940–1950. doi: 10.1109/TBME.2007.901024.

Dibonaventura, M. D. *et al.* (2011) 'Evaluating the health and economic impact of osteoarthritis pain in the workforce: Results from the National Health and Wellness Survey', *BMC Musculoskeletal Disorders*. doi: 10.1186/1471-2474-12-83.

Drake, R. L. (2005) *Gray's anatomy for students*, *Anatomy for students*. Edited by A. W. M. Mitchell, W. Vogl, and H. Gray. Philadelphia: Philadelphia : Elsevier/Churchill Livingstone.

Drake, R. L., Vogl, A. W. and Mitchell, A. W. . (2015) 'Gray's Anatomy for Students, Third Edition', *Gray's Anatomy for Students*. doi: 10.1017/CBO9781107415324.004.

Edwards, R. H. (1981) 'Human muscle function and fatigue.', *Ciba Foundation symposium*.

Eftekhar, N. S. (1976) 'Dislocation and instability complicating low friction arthroplasty of the hip joint', *Clinical Orthopaedics and Related Research*, (121), pp. 120–125. Available at: http://europepmc.org/abstract/MED/991492.

Eitzen, I. *et al.* (2015) 'Gait characteristics, symptoms, and function in persons with hip osteoarthritis: A longitudinal study with 6 to 7 years of follow-up', *Journal of Orthopaedic and Sports Physical Therapy*. doi: 10.2519/jospt.2015.5441.

Felson, D. T. (2013) 'Osteoarthritis as a disease of mechanics', *Osteoarthritis and Cartilage*, 21(1), pp. 10–15. doi: https://doi.org/10.1016/j.joca.2012.09.012.

Fischer, M. C. M. *et al.* (2018) 'Patient-specific musculoskeletal modeling of the hip joint for preoperative planning of total hip arthroplasty: A validation study based on in vivo measurements', *PLoS ONE*. doi: 10.1371/journal.pone.0195376.

Flack, N. A. M. S., Nicholson, H. D. and Woodley, S. J. (2012) 'A review of the anatomy of the hip abductor muscles, gluteus medius, gluteus minimus, and tensor fascia lata', *Clinical Anatomy*. John Wiley & Sons, Ltd, 25(6), pp. 697–708. doi: 10.1002/ca.22004.

Folland, J. P., Mc Cauley, T. M. and Williams, A. G. (2008) 'Allometric scaling of strength measurements to body size', *European Journal of Applied Physiology*, 102(6), pp. 739–745. doi: 10.1007/s00421-007-0654-x.

Foucher, K. C., Hurwitz, D. E. and Wimmer, M. A. (2007) 'Preoperative gait adaptations

persist one year after surgery in clinically well-functioning total hip replacement patients', *Journal of Biomechanics*. doi: 10.1016/j.jbiomech.2007.05.020.

Foucher, K. C. and Wimmer, M. A. (2012) 'Contralateral hip and knee gait biomechanics are unchanged by total hip replacement for unilateral hip osteoarthritis', *Gait and Posture*. doi: 10.1016/j.gaitpost.2011.08.006.

Fukumoto, Y. *et al.* (2013) 'Changes in hip and knee muscle strength in patients following total hip arthroplasty', *Journal of the Japanese Physical Therapy Association = Rigaku ryoho*. JAPANESE PHYSICAL THERAPY ASSOCIATION, 16(1), pp. 22–27. doi: 10.1298/jjpta.Vol16_002.

Gandevia, S. C. (2001) 'Spinal and supraspinal factors in human muscle fatigue', *Physiological Reviews*. doi: 10.1152/physrev.2001.81.4.1725.

Giarmatzis, G. *et al.* (2015) 'Loading of Hip Measured by Hip Contact Forces at Different Speeds of Walking and Running', *Journal of Bone and Mineral Research*, 30(8), pp. 1431–1440. doi: 10.1002/jbmr.2483.

Givens-Heiss, D. L. *et al.* (1992) 'In Vivo Acetabular Contact Pressures During Rehabilitation, Part II: Postacute Phase', *Physical Therapy*. doi: 10.1093/ptj/72.10.700.

Goodpaster, B. H. *et al.* (2008) 'Effects of physical activity on strength and skeletal muscle fat infiltration in older adults: A randomized controlled trial', *Journal of Applied Physiology*. doi: 10.1152/japplphysiol.90425.2008.

Gottschalk, F., Kourosh, S. and Leveau, B. (1989) 'The functional anatomy of tensor fasciae latae and gluteus medius and minimus.', *Journal of anatomy*.

Graichen, F. and Bergmann, G. (1991) 'Four-channel telemetry system for in vivo measurement of hip joint forces', *Journal of Biomedical Engineering*, 13(5), pp. 370–374. doi: https://doi.org/10.1016/0141-5425(91)90016-Z.

Graichen, F., Bergmann, G. and Rohlmann, A. (1999) 'Hip endoprosthesis for in vivo measurement of joint force and temperature', *Journal of Biomechanics*, 32(10), pp. 1113–1117. doi: https://doi.org/10.1016/S0021-9290(99)00110-4.

Greenspan, S. L. *et al.* (1998) 'Fall direction, bone mineral density, and function: Risk factors

for hip fracture in frail nursing home elderly', *American Journal of Medicine*. doi: 10.1016/S0002-9343(98)00115-6.

Grimaldi, A. *et al.* (2009) 'The association between degenerative hip joint pathology and size of the gluteus maximus and tensor fascia lata muscles', *Manual Therapy*. doi: 10.1016/j.math.2008.11.002.

Hurwitz, D. E. *et al.* (1997) 'Gait compensations in patients with osteoarthritis of the hip and their relationship to pain and passive hip motion', *Journal of Orthopaedic Research*. doi: 10.1002/jor.1100150421.

Husted, H. *et al.* (1996) 'Need for bilateral arthroplasty for coxarthrosis. 1,477 replacements in 1,199 patients followed for 0-14 years', *Acta Orthopaedica Scandinavica*. doi: 10.3109/17453679608996660.

Jaric, S. (2002) 'Muscle Strength Testing', *Sports Medicine*, 32(10), pp. 615–631. doi: 10.2165/00007256-200232100-00002.

Kadi, F. *et al.* (2004) 'Satellite cells and myonuclei in young and elderly women and men', *Muscle and Nerve*. doi: 10.1002/mus.10510.

Kainz, H. *et al.* (2017) 'Accuracy and reliability of marker-based approaches to scale the pelvis, thigh, and shank segments in musculoskeletal models', *Journal of Applied Biomechanics*. doi: 10.1123/jab.2016-0282.

Knarr, B. A. *et al.* (2013) 'Muscle volume as a predictor of maximum force generating ability in the plantar flexors post-stroke', *Muscle & Nerve*. doi: 10.1002/mus.23835.

Kovalak, E. *et al.* (2018) 'Assessment of hip abductors by MRI after total hip arthroplasty and effect of fatty atrophy on functional outcome', *Acta Orthopaedica et Traumatologica Turcica*. doi: 10.1016/j.aott.2017.10.005.

Krebs, D. E. *et al.* (1998) 'Hip biomechanics during gait', *Journal of Orthopaedic and Sports Physical Therapy*. doi: 10.2519/jospt.1998.28.1.51.

van der Krogt, M. M., Delp, S. L. and Schwartz, M. H. (2012) 'How robust is human gait to muscle weakness?', *Gait and Posture*. doi: 10.1016/j.gaitpost.2012.01.017.

Kumagai, M. *et al.* (1997) 'Functional evaluation of hip abductor muscles with use of magnetic resonance imaging', *Journal of Orthopaedic Research*. doi: 10.1002/jor.1100150615.

Kurtz, S. *et al.* (2007) 'Projections of primary and revision hip and knee arthroplasty in the United States from 2005 to 2030.', *The Journal of bone and joint surgery. American volume*. United States, 89(4), pp. 780–785. doi: 10.2106/JBJS.F.00222.

Lane, N. E. (2007) 'Osteoarthritis of the hip', *New England Journal of Medicine*. doi: 10.1056/NEJMcp071112.

Lenaerts, G. *et al.* (2008) 'Subject-specific hip geometry affects predicted hip joint contact forces during gait', *Journal of Biomechanics*, 41(6), pp. 1243–1252. doi: https://doi.org/10.1016/j.jbiomech.2008.01.014.

Leskinen, T. *et al.* (2009) 'Leisure-time physical activity and high-risk fat: A longitudinal population-based twin study', *International Journal of Obesity*. doi: 10.1038/ijo.2009.170.

Lespasio, M. J. *et al.* (2018) 'Hip Osteoarthritis: A Primer', *The Permanente journal*. doi: 10.7812/TPP/17-084.

Li, J. *et al.* (2014) 'Hip contact forces in asymptomatic total hip replacement patients differ from normal healthy individuals: Implications for preclinical testing', *Clinical Biomechanics*, 29(7), pp. 747–751. doi: https://doi.org/10.1016/j.clinbiomech.2014.06.005.

Lindberg, H. O. *et al.* (1982) 'Recurrent and Non-Recurrent Dislocation Following Total Hip Arthroplasty', *Acta Orthopaedica Scandinavica*. Taylor & Francis, 53(6), pp. 947–952. doi: 10.3109/17453678208992853.

Loeser, R. F. *et al.* (2012) 'Osteoarthritis: a disease of the joint as an organ', *Arthritis and rheumatism*. 2012/03/05, 64(6), pp. 1697–1707. doi: 10.1002/art.34453.

Loureiro, A. *et al.* (2018) 'Individuals with mild-to-moderate hip osteoarthritis have lower limb muscle strength and volume deficits', *BMC Musculoskeletal Disorders*, 19(1), p. 303. doi: 10.1186/s12891-018-2230-4.

Lumen (2019) *Muscles of the hips and thighs*. Available at: https://courses.lumenlearning.com/ap1x94x1/chapter/muscles-of-the-hips-and-thighs/.

Lyons, K. *et al.* (1983) ‘Timing and relative intensity of hip extensor and abductor muscle action during level and stair ambulation. An EMG study’, *Physical Therapy*. doi: 10.1093/ptj/63.10.1597.

MacInnes, S., Gordon, A. and Mark Wilkinson, J. (2012) ‘Risk Factors for Aseptic Loosening Following Total Hip Arthroplasty’, in. doi: 10.5772/26975.

Madsen, O. R. *et al.* (1997) ‘Body composition and muscle strength in women scheduled for a knee or hip replacement. A comparative study of two groups of osteoarthritic women’, *Clinical Rheumatology*. doi: 10.1007/BF02238761.

Manini, T. M. *et al.* (2007) ‘Reduced physical activity increases intermuscular adipose tissue in healthy young adults’, *American Journal of Clinical Nutrition*.

Marcus, R. L. *et al.* (2010) ‘Skeletal muscle fat infiltration: Impact of age, inactivity, and exercise’, *Journal of Nutrition, Health and Aging*. doi: 10.1007/s12603-010-0081-2.

McNair, P. J. *et al.* (2009) ‘Exercise therapy for the management of osteoarthritis of the hip joint: A systematic review’, *Arthritis Research and Therapy*. doi: 10.1186/ar2743.

Miki, H. *et al.* (2004) ‘Recovery of walking speed and symmetrical movement of the pelvis and lower extremity joints after unilateral THA’, *Journal of Biomechanics*. doi: 10.1016/j.jbiomech.2003.09.009.

Modenese, L., Phillips, A. T. M. and Bull, A. M. J. (2011) ‘An open source lower limb model: Hip joint validation’, *Journal of Biomechanics*. doi: 10.1016/j.jbiomech.2011.06.019.

Müller, M. *et al.* (2011) ‘Age-related appearance of muscle trauma in primary total hip arthroplasty and the benefit of a minimally invasive approach for patients older than 70 years’, *International Orthopaedics*, 35(2), pp. 165–171. doi: 10.1007/s00264-010-1166-6.

Murray, M. P., Gore, D. R. and Clarkson, B. H. (1971) ‘Walking patterns of patients with unilateral hip pain due to osteo-arthritis and avascular necrosis.’, *The Journal of bone and joint surgery. American volume*. doi: 10.2106/00004623-197153020-00006.

Neumann PT FAPTA, D. A. (2010) *Kinesiology of the Musculoskeletal System: Foundations for Rehabilitation*, *Kinesiology of the Musculoskeletal System_Reprint*. doi: 10.1029/2007JG000640/abstract.

Ng, K. C. G. *et al.* (2018) 'Altered Walking and Muscle Patterns Reduce Hip Contact Forces in Individuals With Symptomatic Cam Femoroacetabular Impingement', *American Journal of Sports Medicine*. doi: 10.1177/0363546518787518.

Nolte, D. *et al.* (2016) 'Non-linear scaling of a musculoskeletal model of the lower limb using statistical shape models', *Journal of Biomechanics*. doi: 10.1016/j.jbiomech.2016.09.005.

O'Connor, J. D. *et al.* (2018) 'Long-term hip loading in unilateral total hip replacement patients is no different between limbs or compared to healthy controls at similar walking speeds', *Journal of Biomechanics*, 80, pp. 8–15. doi: https://doi.org/10.1016/j.jbiomech.2018.07.033.

Oberhofer, K., Lorenzetti, S. and Mithraratne, K. (2019) 'Host Mesh Fitting of a Generic Musculoskeletal Model of the Lower Limbs to Subject-Specific Body Surface Data: A Validation Study', *Applied Bionics and Biomechanics*. doi: 10.1155/2019/8381351.

OpenSim (2019) *Tutorial 1 - Intro to Musculoskeletal Modeling*. Available at: https://simtk-confluence.stanford.edu:8443/display/OpenSim/Tutorial+1+-+Intro+to+Musculoskeletal+Modeling.

Orthoinfo (2019) *Total Hip Replacement*. Available at: https://orthoinfo.aaos.org/en/treatment/total-hip-replacement/.

Pai, Y.-C. *et al.* (1994) 'Alterations in Weight-Transfer Capabilities in Adults With Hemiparesis', *Physical Therapy*. doi: 10.1093/ptj/74.7.647.

Patil, S. *et al.* (2008) 'Quality of Life Outcomes in Revision vs Primary Total Hip Arthroplasty. A Prospective Cohort Study', *Journal of Arthroplasty*. doi: 10.1016/j.arth.2007.04.035.

Perry, J. (1992) 'Gait Cycle', in *Gait Analysis: Normal and Pathological Function*. doi: 10.1001.

De Pieri, E. *et al.* (2019) 'Patient characteristics affect hip contact forces during gait', *Osteoarthritis and Cartilage*, 27(6), pp. 895–905. doi: https://doi.org/10.1016/j.joca.2019.01.016.

Pivec, R. *et al.* (2012) 'Hip arthroplasty', in *The Lancet*. doi: 10.1016/S0140-6736(12)60607-2.

Prior, S. J. *et al.* (2007) 'Reduction in midthigh low-density muscle with aerobic exercise training and weight loss impacts glucose tolerance in older men', *Journal of Clinical Endocrinology and Metabolism*. doi: 10.1210/jc.2006-2113.

Puett, D. W. and Griffin, M. R. (1994) 'Published trials of nonmedicinal and noninvasive therapies for hip and knee osteoarthritis', *Annals of Internal Medicine*. doi: 10.7326/0003-4819-121-2-199407150-00010.

Rasch, A. *et al.* (2007) 'Reduced muscle radiological density, cross-sectional area, and strength of major hip and knee muscles in 22 patients with hip osteoarthritis', *Acta Orthopaedica*. doi: 10.1080/17453670710014158.

Rasch, A. *et al.* (2009) 'Persisting muscle atrophy two years after replacement of the hip', *The Journal of Bone and Joint Surgery. British volume*. The British Editorial Society of Bone & Joint Surgery, 91-B(5), pp. 583–588. doi: 10.1302/0301-620X.91B5.21477.

Rasch, A., Dalén, N. and Berg, H. E. (2010) 'Muscle strength, gait, and balance in 20 patients with hip osteoarthritis followed for 2 years after THA', *Acta Orthopaedica*. Taylor & Francis, 81(2), pp. 183–188. doi: 10.3109/17453671003793204.

Reid, K. F. and Fielding, R. A. (2012) 'Skeletal muscle power: A critical determinant of physical functioning in older adults', *Exercise and Sport Sciences Reviews*. doi: 10.1097/JES.0b013e31823b5f13.

Rydell, N. W. (1966) 'Forces Acting on the Femoral Head-Prosthesis: A Study on Strain Gauge Supplied Prostheses in Living Persons', *Acta Orthopaedica Scandinavica*. Taylor & Francis, 37(sup88), pp. 1–132. doi: 10.3109/ort.1966.37.suppl-88.01.

Schmidt, A. *et al.* (2017) 'Unilateral hip osteoarthritis: The effect of compensation strategies and anatomic measurements on frontal plane joint loading', *Journal of Orthopaedic Research*. doi: 10.1002/jor.23444.

Schmitt, D., Vap, A. and Queen, R. M. (2015) 'Effect of end-stage hip, knee, and ankle osteoarthritis on walking mechanics', *Gait and Posture*. doi: 10.1016/j.gaitpost.2015.07.005.

Schultz, E. and Lipton, B. H. (1982) ‘Skeletal muscle satellite cells: Changes in proliferation potential as a function of age’, *Mechanisms of Ageing and Development*, 20(4), pp. 377–383. doi: https://doi.org/10.1016/0047-6374(82)90105-1.

Schwachmeyer, V. *et al.* (2013) ‘In Vivo Hip Joint Loading during Post-Operative Physiotherapeutic Exercises’, *PloS one*. Public Library of Science, 8(10), p. e77807. doi: 10.1371/journal.pone.0077807.

Sciorati, C. *et al.* (2015) ‘Fat deposition and accumulation in the damaged and inflamed skeletal muscle: Cellular and molecular players’, *Cellular and Molecular Life Sciences*. doi: 10.1007/s00018-015-1857-7.

Scovil, C. Y. and Ronsky, J. L. (2006) ‘Sensitivity of a Hill-based muscle model to perturbations in model parameters’, *Journal of Biomechanics*. doi: 10.1016/j.jbiomech.2005.06.005.

Shakoor, N. *et al.* (2002) ‘Nonrandom evolution of end-stage osteoarthritis of the lower limbs’, *Arthritis and Rheumatism*. doi: 10.1002/art.10649.

Shakoor, N. *et al.* (2003) ‘Asymmetric knee loading in advanced unilateral hip osteoarthritis’, *Arthritis and Rheumatism*. doi: 10.1002/art.11034.

Sicard-Rosenbaum, L., Light, K. E. and Behrman, A. L. (2002) ‘Gait, lower extremity strength, and self-assessed mobility after hip arthroplasty’, *Journals of Gerontology - Series A Biological Sciences and Medical Sciences*. doi: 10.1093/gerona/57.1.M47.

Silva, J. M. de S. *et al.* (2018) ‘Muscle wasting in osteoarthritis model induced by anterior cruciate ligament transection’, *PloS one*. Public Library of Science, 13(4), pp. e0196682–e0196682. doi: 10.1371/journal.pone.0196682.

Skalshøi, O. *et al.* (2015) ‘Walking patterns and hip contact forces in patients with hip dysplasia’, *Gait & Posture*, 42(4), pp. 529–533. doi: https://doi.org/10.1016/j.gaitpost.2015.08.008.

Soderberg, G. L. and Dostal, W. F. (1978) ‘Electromyographic study of three parts of the gluteus medius muscle during functional activities’, *Physical Therapy*. doi: 10.1093/ptj/58.6.691.

Suetta, C. *et al.* (2004) ‘Training-induced changes in muscle CSA, muscle strength, EMG, and rate of force development in elderly subjects after long-term unilateral disuse’, *Journal of Applied Physiology*. doi: 10.1152/japplphysiol.01307.2003.

Suetta, C. *et al.* (2007) ‘Muscle size, neuromuscular activation, and rapid force characteristics in elderly men and women: Effects of unilateral long-term disuse due to hip-osteoarthritis’, *Journal of Applied Physiology*. doi: 10.1152/japplphysiol.00067.2006.

Suwarganda, E. K. *et al.* (2019) ‘Minimal medical imaging can accurately reconstruct geometric bone models for musculoskeletal models’, *PLoS ONE*. doi: 10.1371/journal.pone.0205628.

Thelen, D. G. and Anderson, F. C. (2006) ‘Using computed muscle control to generate forward dynamic simulations of human walking from experimental data’, *Journal of Biomechanics*. doi: 10.1016/j.jbiomech.2005.02.010.

Tuttle, L. J. *et al.* (2011) ‘Lower Physical Activity Is Associated With Higher Intermuscular Adipose Tissue in People With Type 2 Diabetes and Peripheral Neuropathy’, *Physical Therapy*. doi: 10.2522/ptj.20100329.

Uezumi, A., Ikemoto-Uezumi, M. and Tsuchida, K. (2014) ‘Roles of nonmyogenic mesenchymal progenitors in pathogenesis and regeneration of skeletal muscle’, *Frontiers in Physiology*. doi: 10.3389/fphys.2014.00068.

University Standford (2013) ‘OpenSim Documentation’, *How Inverse Kinematics Works*.

Valente, G. *et al.* (2014) ‘Are subject-specific musculoskeletal models robust to the uncertainties in parameter identification?’, *PLoS ONE*. doi: 10.1371/journal.pone.0112625.

Valente, G., Taddei, F. and Jonkers, I. (2013) ‘Influence of weak hip abductor muscles on joint contact forces during normal walking: Probabilistic modeling analysis’, *Journal of Biomechanics*. doi: 10.1016/j.jbiomech.2013.06.030.

Vanhegan, I. S. *et al.* (2012) ‘A financial analysis of revision hip arthroplasty’, *The Journal of Bone and Joint Surgery. British volume*. doi: 10.1302/0301-620x.94b5.27073.

Visser, M. *et al.* (2002) ‘Leg muscle mass and composition in relation to lower extremity performance in men and women aged 70 to 79: The Health, Aging and Body Composition

Study', *Journal of the American Geriatrics Society*. doi: 10.1046/j.1532-5415.2002.50217.x.

Vu, H. T. T. *et al.* (2018) 'ED-FNN: A new deep learning algorithm to detect percentage of the gait cycle for powered prostheses', *Sensors (Switzerland)*. doi: 10.3390/s18072389.

Wadsworth, J. B., Smidt, G. L. and Johnston, R. C. (1972) 'Gait characteristics of subjects with hip disease.', *Physical therapy*. doi: 10.1093/ptj/52.8.829.

Wan, J. J. *et al.* (2017) 'Muscle fatigue: General understanding and treatment', *Experimental and Molecular Medicine*. doi: 10.1038/emm.2017.194.

Weinhandl, J. T. and Bennett, H. J. (2019) 'Musculoskeletal model choice influences hip joint load estimations during gait', *Journal of Biomechanics*, 91, pp. 124–132. doi: https://doi.org/10.1016/j.jbiomech.2019.05.015.

Wesseling, M. *et al.* (2015) 'Muscle optimization techniques impact the magnitude of calculated hip joint contact forces', *Journal of Orthopaedic Research*. John Wiley & Sons, Ltd, 33(3), pp. 430–438. doi: 10.1002/jor.22769.

Wesseling, M. *et al.* (2018) 'Longitudinal joint loading in patients before and up to one year after unilateral total hip arthroplasty', *Gait & Posture*, 61, pp. 117–124. doi: https://doi.org/10.1016/j.gaitpost.2018.01.002.

Winther, S. B. *et al.* (2016) 'Muscular strength after total hip arthroplasty', *Acta Orthopaedica*. Taylor & Francis, 87(1), pp. 22–28. doi: 10.3109/17453674.2015.1068032.

Wootten, M. E., Kadaba, M. P. and Cochran, G. V. B. (1990) 'Dynamic electromyography. II. Normal patterns during gait', *Journal of Orthopaedic Research*. John Wiley & Sons, Ltd, 8(2), pp. 259–265. doi: 10.1002/jor.1100080215.

World Health Organization (2013) 'Chronic rheumatic conditions', *Chronic deseases and health promotion*.

Zacharias, A. *et al.* (2016) 'Hip abductor muscle volume in hip osteoarthritis and matched controls', *Osteoarthritis and Cartilage*, 24(10), pp. 1727–1735. doi: https://doi.org/10.1016/j.joca.2016.05.002.

Zacharias, A. *et al.* (2017) 'Gluteal muscle atrophy and fatty deposits increase with

advancing hip osteoarthritis', *Journal of Science and Medicine in Sport*. doi: 10.1016/j.jsams.2016.12.072.

Zahar, A., Rastogi, A. and Kendoff, D. (2013) 'Dislocation after total hip arthroplasty', *Current reviews in musculoskeletal medicine*. Springer US, 6(4), pp. 350–356. doi: 10.1007/s12178-013-9187-6.

Zhang, J., Malcolm, D., *et al.* (2014) 'An anatomical region-based statistical shape model of the human femur', *Computer Methods in Biomechanics and Biomedical Engineering: Imaging and Visualization*. doi: 10.1080/21681163.2013.878668.

Zhang, J., Sorby, H., *et al.* (2014) 'The MAP client: User-friendly musculoskeletal modelling workflows', in *Lecture Notes in Computer Science (including subseries Lecture Notes in Artificial Intelligence and Lecture Notes in Bioinformatics)*. doi: 10.1007/978-3-319-12057-7_21.

Zhang, J. *et al.* (2016) 'Lower limb estimation from sparse landmarks using an articulated shape model', *Journal of Biomechanics*. doi: 10.1016/j.jbiomech.2016.10.021.

A-1. Appendix A – OpenSim Modelling

Patient009 RH

Walking6	Frames06
Backward	
FP1	Right
FP2	Left
General_FirstFrame	31
Right_Foot Strike	375
Right_Foot Off	494
Right_End GC	572
Left_Foot Strike	275
Left_Foot Off	4
Lefrt_End GC	473
General_LastFrame	636

Table A. 1: Patient009 RH walking trail & frame, walking direction, force plate (FP) and gait cycle details.

Patient014 SP

Walking8	Frames08
backward	
FP4	Left
FP1	Right
General_FirstFrame	66
Left_Foot Strike	119
Left_Foot Off	189
Left_End GC	239
Right_Foot Strike	295
Right_Foot Off	370
Right_End GC	415
General_LastFrame	449

Table A. 2: Patient014 SP walking trail & frame, walking direction, force plate (FP) and gait cycle details.

Patient016 AF

Walking3	**Frames03**	**Walking4**	**Frames04**
forward		**backward**	
FP1	Left	**FP1**	Right
General_FirstFrame	186	**General_FirstFrame**	193
Left_Foot Strike	262	**Right_Foot Strike**	898
Left_Foot Off	402	**Right_Foot Off**	1010
Left_End GC	426	**Right_End GC**	1054
General_LastFrame	1081	**General_LastFrame**	1166

Table A. 3: Patient016 AF walking trail & frame, walking direction, force plate (FP) and gait cycle details.

Patient044 JS

Walking1	Frames01	**Walking9 - final**	Frames09
forward		**forward**	
FP1	Right	**FP1**	Left
FP2	Left	**FP2**	Right
General_FirstFrame	61	**General_FirstFrame**	37
Right_Foot Strike	104	**Left_Foot Strike**	121
Right_Foot Off	172	**Left_Foot Off**	196
Right_End GC	215	**Left_End GC**	245
Left_Foot Strike	157	**Right_Foot Strike**	182
Left_Foot Off	228	**Right_Foot Off**	261
Left_End GC	271	**Right_End GC**	306
General_LastFrame	451	**General_LastFrame**	531

Table A. 4: Patient044 JS walking trail & frame, walking direction, force plate (FP) and gait cycle details.

Patient046 BA

Walking12 - final	Frames12	**Walking7**	Frames07
backward		**forward**	
FP1	Left	**FP1**	Right
General_FirstFrame	67	**General_FirstFrame**	126
Left_Foot Strike	226	**Right_Foot Strike**	199
Left_Foot Off	313	**Right_Foot Off**	280
Left_End GC	361	**Right_End GC**	337
General_LastFrame	433	**General_LastFrame**	453

Table A. 5: Patient046 BA walking trail & frame, walking direction, force plate (FP) and gait cycle details.

Patient051 JO

Walking2 - final	Frames02	**Walking13**	Frames13
backward		**backward**	
FP2	Left	**FP1**	Right
General_FirstFrame	107	**General_FirstFrame**	84
Left_Foot Strike	146	**Right_Foot Strike**	215
Left_Foot Off	221	**Right_Foot Off**	285
Left_End GC	265	**Right_End GC**	335
General_LastFrame	395	**General_LastFrame**	386

Table A. 6: Patient051 JO walking trail & frame, walking direction, force plate (FP) and gait cycle details.

B-1. Appendix B – Linear vs Statistical Shape Scaling

1. Data Analysis MATLAB

```
D = xlsread('Studyone.xlsx')
figure;

xA = D(:,4);
%Bahl Model Right Leg - Stance Phase
xB = D(:,1);
Mb = (max(xB)/(69.92*9.81))
plot(xA,xB,'LineWidth',3);
hold on

%Gait2392 Model Right Leg - Stance Phase
xG = D(:,2);
Mg = (max(xG)/(69.92*9.81))
plot(xA,xG,'LineWidth',3);

xlabel ('Stance Phase (100%)')
ylabel ('Resultant Hip Contact Force (N)')
title ('Study One')
legend ({'Bahl Model (6.6BW)','Gait2392 (3.3BW)'})
```

2. Results

Table B.1 Maximum isometric forces and resultant muscle forces for gait2392 and Bahl model for Patient009 RH

Muscles	Max Isometric Force		Peak Muscle Force	
	Bahl	**Gait2392**	**Bahl**	**Gait2392**
glut_med1_r	2048	707	200 (spike at 500)	200
glut_med2_r	1432.5	495	225	125
glut_med3_r	1632.5	564	325	175
glut_min1_r	675	233	50	45
glut_min2_r	713	246	47	55
glut_min3_r	808	279	55	65
semimem_r	3220	1112	400 (spike at 1250)	600
semiten_r	1025	354	45	113
bifemlh_r	2240	773	200	250
bifemsh_r	2010	694	125	375
sar_r	390	135	25 (spike at 160)	32
add_long_r	1568	541	42	100
add_brev_r	1073	370	18	75
add_mag1_r	953	329	15	55
add_mag2_r	858	296	10	47
add_mag3_r	1220	421	25 (spike at 400)	70
tfl_r	583	201	77	47
pect_r	665	230	8.5	62
grac_r	405	140	9	27
glut_max1_r	1433	495	160	62
glut_max2_r	2048	707	350	47
glut_max3_r	1380	476	75	62
iliacus_r	2683	926	700	325
psoas_r	2783	961	1100	350
quad_fem_r	953	329	700	40

gem_r	410	142	16	30
peri_r	1110	383	160	70
rect_fem_r	2923	1009	360	240
vas_med_r	3235	1117	55 (spike at 140)	80
vas_int_r	3413	1178	60 (spike at 160)	90
vas_lat_r	4678	1615	120 (spike at 275)	110

C-1. Appendix C – Study Two

1. Methodology

Patient009 RH				
Abbreviation	**Gait2392**	**Delp**	**Carhart**	**Bahl**
glut_med1_r	707	475	471	2048
glut_med2_r	495	328	330	1432.5
glut_med3_r	564	375	375	1632.5
glut_min1_r	233	155	155	675
glut_min2_r	246	164	164	713
glut_min3_r	279	186	186	808
semimem_r	1112	889	889	3220
semiten_r	354	285	283	1025
bifemlh_r	773	621	619	2240
bifemsh_r	694	345	347	2010
sar_r	135	91	90	390
add_long_r	541	362	361	1568
add_brev_r	370	246	247	1073
add_mag1_r	329	298	299	953
add_mag2_r	296	268	269	858
add_mag3_r	421	384	383	1220
tfl_r	201	134	134	583
pect_r	230	151	153	665
grac_r	140	95	93	405
glut_max1_r	495	328	330	1433
glut_max2_r	707	475	471	2048
glut_max3_r	476	319	318	1380
iliacus_r	926	371	370	2683
psoas_r	961	319	320	2783
quad_fem_r	329	220	219	953
gem_r	142	95	94	410
peri_r	383	255	255	1110

rect_fem_r	1009	673	672	2923
vas_med_r	1117	1118	1117	3235
vas_int_r	1178	1066	1178	3413
vas_lat_r	1615	1614	1615	4678
med_gas_r	1345	962	961	
lat_gas_r	589	423	421	
soleus_r	3063	2442	2450	
tib_post_r	1371	1096	1096	
flex_dig_r	268	268	268	
flex_hal_r	278	276	278	
tib_ant_r	781	518	520	
per_brev_r	375	302	300	
per_long_r	814	652	651	
per_tert_r	155	78	78	
ext_dig_r	442	293	520	
ext_hal_r	140	95	93	
ercspn_r	707	1079	1079	
ercspn_l	495	1079	1079	
intobl_r	564	388	388	
intobl_l	233	388	388	
extobl_r	246	388	388	
extobl_l	279	388	388	

2. Data Analysis MATLAB

```
E = xlsread('Study two.xlsx')
figure;

xA = E(:,6);
%Bahl Model Right Leg - Stance Phase
xB = E(:,1);
Mb = (max(xB)/(69.92*9.81))
plot(xA,xB,'LineWidth',3);
hold on


%Carhart Model Right Leg - Stance Phase
xC = E(:,2);
Mc = (max(xC)/(69.92*9.81))
plot(xA,xC,'LineWidth',3);
hold on

%Delp Model Right Leg - Stance Phase
xD = E(:,3);
Md = (max(xD)/(69.92*9.81))
plot(xA,xD,'LineWidth',3);
hold on

%Gait2392 Model Right Leg - Stance Phase
xG = E(:,4);
Mg = (max(xG)/(69.92*9.81))
plot(xA,xG,'LineWidth',3);
xlabel ('Stance Phase (100%)')
ylabel ('Hip Contact Force (N)')
title ('Study Two - Joint Contact Forces')
legend ({'Bahl (6.8BW)','Carhart  (3.6BW)','Delp  (3.6BW)','Gait2392  (4.1BW)'})
```

D-1 Appendix D – Study Three

1.0 Data Analysis MATLAB

1.1 Resultant HCF

```
U = xlsread('Unaffected Leg.xlsx')
A = xlsread('Affected Leg.xlsx')

figure;
format LongG
%Patient 009 - BA - Affected
xA = A(:,2);
pA = A(:,3);
Ma = (max(pA)/(69.92*9.81))

plot(xA,pA,'LineWidth',3);
hold on

%Patient 009 - BA - Unaffected
xU = U(:,2);
pU = U(:,3);
Mu = (max(pU)/(69.92*9.81))
plot(xU,pU,'LineWidth',3);
hold on

xlabel ('Gait Cycle (100%)')
ylabel ('Hip Contact Force (N)')
title ('Patient009 - RH')
legend ({'Affected (4.3BW)','Unaffected (3.6BW)'})
```

1.2 Gait Muscle Patterns

```
A = xlsread('Patient009L.xlsx') %rh
B = xlsread('Patient014L.xlsx') %sp
C = xlsread('Patient016R.xlsx') %af
D = xlsread('Patient044L.xlsx') %js
E = xlsread('Patient046R.xlsx') %ba
F = xlsread('Patient051R.xlsx') %jo
```

```
figure

%Gluteus Medius
x1 = A(:,2); %009
rh = A(:,3);
x2 = B(:,2); %014
sp = B(:,3);
x3 = C(:,2); %016
af = C(:,3);
x4 = D(:,2); %044
js = D(:,3);
x5 = E(:,2); %046
ba = E(:,3);
x6 = F(:,2); %051
jo = F(:,3);
plot (x1,rh,'LineWidth',1)
hold on
plot (x2,sp,'LineWidth',1)
hold on
plot (x3,af,'LineWidth',1)
hold on
plot (x4,js,'LineWidth',1)
hold on
plot (x5,ba,'LineWidth',1)
hold on
plot (x6,jo,'LineWidth',1)
legend ({'009','014','016','044','046','051'})
xlabel ('Gait Cycle (100%)')
ylabel ('Hip Contact Force (N)')
title ('Gluteus Medius')

figure
%Gluteus Minimus
x1 = A(:,2); %009
rh = A(:,4);
x2 = B(:,2); %014
sp = B(:,4);
x3 = C(:,2); %016
af = C(:,4);
```

```
x4 = D(:,2); %044
js = D(:,4);
x5 = E(:,2); %046
ba = E(:,4);
x6 = F(:,2); %051
jo = F(:,4);
plot (x1,rh,'LineWidth',1)
hold on
plot (x2,sp,'LineWidth',1)
hold on
plot (x3,af,'LineWidth',1)
hold on
plot (x4,js,'LineWidth',1)
hold on
plot (x5,ba,'LineWidth',1)
hold on
plot (x6,jo,'LineWidth',1)
xlabel ('Gait Cycle (100%)')
ylabel ('Hip Contact Force (N)')
title ('Gluteus Minimus')
legend ({'009','014','016','044','046','051'})
xlabel ('Gait Cycle (100%)')
ylabel ('Hip Contact Force (N)')

figure
x1 = A(:,2); %009
rh = A(:,5);
x2 = B(:,2); %014
sp = B(:,5);
x3 = C(:,2); %016
af = C(:,5);
x4 = D(:,2); %044
js = D(:,5);
x5 = E(:,2); %046
ba = E(:,5);
x6 = F(:,2); %051
jo = F(:,5);
plot (x1,rh,'LineWidth',1)
hold on
plot (x2,sp,'LineWidth',1)
```

```
hold on
plot (x3,af,'LineWidth',1)
hold on
plot (x4,js,'LineWidth',1)
hold on
plot (x5,ba,'LineWidth',1)
hold on
plot (x6,jo,'LineWidth',1)
title ('Adductor Magnus')
legend ({'009','014','016','044','046','051'})
xlabel ('Gait Cycle (100%)')
ylabel ('Hip Contact Force (N)')

figure
x1 = A(:,2); %009
rh = A(:,6);
x2 = B(:,2); %014
sp = B(:,6);
x3 = C(:,2); %016
af = C(:,6);
x4 = D(:,2); %044
js = D(:,6);
x5 = E(:,2); %046
ba = E(:,6);
x6 = F(:,2); %051
jo = F(:,6);
plot (x1,rh,'LineWidth',1)
hold on
plot (x2,sp,'LineWidth',1)
hold on
plot (x3,af,'LineWidth',1)
hold on
plot (x4,js,'LineWidth',1)
hold on
plot (x5,ba,'LineWidth',1)
hold on
plot (x6,jo,'LineWidth',1)
title ('Gluteus Maximus')
legend ({'009','014','016','044','046','051'})
xlabel ('Gait Cycle (100%)')
```

```
ylabel ('Hip Contact Force (N)')

figure
x1 = A(:,2); %009
rh = A(:,7);
x2 = B(:,2); %014
sp = B(:,7);
x3 = C(:,2); %016
af = C(:,7);
x4 = D(:,2); %044
js = D(:,7);
x5 = E(:,2); %046
ba = E(:,7);
x6 = F(:,2); %051
jo = F(:,7);
plot (x1,rh,'LineWidth',1)
hold on
plot (x2,sp,'LineWidth',1)
hold on
plot (x3,af,'LineWidth',1)
hold on
plot (x4,js,'LineWidth',1)
hold on
plot (x5,ba,'LineWidth',1)
hold on
plot (x6,jo,'LineWidth',1)
title ('Iliopsoas')
legend ({'009','014','016','044','046','051'})
xlabel ('Gait Cycle (100%)')
ylabel ('Hip Contact Force (N)')

figure
x1 = A(:,2); %009
rh = A(:,8);
x2 = B(:,2); %014
sp = B(:,8);
x3 = C(:,2); %016
af = C(:,8);
x4 = D(:,2); %044
js = D(:,8);
```

```
x5 = E(:,2); %046
ba = E(:,8);
x6 = F(:,2); %051
jo = F(:,8);
plot (x1,rh,'LineWidth',1)
hold on
plot (x2,sp,'LineWidth',1)
hold on
plot (x3,af,'LineWidth',1)
hold on
plot (x4,js,'LineWidth',1)
hold on
plot (x5,ba,'LineWidth',1)
hold on
plot (x6,jo,'LineWidth',1)
title ('Semimembranosus')
legend ({'009','014','016','044','046','051'})
xlabel ('Gait Cycle (100%)')
ylabel ('Hip Contact Force (N)')

figure
x1 = A(:,2); %009
rh = A(:,9);
x2 = B(:,2); %014
sp = B(:,9);
x3 = C(:,2); %016
af = C(:,9);
x4 = D(:,2); %044
js = D(:,9);
x5 = E(:,2); %046
ba = E(:,9);
x6 = F(:,2); %051
jo = F(:,9);
plot (x1,rh,'LineWidth',1)
hold on
plot (x2,sp,'LineWidth',1)
hold on
plot (x3,af,'LineWidth',1)
hold on
plot (x4,js,'LineWidth',1)
```

```
hold on
plot (x5,ba,'LineWidth',1)
hold on
plot (x6,jo,'LineWidth',1)
title ('Semitendinosus')
legend ({'009','014','016','044','046','051'})
xlabel ('Gait Cycle (100%)')
ylabel ('Hip Contact Force (N)')

figure
x1 = A(:,2); %009
rh = A(:,10);
x2 = B(:,2); %014
sp = B(:,10);
x3 = C(:,2); %016
af = C(:,10);
x4 = D(:,2); %044
js = D(:,10);
x5 = E(:,2); %046
ba = E(:,10);
x6 = F(:,2); %051
jo = F(:,10);
plot (x1,rh,'LineWidth',1)
hold on
plot (x2,sp,'LineWidth',1)
hold on
plot (x3,af,'LineWidth',1)
hold on
plot (x4,js,'LineWidth',1)
hold on
plot (x5,ba,'LineWidth',1)
hold on
plot (x6,jo,'LineWidth',1)
title ('Biceps Femoris Long Head')
legend ({'009','014','016','044','046','051'})
xlabel ('Gait Cycle (100%)')
ylabel ('Hip Contact Force (N)')

figure
x1 = A(:,2); %009
```

```
rh = A(:,11);
x2 = B(:,2); %014
sp = B(:,11);
x3 = C(:,2); %016
af = C(:,11);
x4 = D(:,2); %044
js = D(:,11);
x5 = E(:,2); %046
ba = E(:,11);
x6 = F(:,2); %051
jo = F(:,11);
plot (x1,rh,'LineWidth',1)
hold on
plot (x2,sp,'LineWidth',1)
hold on
plot (x3,af,'LineWidth',1)
hold on
plot (x4,js,'LineWidth',1)
hold on
plot (x5,ba,'LineWidth',1)
hold on
plot (x6,jo,'LineWidth',1)
title ('Biceps Femoris Short Head')
legend ({'009','014','016','044','046','051'})
xlabel ('Gait Cycle (100%)')
ylabel ('Hip Contact Force (N)')

figure
x1 = A(:,2); %009
rh = A(:,12);
x2 = B(:,2); %014
sp = B(:,12);
x3 = C(:,2); %016
af = C(:,12);
x4 = D(:,2); %044
js = D(:,12);
x5 = E(:,2); %046
ba = E(:,12);
x6 = F(:,2); %051
jo = F(:,12);
```

```
plot (x1,rh,'LineWidth',1)
hold on
plot (x2,sp,'LineWidth',1)
hold on
plot (x3,af,'LineWidth',1)
hold on
plot (x4,js,'LineWidth',1)
hold on
plot (x5,ba,'LineWidth',1)
hold on
plot (x6,jo,'LineWidth',1)
title ('Sartorius')
legend ({'009','014','016','044','046','051'})
xlabel ('Gait Cycle (100%)')
ylabel ('Hip Contact Force (N)')

figure
x1 = A(:,2); %009
rh = A(:,13);
x2 = B(:,2); %014
sp = B(:,13);
x3 = C(:,2); %016
af = C(:,13);
x4 = D(:,2); %044
js = D(:,13);
x5 = E(:,2); %046
ba = E(:,13);
x6 = F(:,2); %051
jo = F(:,13);
plot (x1,rh,'LineWidth',1)
hold on
plot (x2,sp,'LineWidth',1)
hold on
plot (x3,af,'LineWidth',1)
hold on
plot (x4,js,'LineWidth',1)
hold on
plot (x5,ba,'LineWidth',1)
hold on
plot (x6,jo,'LineWidth',1)
```

```
title ('Adductor Longus')
legend ({'009','014','016','044','046','051'})
xlabel ('Gait Cycle (100%)')
ylabel ('Hip Contact Force (N)')

figure
x1 = A(:,2); %009
rh = A(:,14);
x2 = B(:,2); %014
sp = B(:,14);
x3 = C(:,2); %016
af = C(:,14);
x4 = D(:,2); %044
js = D(:,14);
x5 = E(:,2); %046
ba = E(:,14);
x6 = F(:,2); %051
jo = F(:,14);
plot (x1,rh,'LineWidth',1)
hold on
plot (x2,sp,'LineWidth',1)
hold on
plot (x3,af,'LineWidth',1)
hold on
plot (x4,js,'LineWidth',1)
hold on
plot (x5,ba,'LineWidth',1)
hold on
plot (x6,jo,'LineWidth',1)
title ('Adductor Brevis')
legend ({'009','014','016','044','046','051'})
xlabel ('Gait Cycle (100%)')
ylabel ('Hip Contact Force (N)')

figure
x1 = A(:,2); %009
rh = A(:,15);
x2 = B(:,2); %014
sp = B(:,15);
x3 = C(:,2); %016
```

```
af = C(:,15);
x4 = D(:,2); %044
js = D(:,15);
x5 = E(:,2); %046
ba = E(:,15);
x6 = F(:,2); %051
jo = F(:,15);
plot (x1,rh,'LineWidth',1)
hold on
plot (x2,sp,'LineWidth',1)
hold on
plot (x3,af,'LineWidth',1)
hold on
plot (x4,js,'LineWidth',1)
hold on
plot (x5,ba,'LineWidth',1)
hold on
plot (x6,jo,'LineWidth',1)
title ('Tensor Fasciae Latae')
legend ({'009','014','016','044','046','051'})
xlabel ('Gait Cycle (100%)')
ylabel ('Hip Contact Force (N)')

figure
x1 = A(:,2); %009
rh = A(:,16);
x2 = B(:,2); %014
sp = B(:,16);
x3 = C(:,2); %016
af = C(:,16);
x4 = D(:,2); %044
js = D(:,16);
x5 = E(:,2); %046
ba = E(:,16);
x6 = F(:,2); %051
jo = F(:,16);
plot (x1,rh,'LineWidth',1)
hold on
plot (x2,sp,'LineWidth',1)
hold on
```

```
plot (x3,af,'LineWidth',1)
hold on
plot (x4,js,'LineWidth',1)
hold on
plot (x5,ba,'LineWidth',1)
hold on
plot (x6,jo,'LineWidth',1)
title ('Gracilis')
legend ({'009','014','016','044','046','051'})
xlabel ('Gait Cycle (100%)')
ylabel ('Hip Contact Force (N)')

figure
x1 = A(:,2); %009
rh = A(:,17);
x2 = B(:,2); %014
sp = B(:,17);
x3 = C(:,2); %016
af = C(:,17);
x4 = D(:,2); %044
js = D(:,17);
x5 = E(:,2); %046
ba = E(:,17);
x6 = F(:,2); %051
jo = F(:,17);
plot (x1,rh,'LineWidth',1)
hold on
plot (x2,sp,'LineWidth',1)
hold on
plot (x3,af,'LineWidth',1)
hold on
plot (x4,js,'LineWidth',1)
hold on
plot (x5,ba,'LineWidth',1)
hold on
plot (x6,jo,'LineWidth',1)
title ('Rectus Femoris')
legend ({'009','014','016','044','046','051'})
xlabel ('Gait Cycle (100%)')
ylabel ('Hip Contact Force (N)')
```

```
figure
x1 = A(:,2); %009
rh = A(:,18);
x2 = B(:,2); %014
sp = B(:,18);
x3 = C(:,2); %016
af = C(:,18);
x4 = D(:,2); %044
js = D(:,18);
x5 = E(:,2); %046
ba = E(:,18);
x6 = F(:,2); %051
jo = F(:,18);
plot (x1,rh,'LineWidth',1)
hold on
plot (x2,sp,'LineWidth',1)
hold on
plot (x3,af,'LineWidth',1)
hold on
plot (x4,js,'LineWidth',1)
hold on
plot (x5,ba,'LineWidth',1)
hold on
plot (x6,jo,'LineWidth',1)
title ('Vastus Medialis')
legend ({'009','014','016','044','046','051'})
xlabel ('Gait Cycle (100%)')
ylabel ('Hip Contact Force (N)')

figure
x1 = A(:,2); %009
rh = A(:,19);
x2 = B(:,2); %014
sp = B(:,19);
x3 = C(:,2); %016
af = C(:,19);
x4 = D(:,2); %044
js = D(:,19);
x5 = E(:,2); %046
```

```
ba = E(:,19);
x6 = F(:,2); %051
jo = F(:,19);
plot (x1,rh,'LineWidth',1)
hold on
plot (x2,sp,'LineWidth',1)
hold on
plot (x3,af,'LineWidth',1)
hold on
plot (x4,js,'LineWidth',1)
hold on
plot (x5,ba,'LineWidth',1)
hold on
plot (x6,jo,'LineWidth',1)
title ('Vastus Intermedius')
legend ({'009','014','016','044','046','051'})
xlabel ('Gait Cycle (100%)')
ylabel ('Hip Contact Force (N)')

figure
x1 = A(:,2); %009
rh = A(:,20);
x2 = B(:,2); %014
sp = B(:,20);
x3 = C(:,2); %016
af = C(:,20);
x4 = D(:,2); %044
js = D(:,20);
x5 = E(:,2); %046
ba = E(:,20);
x6 = F(:,2); %051
jo = F(:,20);
plot (x1,rh,'LineWidth',1)
hold on
plot (x2,sp,'LineWidth',1)
hold on
plot (x3,af,'LineWidth',1)
hold on
plot (x4,js,'LineWidth',1)
hold on
```

```
plot (x5,ba,'LineWidth',1)
hold on
plot (x6,jo,'LineWidth',1)
title ('Vastus Lateralis')
legend ({'009','014','016','044','046','051'})
xlabel ('Gait Cycle (100%)')
ylabel ('Hip Contact Force (N)')
```

1.3 Anterior to Posterior

```
A = xlsread('Patient009.xlsx')
B = xlsread('Patient014.xlsx')

figure
x1 = A(:,2);
r1 = A(:,3); %Base model
r2 = A(:,4);
r3 = A(:,5);
r4 = A(:,6);
plot (x1,r1, 'LineWidth',2)
hold on
plot (x1,r2, 'LineWidth',2)
hold on
plot (x1,r3, 'LineWidth',2)
hold on
plot (x1,r4, 'LineWidth',2)

legend ({'Base','20% reduction','40% reduction','60% reduction'})
xlabel ('Gait Cycle (100%)')
ylabel ('Hip Contact Force (N)')
title ('Anterior to Posterior Force Patient009')

figure
x1 = B(:,2);
r1 = B(:,3); %Base model
r2 = B(:,4);
r3 = B(:,5);
r4 = B(:,6);
```

```
plot (x1,r1, 'LineWidth',2)
hold on
plot (x1,r2, 'LineWidth',2)
hold on
plot (x1,r3, 'LineWidth',2)
hold on
plot (x1,r4, 'LineWidth',2)

legend ({'Base','20% reduction','40% reduction','60% reduction'})
xlabel ('Gait Cycle (100%)')
ylabel ('Hip Contact Force (N)')
title ('Anterior to Posterior Force Patient014')
```

1.4 Asymmetry

```
A = xlsread('Base009.xlsx') %Base Model
B = xlsread('00920.xlsx') %20 Reduction
C = xlsread('00940.xlsx') %40 Reduction
D = xlsread('00960.xlsx') %60 Reduction

figure
%Gluteus Medius
subplot (4,2,1)
x1 = A(:,2);
m1 = A(:,3); %base
m2 = B(:,3); %20
m3 = C(:,3); %40
m4 = D(:,3); %60

plot (x1,m1,'LineWidth',2,'color',[0.15 0.2 0.05])
hold on
plot (x1,m2,'LineWidth',2,'color',[0.3 0.4 0.35])
hold on
plot (x1,m3,'LineWidth',2,'color',[0.5 0.6 0.55])
hold on
plot (x1,m4,'LineWidth',2,'color',[0.7 0.8 0.75])
title ('Gluteus Medius')
legend ({'Base','20','40','60'})
```

```
%Gluteus Minimus
subplot (4,2,2)
x1 = A(:,2);
m1 = A(:,4); %base
m2 = B(:,4); %20
m3 = C(:,4); %40
m4 = D(:,4); %60

plot (x1,m1,'LineWidth',2,'color',[0.15 0.2 0.05])
hold on
plot (x1,m2,'LineWidth',2,'color',[0.3 0.4 0.35])
hold on
plot (x1,m3,'LineWidth',2,'color',[0.5 0.6 0.55])
hold on
plot (x1,m4,'LineWidth',2,'color',[0.7 0.8 0.75])
title ('Gluteus Minimus')


%Sartorius
subplot (4,2,3)
x1 = A(:,2);
m1 = A(:,5); %base
m2 = B(:,5); %20
m3 = C(:,5); %40
m4 = D(:,5); %60

plot (x1,m1,'LineWidth',2,'color',[0.15 0.2 0.05])
hold on
plot (x1,m2,'LineWidth',2,'color',[0.3 0.4 0.35])
hold on
plot (x1,m3,'LineWidth',2,'color',[0.5 0.6 0.55])
hold on
plot (x1,m4,'LineWidth',2,'color',[0.7 0.8 0.75])
title ('Sartorius')


%Tensor Fascia Latae
subplot (4,2,4)
x1 = A(:,2);
```

```
m1 = A(:,6); %base
m2 = B(:,6); %20
m3 = C(:,6); %40
m4 = D(:,6); %60

plot (x1,m1,'LineWidth',2,'color',[0.15 0.2 0.05])
hold on
plot (x1,m2,'LineWidth',2,'color',[0.3 0.4 0.35])
hold on
plot (x1,m3,'LineWidth',2,'color',[0.5 0.6 0.55])
hold on
plot (x1,m4,'LineWidth',2,'color',[0.7 0.8 0.75])
title ('Tensor Fascia Latae')



%Gluteus Maximus
subplot (4,2,5)
x1 = A(:,2);
m1 = A(:,7); %base
m2 = B(:,7); %20
m3 = C(:,7); %40
m4 = D(:,7); %60

plot (x1,m1,'LineWidth',2,'color',[0.15 0.2 0.05])
hold on
plot (x1,m2,'LineWidth',2,'color',[0.3 0.4 0.35])
hold on
plot (x1,m3,'LineWidth',2,'color',[0.5 0.6 0.55])
hold on
plot (x1,m4,'LineWidth',2,'color',[0.7 0.8 0.75])
title ('Gluteus Maximus ')



%Rectus Femoris
subplot (4,2,6)
x1 = A(:,2);
m1 = A(:,8); %base
m2 = B(:,8); %20
m3 = C(:,8); %40
```

```
m4 = D(:,8); %60

plot (x1,m1,'LineWidth',2,'color',[0.15 0.2 0.05])
hold on
plot (x1,m2,'LineWidth',2,'color',[0.3 0.4 0.35])
hold on
plot (x1,m3,'LineWidth',2,'color',[0.5 0.6 0.55])
hold on
plot (x1,m4,'LineWidth',2,'color',[0.7 0.8 0.75])
title ('Rectus Femoris')



%Piriformis
subplot (4,2,7)
x1 = A(:,2);
m1 = A(:,9); %base
m2 = B(:,9); %20
m3 = C(:,9); %40
m4 = D(:,9); %60

plot (x1,m1,'LineWidth',2,'color',[0.15 0.2 0.05])
hold on
plot (x1,m2,'LineWidth',2,'color',[0.3 0.4 0.35])
hold on
plot (x1,m3,'LineWidth',2,'color',[0.5 0.6 0.55])
hold on
plot (x1,m4,'LineWidth',2,'color',[0.7 0.8 0.75])
title ('Piriformis')
```

D-1.1 Patient009 RH Muscle Forces

2.1 Methodology

Table D. 1: Patient009 RH maximum isometric forces (N) for base model and muscle asymmetry; 20%, 40% and 60% for three components of gluteus medius and minimus.

Reduction in Left hip		Muscle Asymmetry Reductions		
Abbreviation	Base Model	20% Red	40% Red	60% Red
glut_med1_l	475	380	285	190
glut_med2_l	327	262	196	131
glut_med3_l	375	300	225	150
glut_min1_l	155	124	93	62
glut_min2_l	164	131	98	66
glut_min3_l	186	149	112	74

2.2 Results

Table D. 2: Patient009 RH maximum isometric forces (N) and individual muscle forces (N) for base model, contralateral and muscle asymmetry; 20%, 40% and 60%

Patient009.			**Resultant Muscle Force(Left Leg)**			
Muscles	Max Forces	Unaffected Right Leg	Base Model	20% Reduction	40% Reduction	60% Reduction
glut_med1	475	300	418	370	275	195
glut_med2	328	225	233	250	220	147
glut_med3	375	325	270	225	190	171
glut_min1	155	150	50	62	85	60
glut_min2	164	150	60	70	93	70
glut_min3	186	150	80	90	120	90
Semimem	889	400	50	50	55	300
Semiten	285	150	30	27	27	22
Bifemlh	621	350	45	45	40	30
Bifemsh	345	325	110	120	120	160
Sar	91	90	40	60	50	90
add_long	362	400	65	67	60	65
add_brev	246	22.5	10	10	10	8
add_mag1	298	17.5	5	5	4	3
add_mag2	268	35	3	3	2	2
add_mag3	384	300	4	3	3	4
Tfl	134	134	70	110	140	150
Pect	151	150	4	4	4	4
Grac	95	100	4	4	4	4
glut_max1	328	160	100	85	166	225
glut_max2	475	350	60	130	175	300
glut_max3	319	80	3	4	3	3
iliacus	371	400	175	200	175	175
Psoas	319	400	125	150	139	150
quad_fem	220	140	25	35	35	35

Gem	95	20	8	9	11	10
Peri	255	170	100	130	150	180
rect_fem	673	700	300	325	400	800
vas_med	1118	70	22	17	14	14
vas_int	1066	70	25	32	20	20
vas_lat	1614	150	45	18	13	13

D-1.2 Patient014 SP Muscle Forces

3.1 Methodology

Table D. 3: Patient014 SP maximum isometric forces (N) for base model and muscle asymmetry; 20%, 40% and 60% for three components of gluteus medius and minimus.

Reduction in Left hip		Muscle Asymmetry Reductions		
Abbreviation	ScaledFile Value	20% Red	40% Red	60% Red
glut_med1_l	630	504	378	252
glut_med2_l	435	348	261	174
glut_med3_l	499	399	299	200
glut_min1_l	206	165	124	82
glut_min2_l	218	174	131	87
glut_min3_l	246	197	148	98

3.2 Results

Table D. 4: Patient014 SP maximum isometric forces (N) and individual muscle forces (N) for base model, contralateral and muscle asymmetry; 20%, 40% and 60%

Patient014.			**Resultant Muscle Force (Left Leg)**			
Muscles	Max Force	Unaffected Leg – Right	Base Model	20% Reduction	40% Reduction	60% Reduction
glut_med1	630	500	550	450	350	225
glut_med2	435	230	300	300	225	160
glut_med3	499	195	150	125	100	140
glut_min1	206	215	200	160	120	80
glut_min2	218	225	225	175	130	90
glut_min3	246	60	150	190	150	100
Semimem	1180	500	450	450	450	500
Semiten	378	90	350	350	350	350
Bifemlh	825	325	120	130	125	125
Bifemsh	458	325	450	430	430	430
Sar	120	60	120	120	125	125
add_long	481	275	500	350	440	55
add_brev	327	50	25	15	45	5
add_mag1	395	70	15	5	5	5
add_mag2	355	130	15	5	15	5
add_mag3	510	130	25	50	75	7
Tfl	178	80	175	185	200	208
Pect	201	30	200	200	200	200
Grac	126	20	130	130	120	120
glut_max1	435	90	7	15	150	210
glut_max2	630	175	5	9	25	120
glut_max3	424	90	5	5	5	10
iliacus	493	300	500	500	600	500
Psoas	424	300	450	450	500	450
quad_fem	292	80	130	90	50	55
Gem	126	12	8	8	90	8

Peri	338	90	65	70	70 (peak 430)	70
rect_fem	894	250	325	330	330 (peak 900)	350
vas_med	1484	200	22	50	25 (peak 225)	22
vas_int	1415	190	15	55	25 (peak 275)	22
vas_lat	2143	430	30	80	30 (peak 400)	32

D-1.3 Patient016 AF Muscle Forces

4.1 Methodology

Table D. 5: Patient016 AF maximum isometric forces (N) for base model and muscle asymmetry; 20%, 40% and 60% for three components of gluteus medius and minimus.

Reduction in Right hip		Muscle Asymmetry Reductions		
Abbreviation	ScaledFile Value	20% Red	40% Red	60% Red
glut_med1_l	749	599	449	300
glut_med2_l	517	414	310	207
glut_med3_l	592	474	355	237
glut_min1_l	245	196	147	98
glut_min2_l	259	207	155	104
glut_min3_l	293	234	176	117

4.2Results

Table D. 6: Patient016 AF maximum isometric forces (N) and individual muscle forces (N) for base model, contralateral and muscle asymmetry; 20%, 40% and 60%

Patient016.			**Resultant Muscle Force (Right Leg)**			
Muscles	Scaled Force	Unaffected -Left Leg	No Reduction	20% Reduction	40% Reduction	60% Reduction
glut_med1	749	50	9	12	25	30
glut_med2	517	130	55	57	50	30
glut_med3	592	300	400	314	206	107
glut_min1	245	7	3	3	3	3
glut_min2	259	15	10	10	8	6
glut_min3	293	35	25	22	17	12
Semimem	1402	900	140	140	145	148
Semiten	449	100	5	5	5	5
Bifemlh	980	325	30	45	50	50
Bifemsh	545	350	260	260	275	275
Sar	143	100	75	70	70	73
add_long	572	90	5	5	5	5
add_brev	388	55	4	4	4	5
add_mag1	470	100	6	5	6	9
add_mag2	422	70	5	4	5	5
add_mag3	606	100	8	8	8	8
Tfl	211	35	55	55	60	60
Pect	238	8	2	2	2	2
Grac	150	18	2	2	2	2
glut_max1	517	175	100	135	160	200
glut_max2	749	470	350	350	430	470
glut_max3	504	100	35	35	30	31
iliacus	585	200	150	150	155	152
Psoas	504	100	85	77	82	80
quad_fem	347	80	225	215	210	200
Gem	150	30	60	60	60	60

Peri	402	175	370	409	450	500
rect_fem	1062	250	280	280	278	277
vas_med	1763	175	40	40	40	40
vas_int	1682	200	40	35	37	37
vas_lat	2546	400	80	80	83	80

D-1.4 Patient044 JS Muscle Forces

5.1 Methodology

Table D. 7: Patient044 JS maximum isometric forces (N) for base model and muscle asymmetry; 20%, 40% and 60% for three components of gluteus medius and minimus.

Reduction in Left hip		Muscle Asymmetry Reductions		
Abbreviation	ScaledFile Value	20% Red	40% Red	60% Red
glut_med1_l	553	442	332	221
glut_med2_l	382	306	229	153
glut_med3_l	437	350	262	175
glut_min1_l	181	145	109	72
glut_min2_l	191	153	115	76
glut_min3_l	216	173	130	86

5.2 Results

Table D. 8: Patient044 JS maximum isometric forces (N) and individual muscle forces (N) for base model, contralateral and muscle asymmetry; 20%, 40% and 60%

Patient044.			**Resultant Muscle Force (Left Leg)**			
Muscles	Scaled Force	Unaffected – Right leg	No Reduction	20% Reduction	40% Reduction	60% Reduction
glut_med1	553	550	440	430	355	240
glut_med2	382	370	220	270	240	160
glut_med3	437	100	95	70	50	40
glut_min1	181	175	62	87	105	80
glut_min2	191	175	60	80	110	85
glut_min3	216	150	50	57	120	95
Semimem	1035	600	225	230	235	450
Semiten	332	300	15	15	16	17
Bifemlh	723	460	70	72	72	72
Bifemsh	402	150	175	175	180	180
Sar	106	30	32	35	37	109
add_long	422	125	100	100	100	95
add_brev	286	27	11	11	11	9
add_mag1	347	25	22	22	22	20
add_mag2	311	35	20	20	18	17
add_mag3	447	275	45	47	47	47
Tfl	156	150	60	90	170	200
Pect	176	10	9	9	9	9
Grac	111	9	6	6	5	3
glut_max1	382	65	45	60	100	250
glut_max2	553	150	40	45	50	80
glut_max3	372	110	46	47	45	45
iliacus	432	175	200	200	200	200
Psoas	372	125	140	145	145	145
quad_fem	256	18	14	12	12	12
Gem	111	4	6	7	7	7

Peri	296	55	70	72	75	76
rect_fem	784	600	400	400	380	600
vas_med	1301	80	225	225	225	225
vas_int	1241	70	250	250	260	260
vas_lat	1879	175	480	480	490	490

D-1.5 Patient046 BA Muscle Forces

6.1Methodology

Table D. 9: Patient046 BA maximum isometric forces (N) for base model and muscle asymmetry; 20%, 40% and 60% for three components of gluteus medius and minimus.

Reduction in Right hip		Muscle Asymmetry Reductions		
Abbreviation	ScaledFile Value	20% Red	40% Red	60% Red
glut_med1_l	644	515	386	258
glut_med2_l	445	356	267	178
glut_med3_l	509	407	305	204
glut_min1_l	211	169	127	84
glut_min2_l	222	178	133	89
glut_min3_l	252	202	151	101

6.2Results

Table D. 10: Patient046 BA maximum isometric forces (N) and individual muscle forces (N) for base model, contralateral and muscle asymmetry; 20%, 40% and 60%

Patient046.			**Resultant Muscle Force (Right Leg)**			
Muscles	Scaled Force	Unaffected – Left Leg	No Reduction	20% Reduction	40% Reduction	60% Reduction
glut_med1	644	400	275	275	270	225
glut_med2	445	225	150	145	135	120
glut_med3	509	250	160	140	110	72
glut_min1	211	200	34	30	30	27
glut_min2	222	175	40	35	32	28
glut_min3	252	120	50	45	38	32
Semimem	1205	400	260	275	275	280
Semiten	386	45	27	25	23	22
Bifemlh	843	175	90	90	90	90
Bifemsh	468	400	150	150	150	150
Sar	123	120	30	30	28	35
add_long	492	450	30	22	17	17
add_brev	334	10	4	3	4	4
add_mag1	404	20	4	4	3	3
add_mag2	363	30	4	4	2	3
add_mag3	521	100	32	30	25	17
Tfl	181	200	65	70	80	140
Pect	205	55	6	5	5	4
Grac	129	32	4	4	4	3
glut_max1	445	110	40	55	80	120
glut_max2	644	200	70	80	100	112
glut_max3	433	80	30	27	17	5
iliacus	503	250	225	225	225	215
Psoas	433	200	190	175	175	175
quad_fem	298	11	8	8	7	10
Gem	129	3	5	4	3	4
Peri	345	50	70	80	90	90

rect_fem	913	150	475	470	470	485
vas_med	1516	20	140	140	140	145
vas_int	1445	20	140	130	130	135
vas_lat	2189	30	300	300	300	300

D-1.6 Patient051 Muscle Forces

7.1 Methodology

Table D. 11: Patient051 JO maximum isometric forces (N) for base model and muscle asymmetry; 20%, 40% and 60% for three components of gluteus medius and minimus.

Reduction in right hip		Muscle Asymmetry Reductions		
Abbreviation	ScaledFile Value	20% Red	40% Red	60% Red
glut_med1_l	650	520	390	260
glut_med2_l	449	359	269	180
glut_med3_l	514	411	308	206
glut_min1_l	213	170	128	85
glut_min2_l	224	179	134	90
glut_min3_l	254	203	152	102

7.2 Results

Table D. 12: Patient051 JO maximum isometric forces (N) and individual muscle forces (N) for base model, contralateral and muscle asymmetry; 20%, 40% and 60%

Patient051.			**Resultant Muscle Force (Right Leg)**			
Muscles	Scaled Force	Unaffected Leg – left	No Reduction	20% Reduction	40% Reduction	60% Reduction
glut_med1	650	700	700	600	445	300
glut_med2	449	320	360	350	270	180
glut_med3	514	150	150	115	84	185
glut_min1	213	200	130	160	140	90
glut_min2	224	206	113	150	145	100
glut_min3	254	92	90	113	155	115
Semimem	1217	400	365	365	365	370
Semiten	390	55	35	32	32	35
Bifemlh	850	200	140	138	142	143
Bifemsh	472	325	160	160	160	163
Sar	124	130	37	37	130	130
add_long	496	150	190	185	180	175
add_brev	337	15	11	9	8	6
add_mag1	407	27	25	22	22	19
add_mag2	366	32	22	20	20	18
add_mag3	526	150	65	65	65	64
Tfl	183	175	120	190	205	230
Pect	207	35	20	20	20	18
Grac	130	15	15	15	15	15
glut_max1	449	80	70	95	312	315
glut_max2	650	130	115	130	150	160
glut_max3	437	110	80	80	80	77
iliacus	508	550	275	266	268	270
Psoas	437	450	240	242	242	245
quad_fem	301	27	70	72	72	70
Gem	130	11	11	9	9	10
Peri	348	70	130	130	161	180

rect_fem	921	850	570	600	570	530
vas_med	1530	370	390	400	422	420
vas_int	1459	400	370	378	400	395
vas_lat	2209	800	840	860	905	900

D-1.7 Asymmetry Resultant Hip Contact Forces

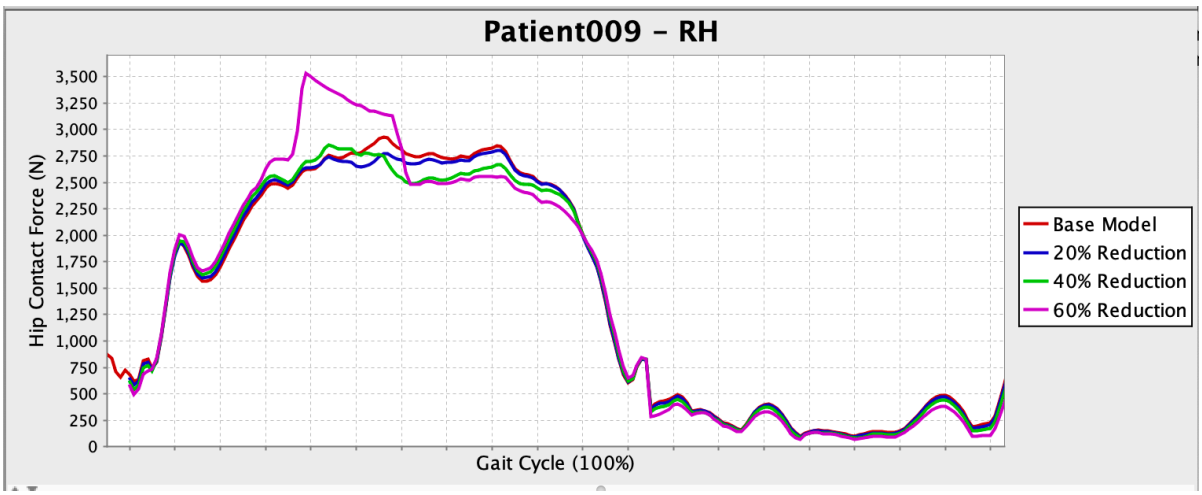

Figure D. 1: Patient009 RH resultant HCF for base (red), muscle asymmetry; 20% (blue), 40% (green) and 60% (purple) over 100% gait cycle.

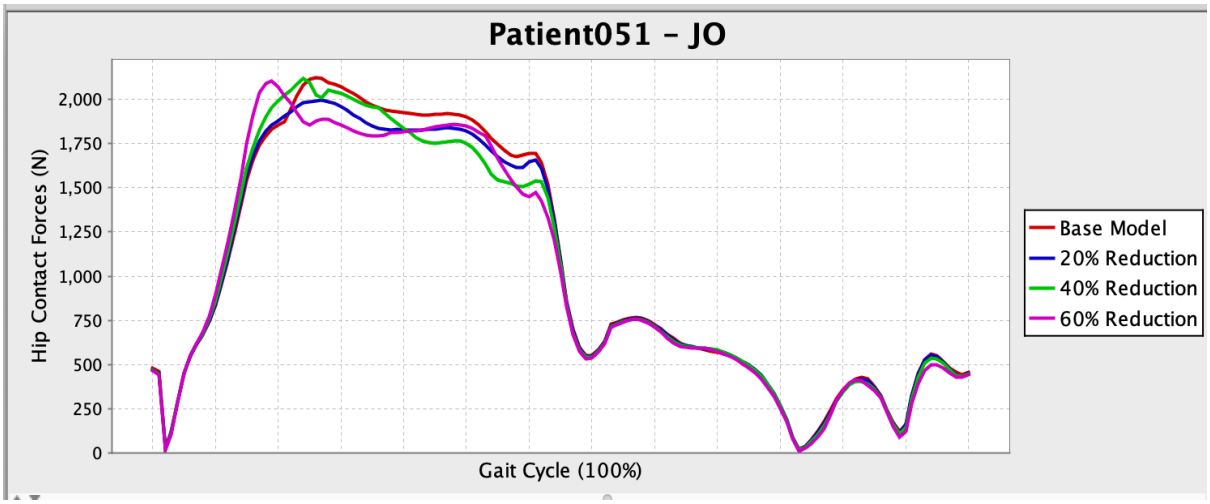

Figure D. 2: Patient051 JO resultant HCF for base (red), muscle asymmetry; 20% (blue), 40% (green) and 60% (purple) over 100% gait cycle.

D-1.8 Muscle Activation During Gait

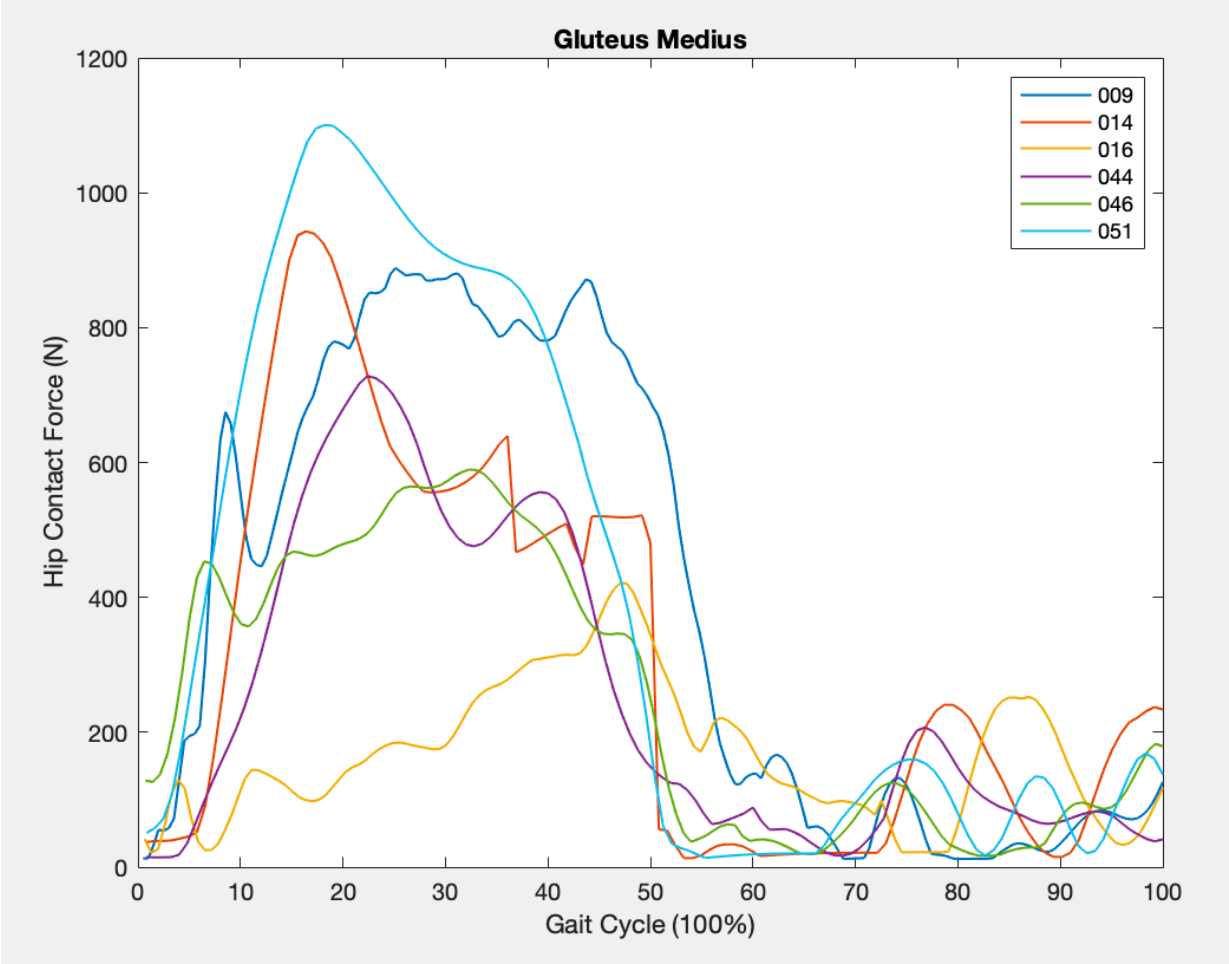

Figure D. 3: Gluteus medius: muscle activation and muscle force for all patients; 009 RH, 014 SP, 016 AF, 044 JS, 046 BA and 051 JO over 100% gait cycle.

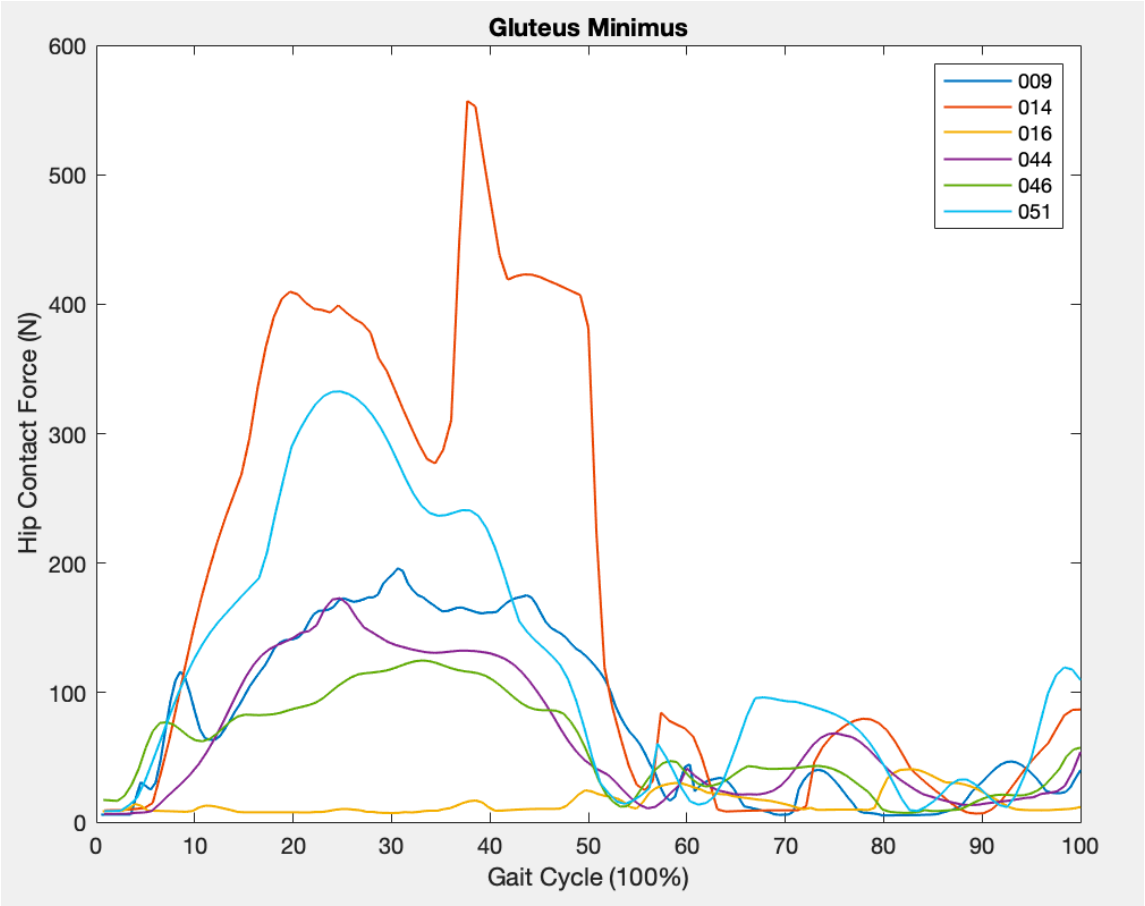

Figure D. 4: Gluteus minimus: muscle activation and muscle force for all patients; 009 RH, 014 SP, 016 AF, 044 JS, 046 BA and 051 JO over 100% gait cycle.

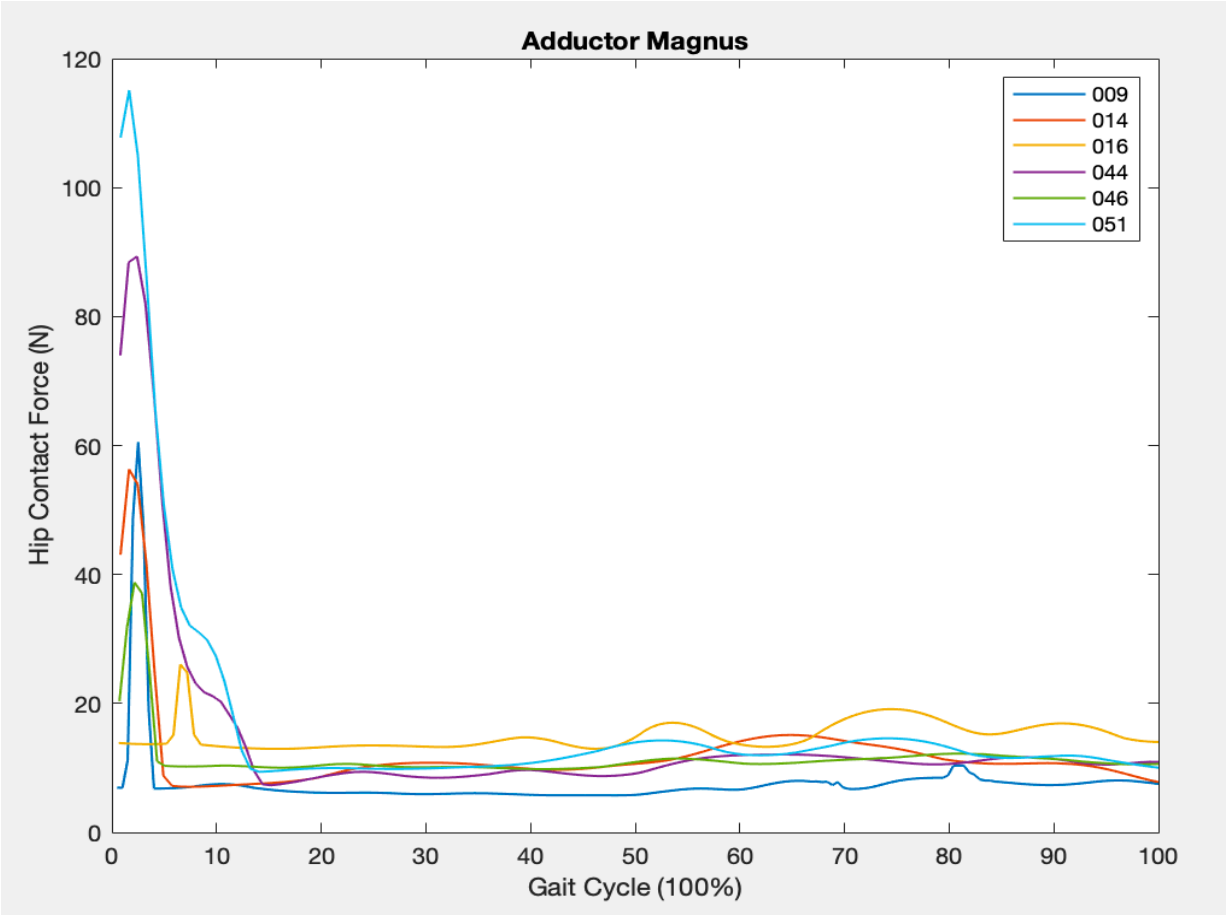

Figure D. 5: Adductor magnus: muscle activation and muscle force for all patients; 009 RH, 014 SP, 016 AF, 044 JS, 046 BA and 051 JO over 100% gait cycle.

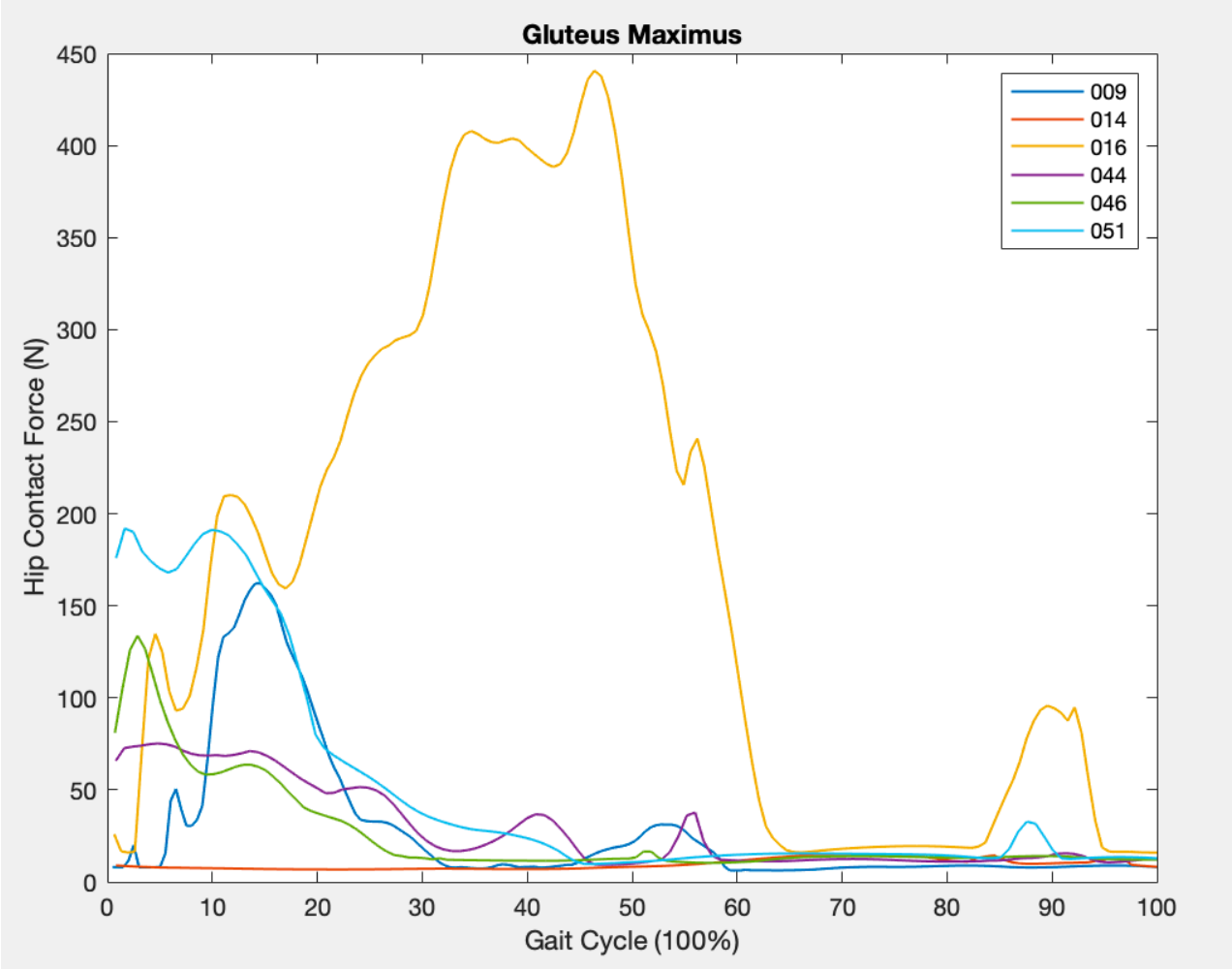

Figure D. 6: Gluteus maximus: muscle activation and muscle force for all patients; 009 RH, 014 SP, 016 AF, 044 JS, 046 BA and 051 JO over 100% gait cycle.

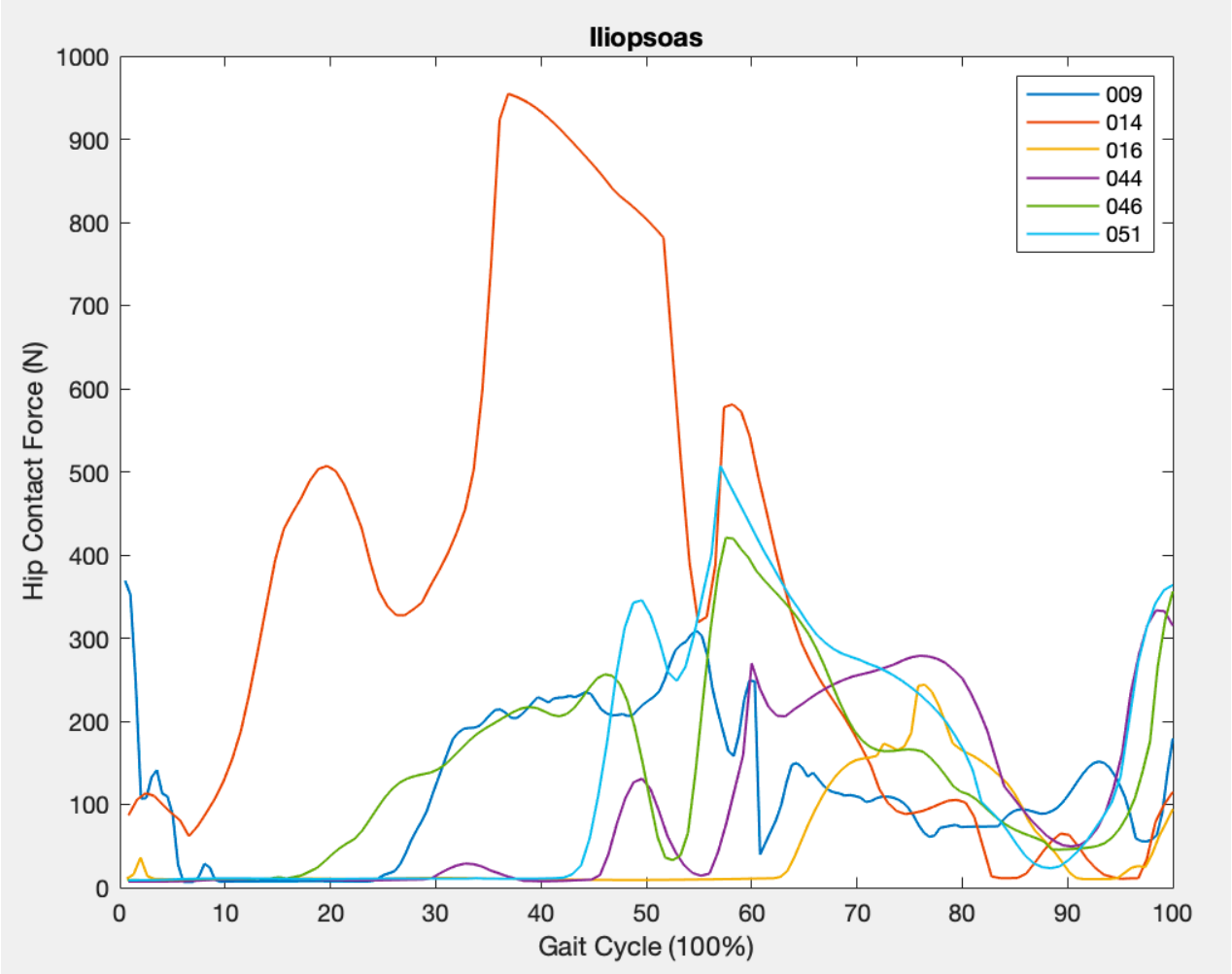

Figure D. 7: Iliopsoas: muscle activation and muscle force for all patients; 009 RH, 014 SP, 016 AF, 044 JS, 046 BA and 051 JO over 100% gait cycle.

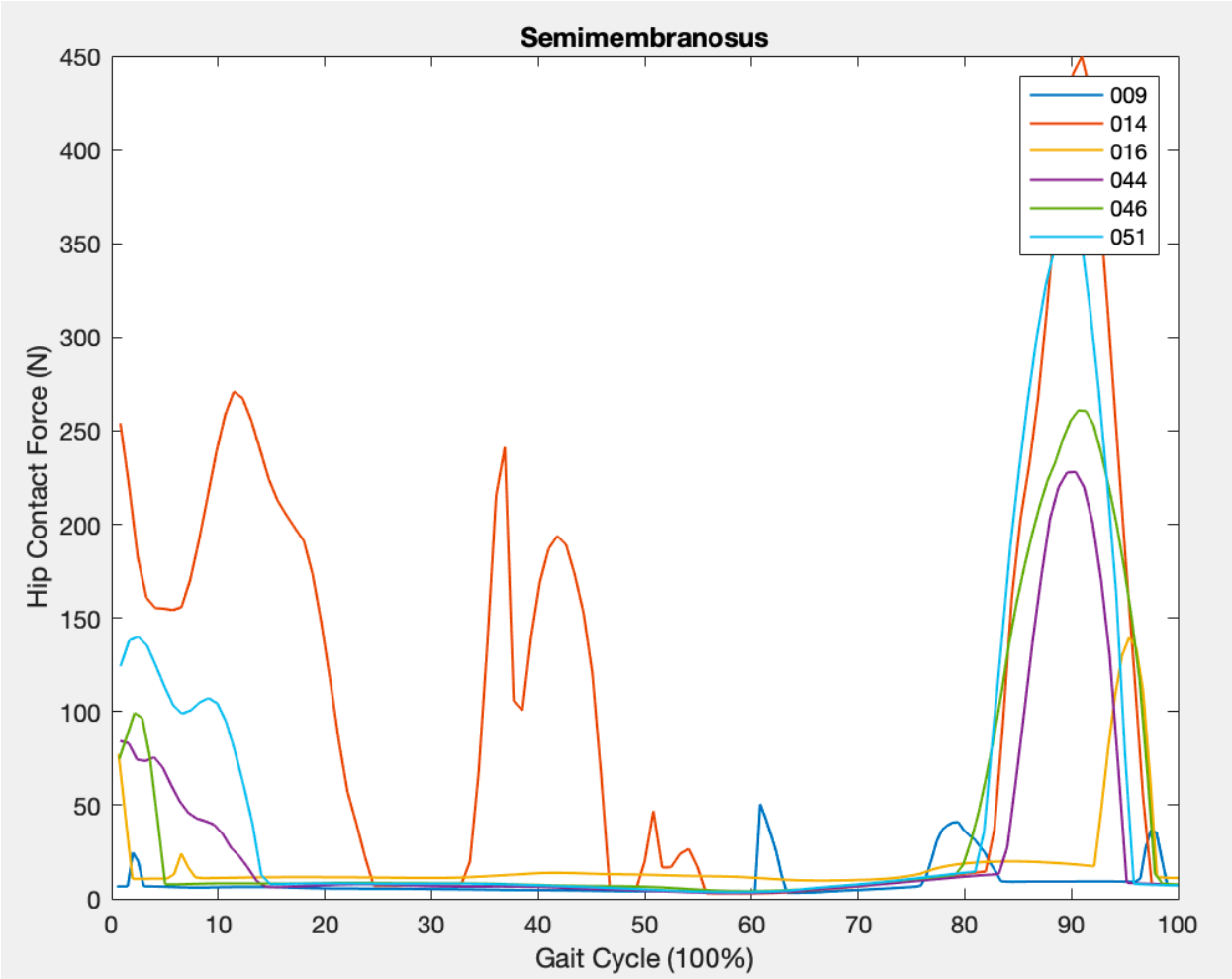

Figure D. 8: Semimembranosus: muscle activation and muscle force for all patients; 009 RH, 014 SP, 016 AF, 044 JS, 046 BA and 051 JO over 100% gait cycle.

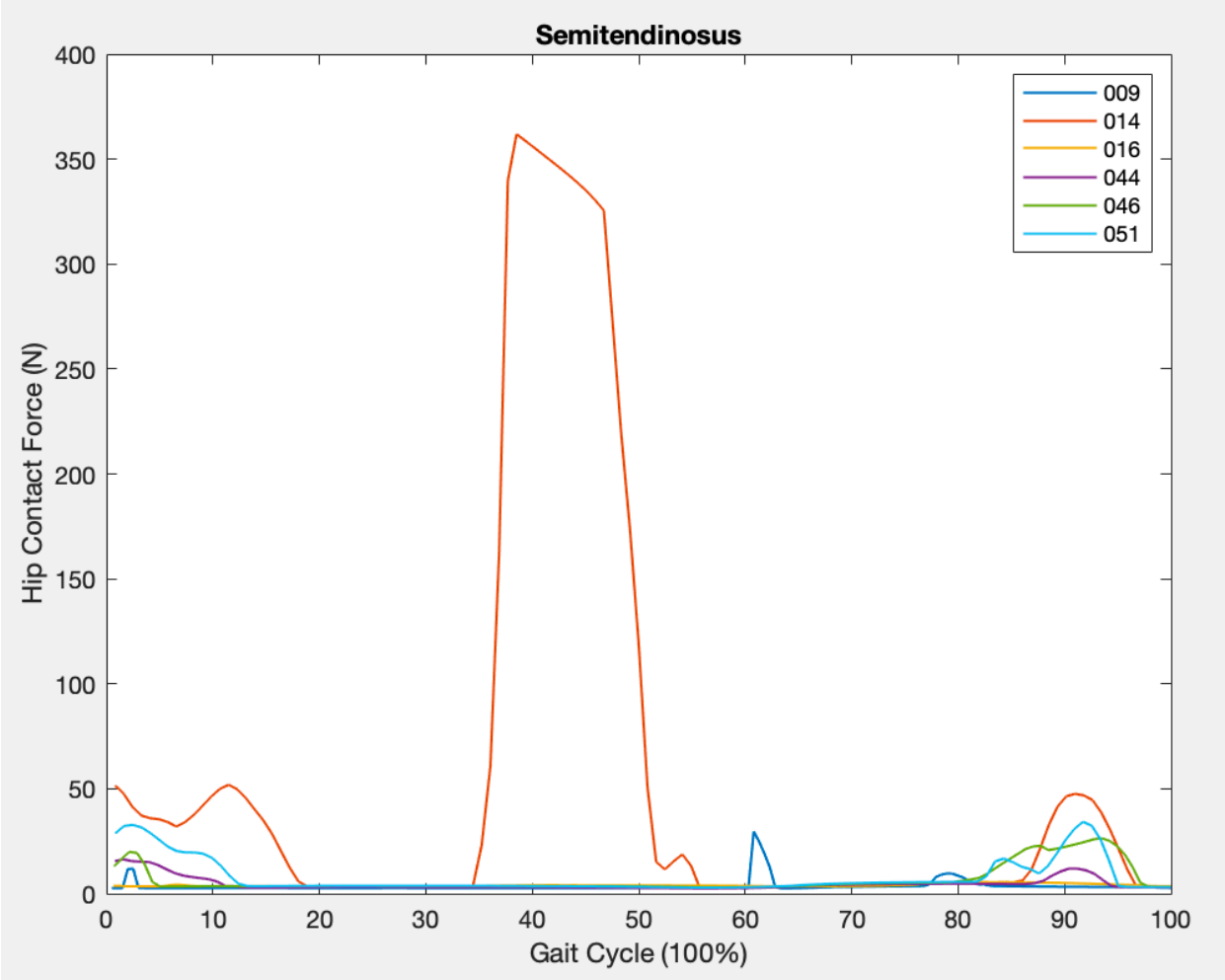

Figure D. 9: Semitendinosus: muscle activation and muscle force for all patients; 009 RH, 014 SP, 016 AF, 044 JS, 046 BA and 051 JO over 100% gait cycle.

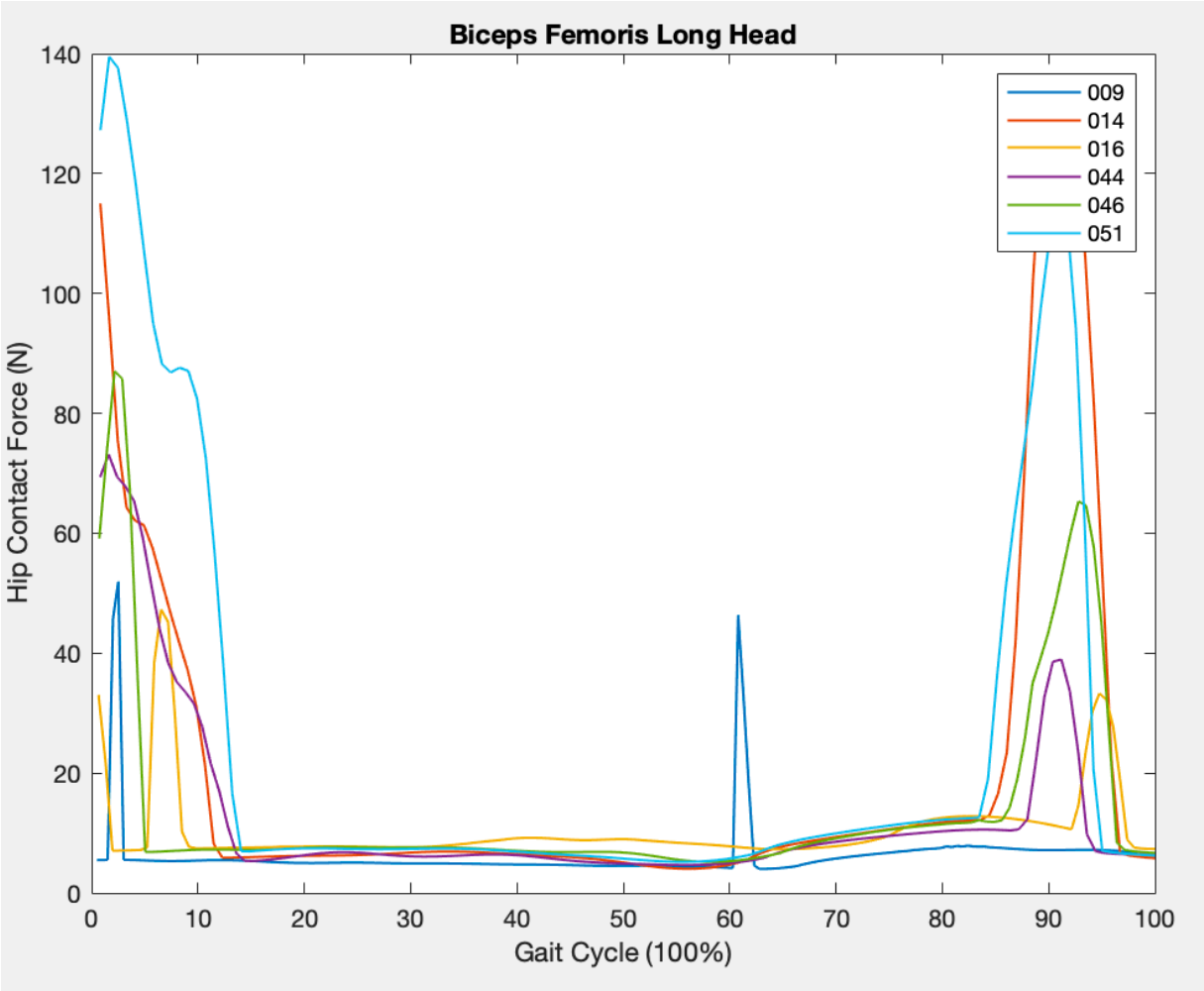

Figure D. 10: Biceps femoris long head: muscle activation and muscle force for all patients; 009 RH, 014 SP, 016 AF, 044 JS, 046 BA and 051 JO over 100% gait cycle.

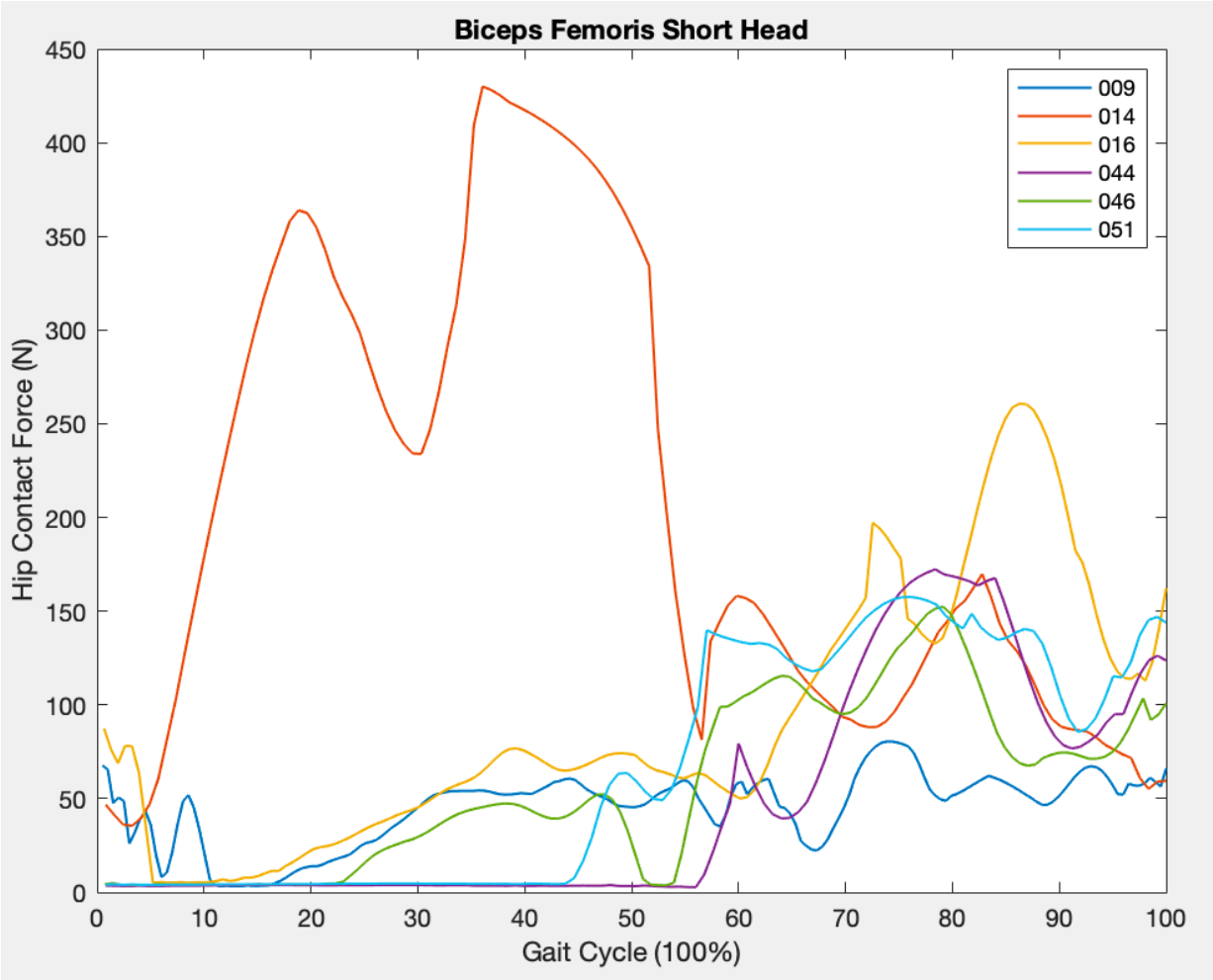

Figure D. 11: Biceps femoris short head: muscle activation and muscle force for all patients; 009 RH, 014 SP, 016 AF, 044 JS, 046 BA and 051 JO over 100% gait cycle.

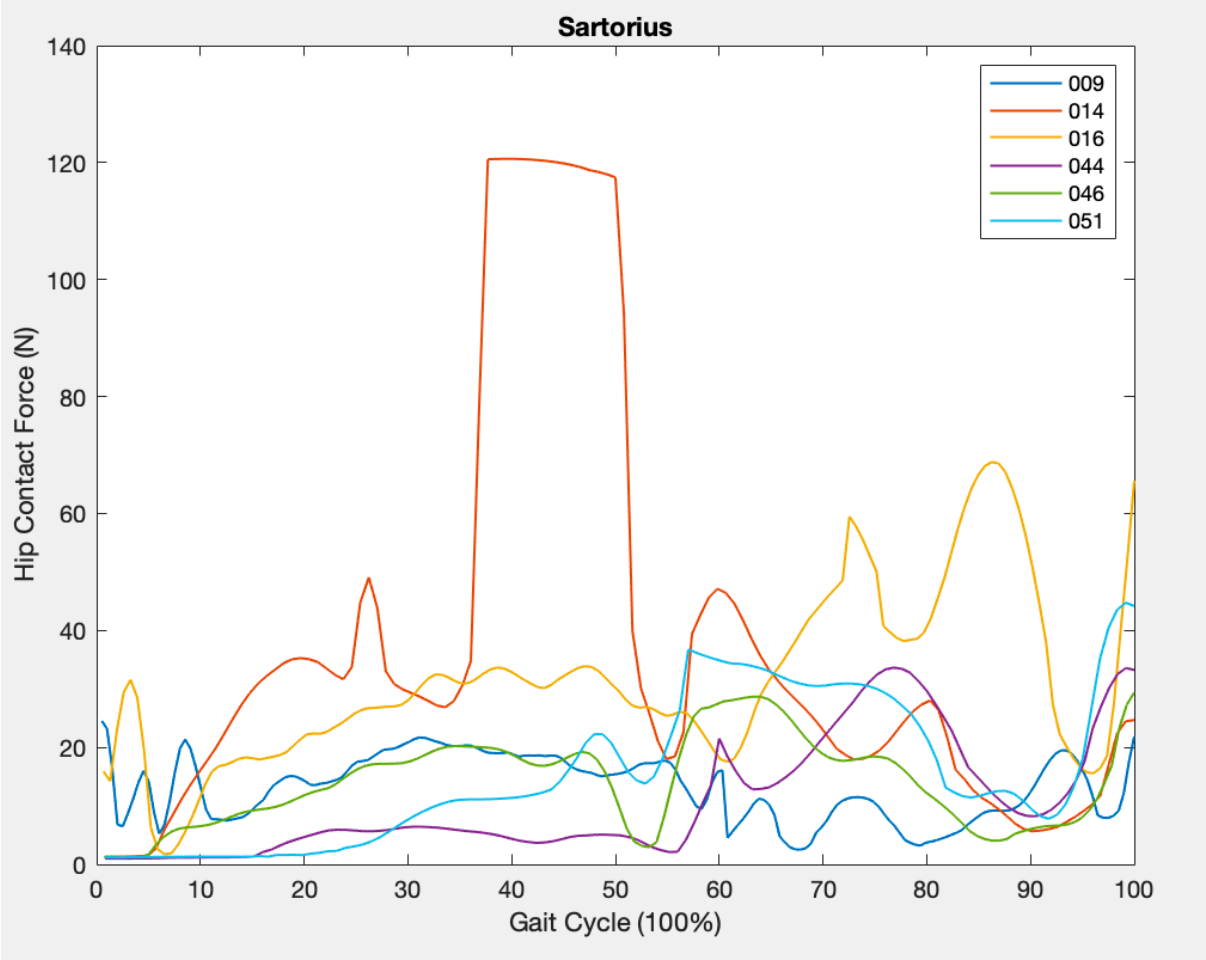

Figure D. 12: Sartorius: muscle activation and muscle force for all patients; 009 RH, 014 SP, 016 AF, 044 JS, 046 BA and 051 JO over 100% gait cycle.

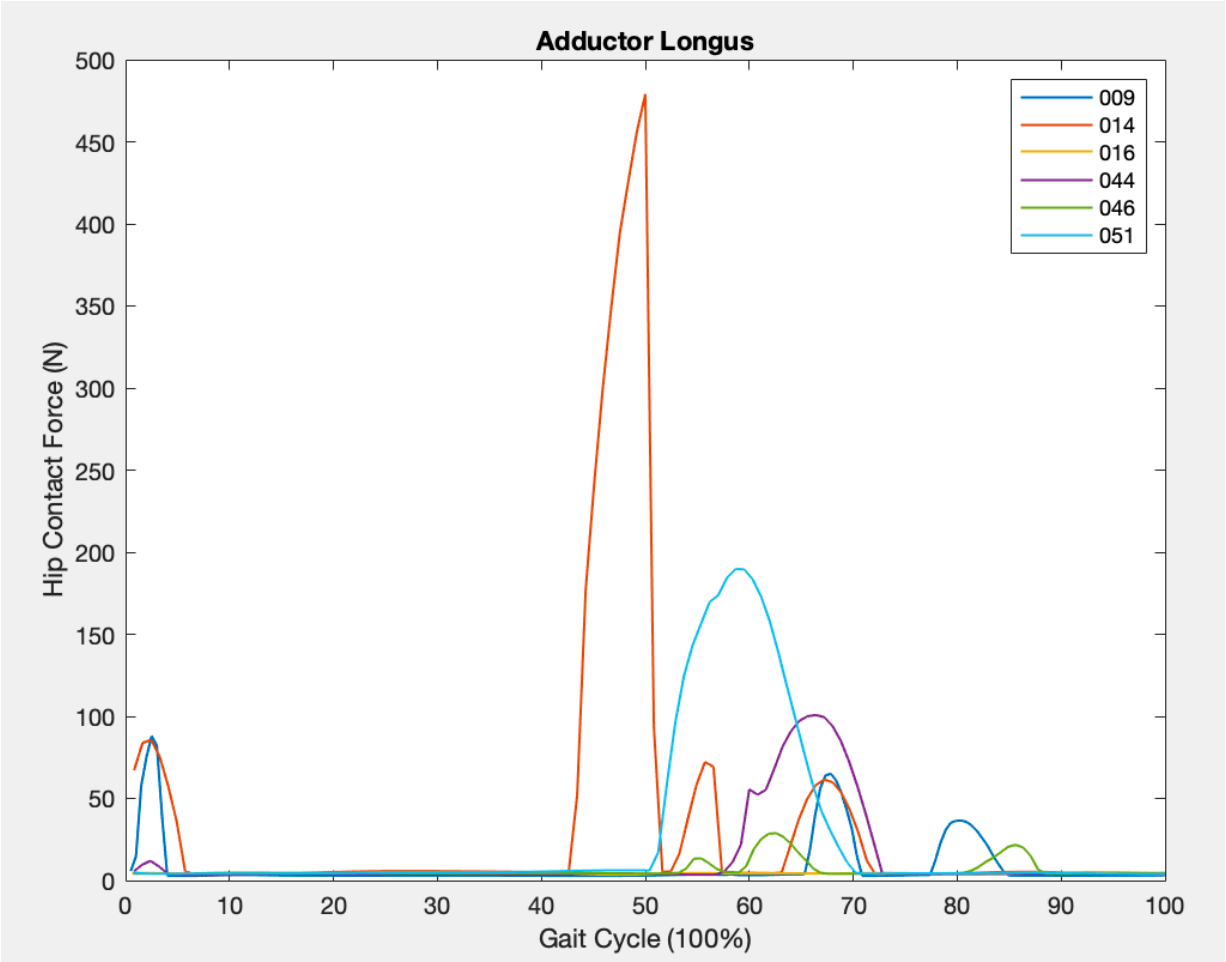

Figure D. 13: Adductor longus: muscle activation and muscle force for all patients; 009 RH, 014 SP, 016 AF, 044 JS, 046 BA and 051 JO over 100% gait cycle.

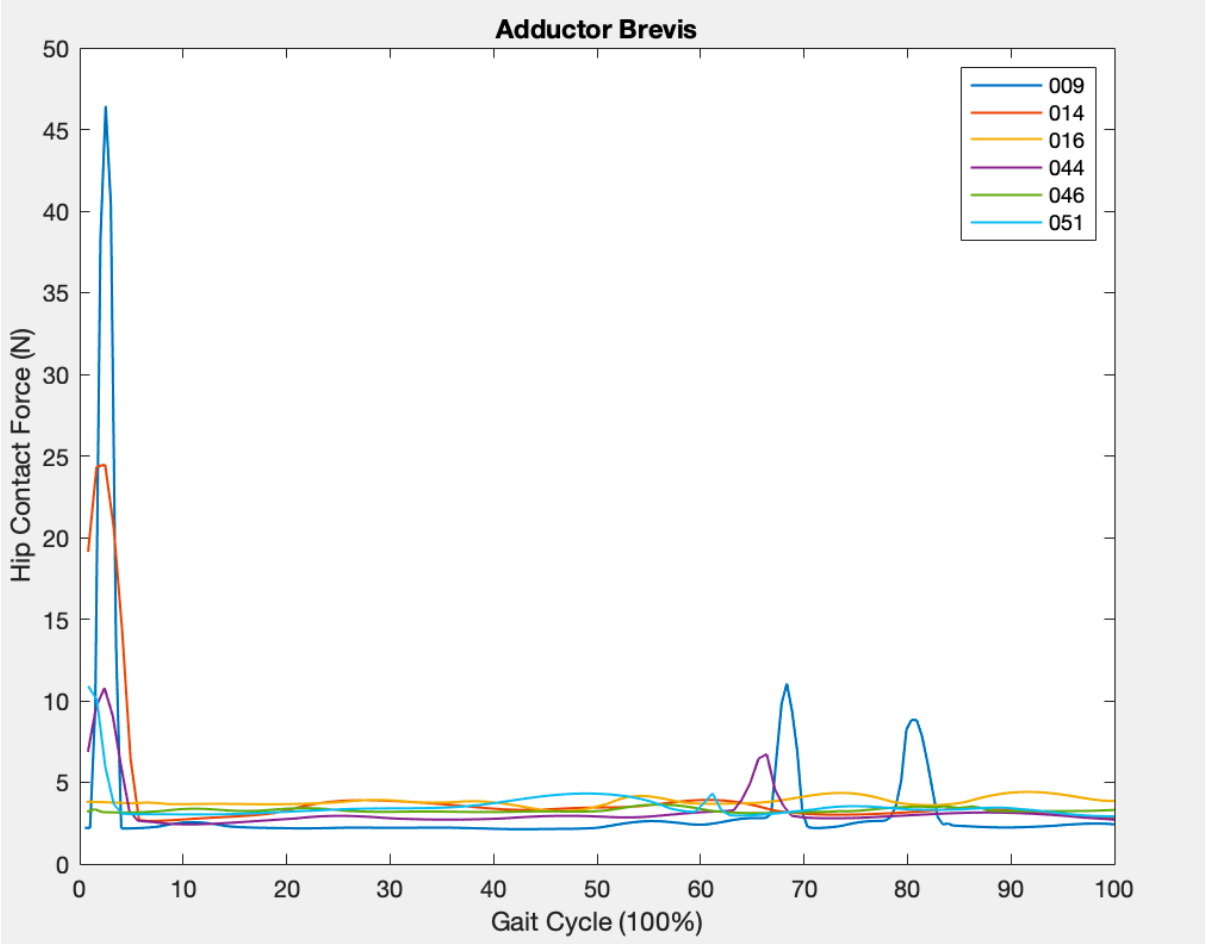

Figure D. 14: Adductor brevis: muscle activation and muscle force for all patients; 009 RH, 014 SP, 016 AF, 044 JS, 046 BA and 051 JO over 100% gait cycle.

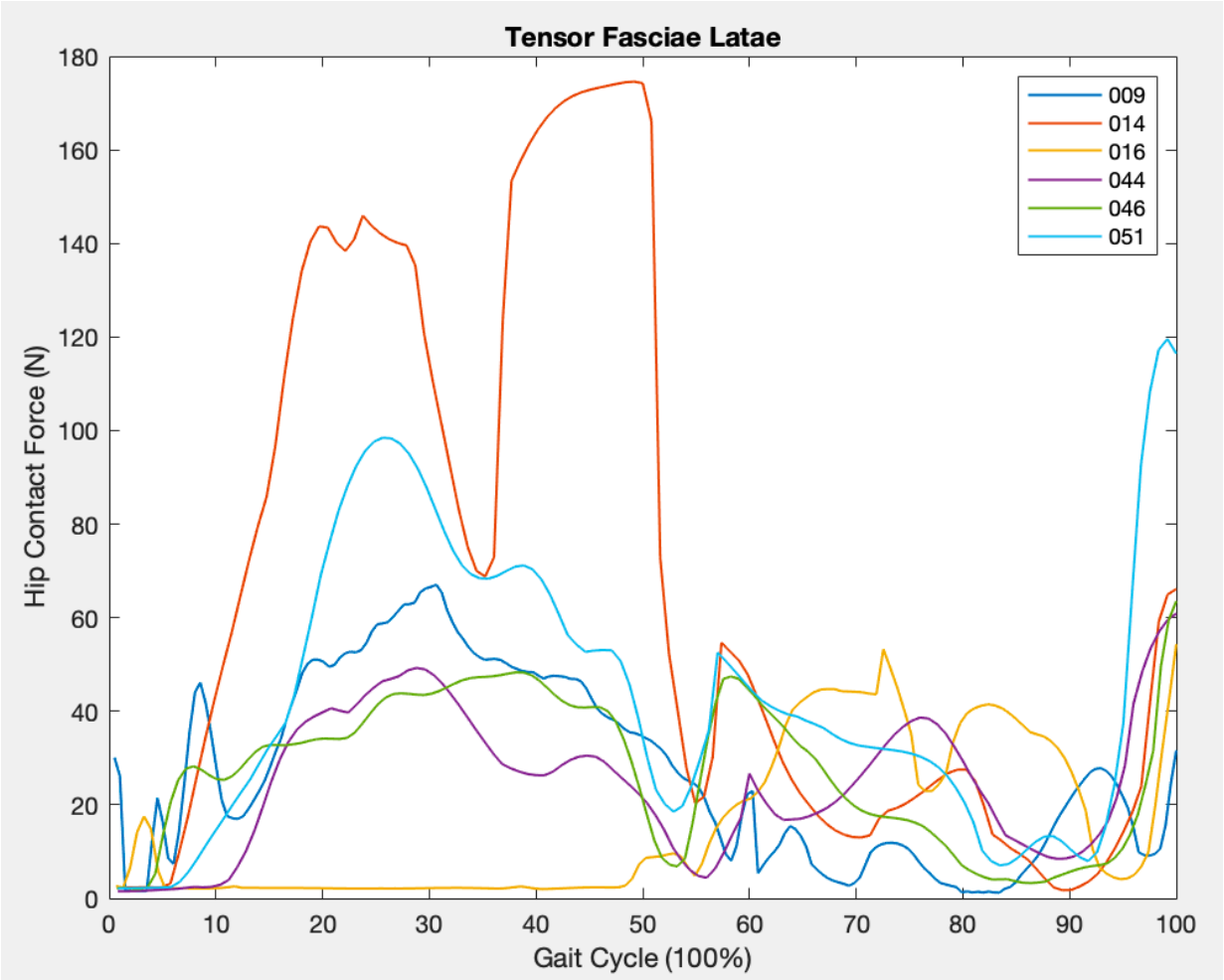

Figure D. 15: Tensor fascia latae: muscle activation and muscle force for all patients; 009 RH, 014 SP, 016 AF, 044 JS, 046 BA and 051 JO over 100% gait cycle.

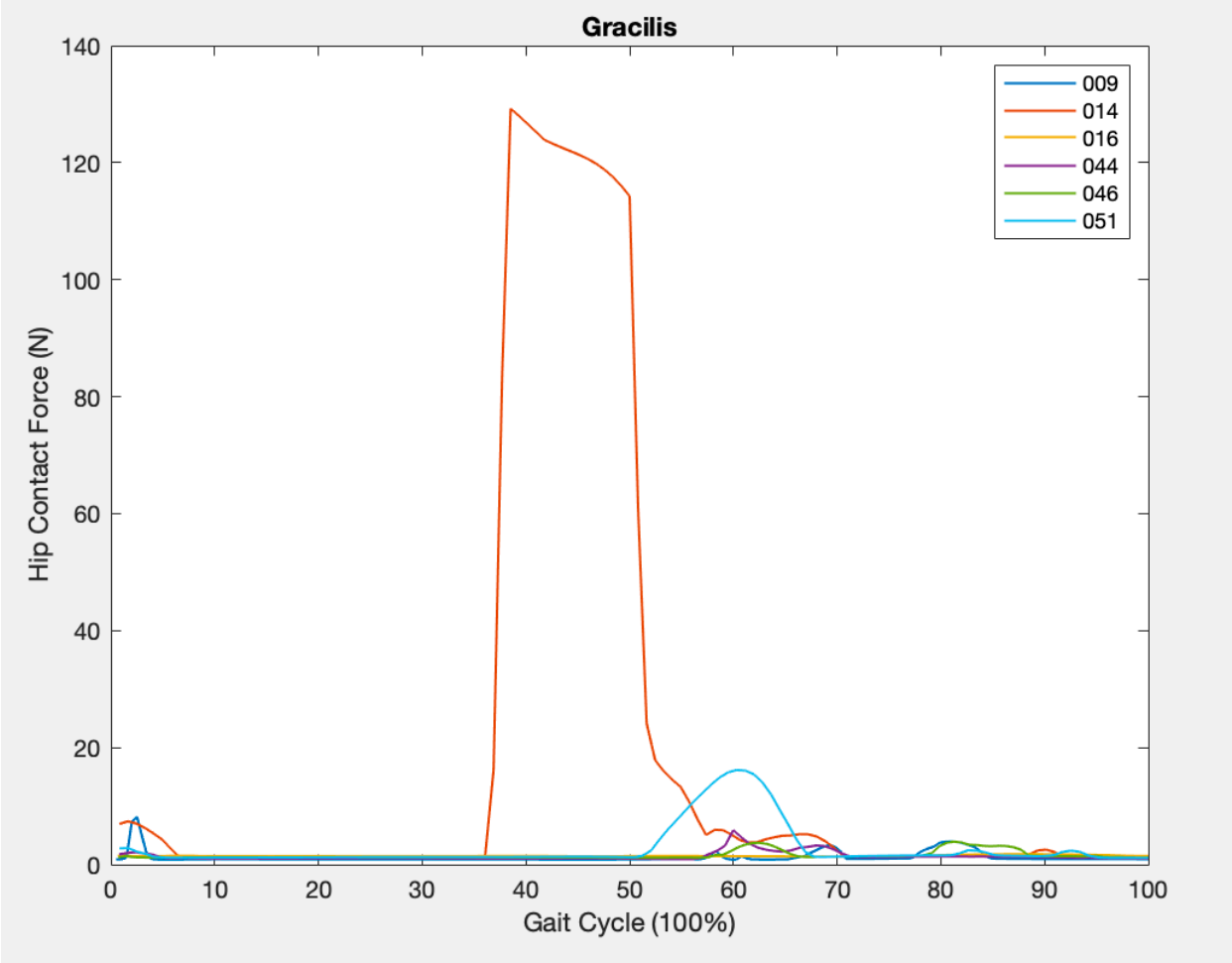

Figure D. 16: Garcilis: muscle activation and muscle force for all patients; 009 RH, 014 SP, 016 AF, 044 JS, 046 BA and 051 JO over 100% gait cycle.

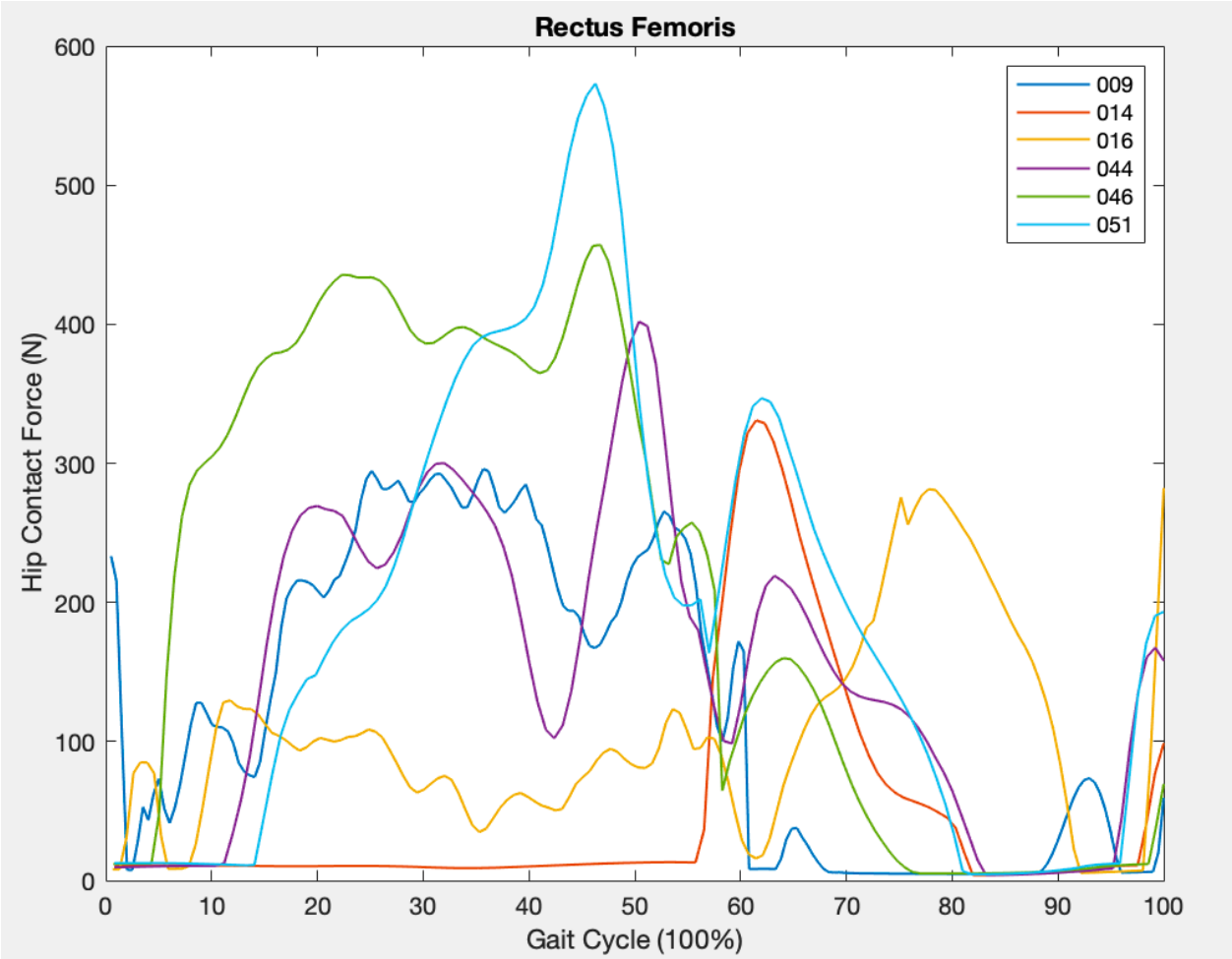

Figure D. 17: Rectus femoris: muscle activation and muscle force for all patients; 009 RH, 014 SP, 016 AF, 044 JS, 046 BA and 051 JO over 100% gait cycle.

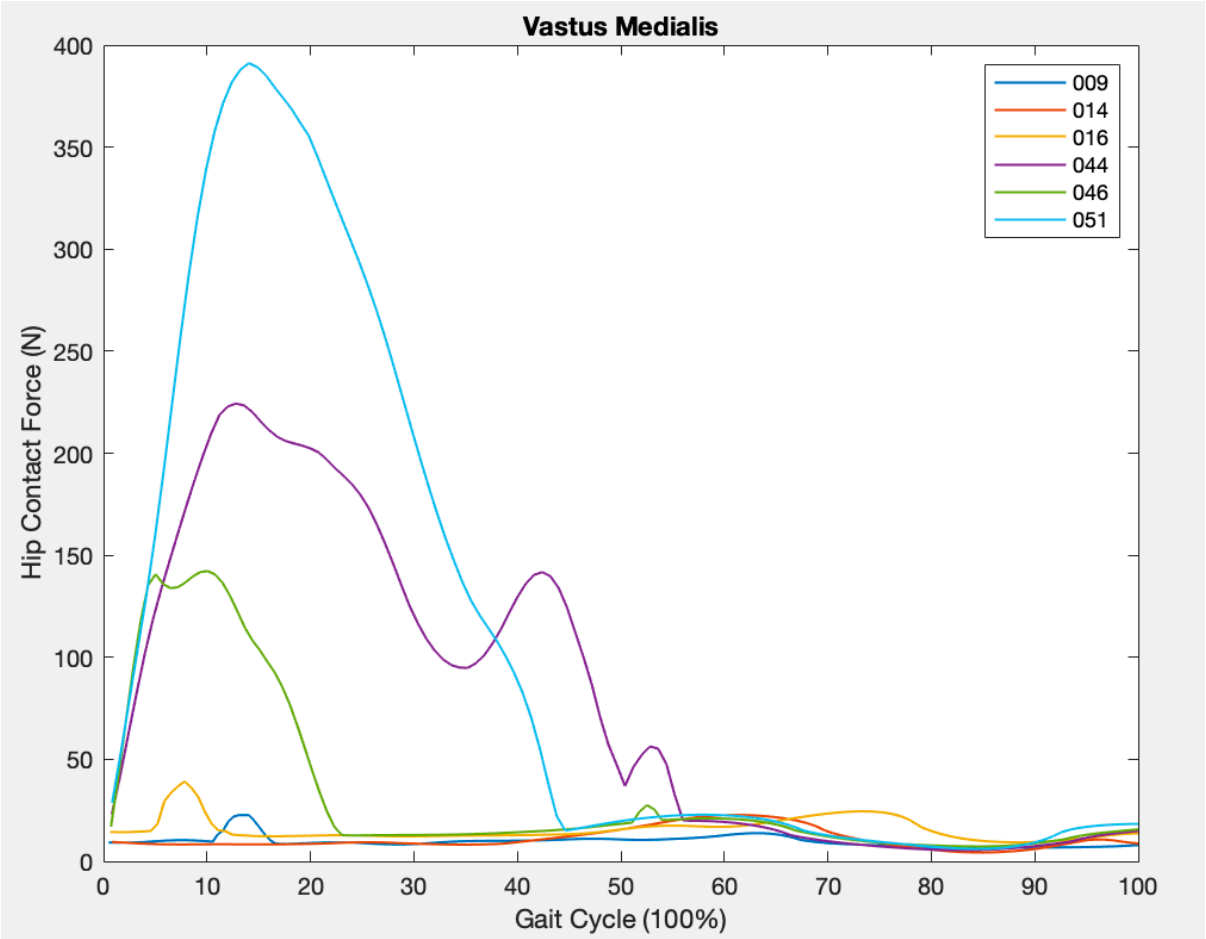

Figure D. 18: Vastus medius: muscle activation and muscle force for all patients; 009 RH, 014 SP, 016 AF, 044 JS, 046 BA and 051 JO over 100% gait cycle.

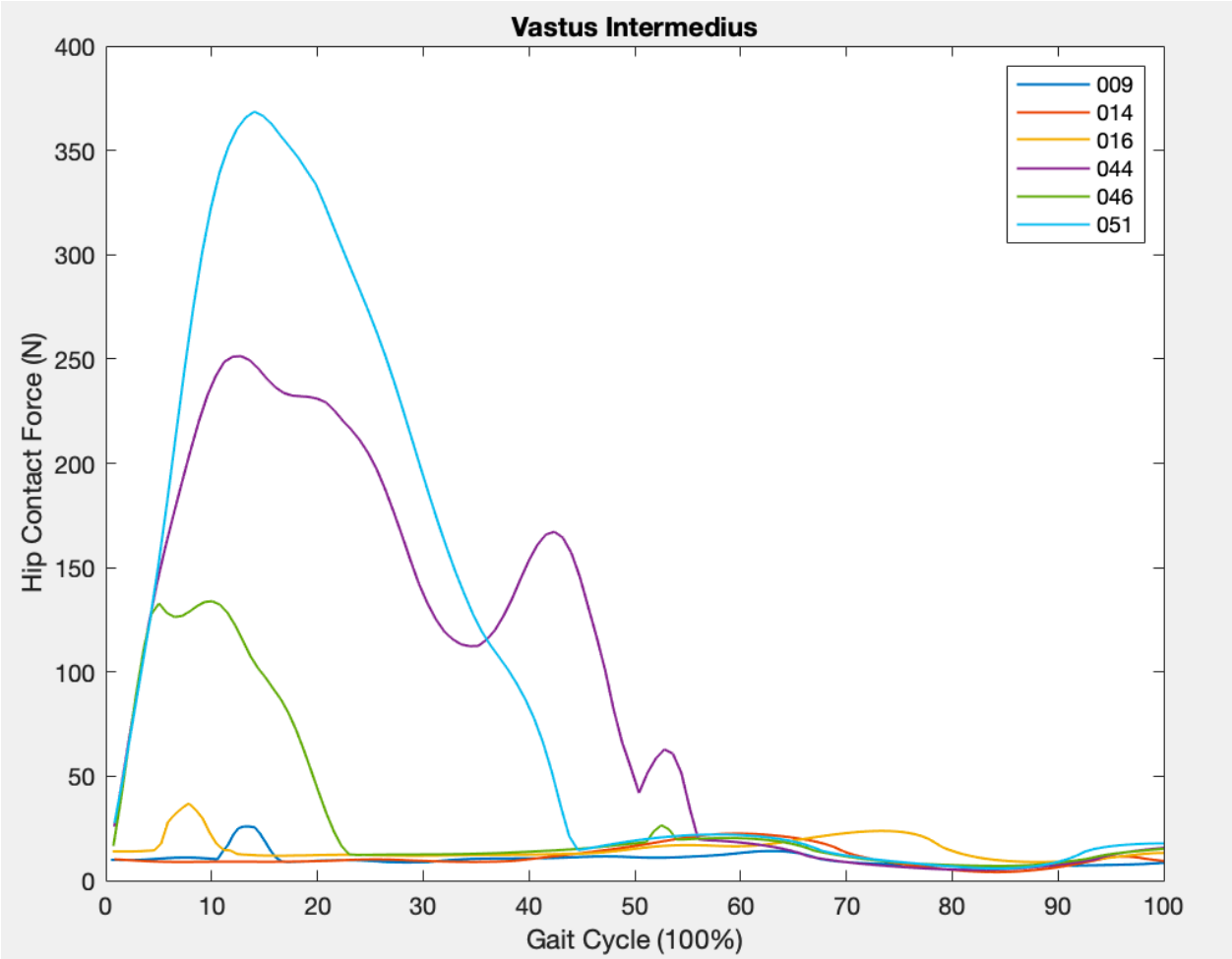

Figure D. 19:Vastus intermedius: muscle activation and muscle force for all patients; 009 RH, 014 SP, 016 AF, 044 JS, 046 BA and 051 JO over 100% gait cycle.

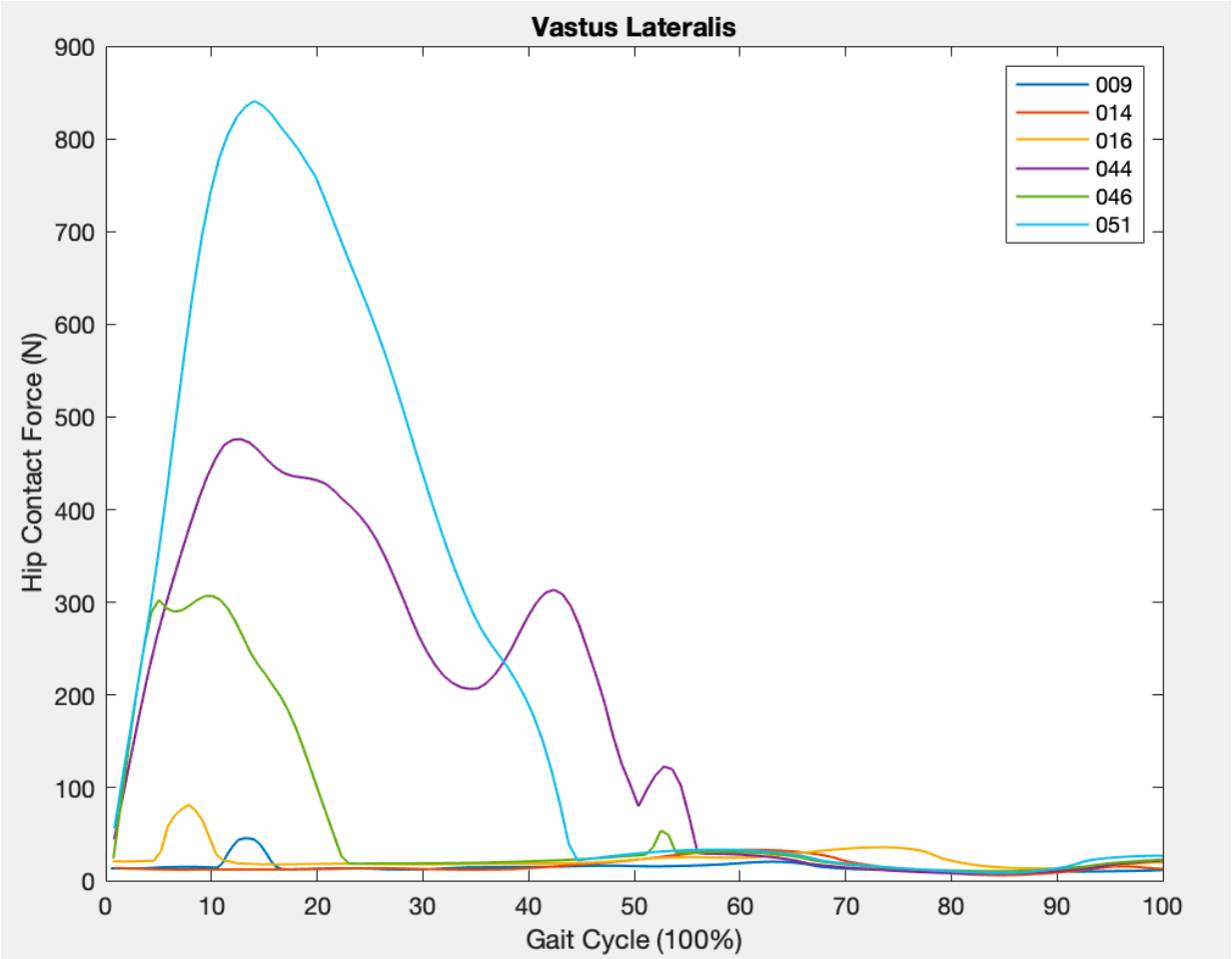

Figure D. 20:Vastus lateralis: muscle activation and muscle force for all patients; 009 RH, 014 SP, 016 AF, 044 JS, 046 BA and 051 JO over 100% gait cycle.